

STATE OF CALIFORNIA DEPARTMENT OF TRANSPORTATION
TECHNICAL REPORT DOCUMENTATION PAGE
 TR0003 (REV. 10/98)

1. REPORT NUMBER CA10-0978	2. GOVERNMENT ASSOCIATION NUMBER	3. RECIPIENT'S CATALOG NUMBER
4. TITLE AND SUBTITLE Diagnosing Chronic Errors in Freeway Loop Detectors from Existing Field hardware.	5. REPORT DATE March 18, 2011	
	6. PERFORMING ORGANIZATION CODE	
7. AUTHOR(S) Benjamin Coifman & Ho Lee	8. PERFORMING ORGANIZATION REPORT NO.	
9. PERFORMING ORGANIZATION NAME AND ADDRESS Ohio State University Department of Civil and Environmental Engineering and Geodetic Science Hitchcock Hall 470 2070 Neil Avenue Columbus, OH 43210	10. WORK UNIT NUMBER	
	11. CONTRACT OR GRANT NUMBER IA 65A0231	
12. SPONSORING AGENCY AND ADDRESS California Department of Transportation Division of Research and Innovation, MS-83 1227 O Street Sacramento CA 95814	13. TYPE OF REPORT AND PERIOD COVERED	
	14. SPONSORING AGENCY CODE Caltrans	
15. SUPPLEMENTAL NOTES		

16. ABSTRACT

Traffic Management applications such as ramp metering, incident detection, travel time prediction, and vehicle classification greatly depend on the accuracy of data collected from inductive loop detectors, but these data are prone to various errors caused by hardware and software problems. The impact of these errors will propagate to the subsequent measurements of flow, occupancy, and speed and can end up affecting traffic control decisions and traveler information. In an effort to improve the quality of loop detector data, this research developed algorithms to automatically identify two types of detector errors that are difficult to diagnose in the field: splashover, the false detection in one lane of a vehicle from an adjacent lane; and pulse breakup, when a single vehicle produces two or more pulses in its lane of travel. While the focus of this study is loop detectors, the present work is likely applicable to emerging detectors seeking to replace loop detectors using wayside mounted sensors. Most of these detectors emulate the operation of loop detectors, so, while the mechanism of splashover and pulse breakup differs across the different detection technologies, its manifestation should be similar in the vehicle actuations.

17. KEY WORDS Inductive Loop Detector, Traffic Monitoring Station, Splashover, Pulse Breakup, Detector Sensitivity, Ground Truth	18. DISTRIBUTION STATEMENT No restrictions. This document is available to the public through the National Technical Information Service, Springfield, VA 22161	
19. SECURITY CLASSIFICATION (of this report) Unclassified	20. NUMBER OF PAGES 139	21. PRICE

Identifying Chronic Errors at Freeway Loop Detectors- Splashover, Pulse Breakup, and Sensitivity Settings

Benjamin Coifman, PhD

Associate Professor
The Ohio State University
Joint appointment with the Department of Civil and Environmental Engineering and Geodetic Science,
and the Department of Electrical and Computer Engineering
Hitchcock Hall 470
2070 Neil Ave, Columbus, OH 43210
Tel: (614) 292-4282
E-mail: Coifman.1@OSU.edu

Ho Lee

Graduate Research Assistant
The Ohio State University
Department of Civil and Environmental Engineering and Geodetic Science,
Hitchcock Hall 470
2070 Neil Ave, Columbus, OH 43210
E-mail: lee.2406@OSU.edu



DISCLAIMER STATEMENT

This document is disseminated in the interest of information exchange. The contents of this report reflect the views of the authors who are responsible for the facts and accuracy of the data presented herein. The contents do not necessarily reflect the official views or policies of the State of California or the Federal Highway Administration. This publication does not constitute a standard, specification or regulation. This report does not constitute an endorsement by the Department of any product described herein.

For individuals with sensory disabilities, this document is available in Braille, large print, audiocassette, or compact disk. To obtain a copy of this document in one of these alternate formats, please contact: the Division of Research and Innovation, MS-83, California Department of Transportation, P.O. Box 942873, Sacramento, CA 94273-0001.

ABSTRACT

Loop detectors are the most common sensors used to collect freeway management data. Data obtained from loop detectors are used for applications such as traveler information, ramp metering, incident detection, travel time prediction, and vehicle classification. The performance of such applications greatly depends on the accuracy of the detector data. Unfortunately, data collected from loop detectors are frequently prone to chronic errors caused by hardware and software problems. Detector errors degrade the accuracy of detector data, and the impact of these errors will propagate to subsequent measurements of flow, occupancy, and speed from the loop detectors. In the end, unreliable data incorporating detector errors undermine the control decisions based on the detector's data and traveler information provided to drivers.

There has been considerable research to screen the quality of loop detector data from aggregate measurements and more recently individual vehicle actuations. However, some significant detector errors have not received much attention due to the difficulty of identifying their occurrence. This research looks at two such errors: splashover, the false detection in one lane of a vehicle from an adjacent lane; and pulse breakup, the division of a single pulse from a vehicle that breaks up into two or more pulses. Algorithms are developed to identify these errors using loop detector data. The development process employs concurrent video-recorded ground truth data, though the algorithms themselves only use data from the loop detectors. Splashover and pulse breakup are often related, arising from the detectors being set too sensitive, or not sensitive enough, respectively.

First, the splashover detection algorithm is designed to find detectors exhibiting chronic splashover problems. At the crux of this algorithm is the fact that an erroneous pulse arising from splashover in one lane should usually be bounded by the valid pulse from the vehicle in its lane of travel. The algorithm calculates the rate of suspected splashover, i.e., the percentage of pulses in the subject lane that are bounded by a pulse in an adjacent lane. But a difficulty arises because any given splashover event in the data stream is usually indistinguishable from the non-error event of two vehicles passing the detector station at the same time. To control for these valid concurrent actuations we calculate an expected rate of false positives as a function of the observed traffic conditions.

Next, the pulse breakup detection algorithm is designed to identify the presence of individual pulse breakup events. The algorithm begins with the comparison of on-times from the two successive pulses bounding a given short off-time, but then employs several heuristic comparisons of the adjacent

on-times with respect to traffic conditions to refine the performance. A total of six steps are included in the algorithm. If two successive pulses satisfy all of the steps, these pulses are a suspected pulse breakup. Otherwise, these pulses are considered to arise from non-pulse breakup, e.g., tailgating. The process is repeated over all pulses in each lane.

Prior to applying these algorithms, one must ensure that the detector sensitivity is set correctly, as discussed in Appendix A. The splashover algorithm is presented before the pulse breakup algorithm because it is envisioned that in practice the algorithms would be applied in this order, since any given splashover event may also appear to be a pulse breakup event if it is too close to a valid pulse when looking strictly at the data stream in a single lane. The algorithms for splashover and for pulse breakup were tested over 15 detector stations in Columbus, Ohio, with concurrent video-record ground truth data, and the algorithms exhibited good performance.

While the focus of this study is loop detectors, the present work is likely applicable to emerging detectors as well. The emerging detectors seek to replace loop detectors using wayside mounted sensors, but most of these detectors emulate the operation of loop detectors. So, while the mechanism of splashover and pulse breakup differs across the different detection technologies, the manifestation should be similar in the vehicle actuations.

Detector error detection enabled by the research could lead to a very inexpensive means to improve the quality of loop detector data at existing loop detector stations. After further refinement, in the short term the algorithms could be incorporated into a field diagnostic tool to assess the performance of a given station. In the longer run, the tests should be incorporated into the regular controller software so that the controller can continually assess the health of the detectors. The research should benefit the various applications employing a loop detector data, e.g., traffic control, traveler information, transportation planning, and traffic flow theory.

TABLE OF CONTENTS

1	INTRODUCTION	1-1
1.1	OBJECTIVES OF THE STUDY	1-2
1.2	BACKGROUND AND LITERATURE REVIEW	1-3
1.3	OVERVIEW.....	1-5
2	DATA DESCRIPTION.....	2-1
2.1	LOOP DETECTOR OVERVIEW	2-1
2.1.1	<i>Single loop detectors.....</i>	<i>2-1</i>
2.1.2	<i>Dual loop detectors.....</i>	<i>2-4</i>
2.2	DATA SOURCES	2-5
2.2.1	<i>Loop detector data.....</i>	<i>2-5</i>
2.2.2	<i>Ground truth data</i>	<i>2-5</i>
3	AN ALGORITHM TO IDENTIFY DETECTORS EXHIBITING CHRONIC SPLASHOVER .	3-1
3.1	THE NATURE OF SPLASHOVER.....	3-2
3.2	DEVELOPMENT OF AN ALGORITHM TO IDENTIFY LOOP DETECTORS WITH SPLASHOVER.....	3-5
3.2.1	<i>Expected number of false positives</i>	<i>3-6</i>
3.2.2	<i>The adjusted rate of suspected splashover</i>	<i>3-7</i>
3.3	OPTIMAL APPLICATION PERIODS.....	3-9
3.4	EVALUATION OF THE ALGORITHM	3-10
3.4.1	<i>Application and results.....</i>	<i>3-11</i>
3.4.2	<i>A comparison of algorithm performance.....</i>	<i>3-12</i>
3.4.3	<i>Brief before and after study of loop detector sensitivity</i>	<i>3-13</i>
4	AN ALGORITHM TO IDENTIFY PULSE BREAKUP	4-1
4.1	PREVIOUS RESEARCH RELATED TO PULSE BREAKUP	4-3
4.2	DEVELOPMENT OF A NEW ALGORITHM TO IDENTIFY PULSE BREAKUP	4-5
4.2.1	<i>Dynamic off-time.....</i>	<i>4-6</i>
4.2.2	<i>Ratio of on-times.....</i>	<i>4-8</i>
4.2.3	<i>Ratio of off-time and preceding on-time</i>	<i>4-9</i>
4.2.4	<i>20th percentile off-time.....</i>	<i>4-10</i>
4.2.5	<i>Maximum vehicle length.....</i>	<i>4-11</i>
4.2.6	<i>The pulse breakup detection algorithm for single loop detectors.....</i>	<i>4-12</i>
4.3	EVALUATION OF THE PULSE BREAKUP DETECTION ALGORITHM FOR SINGLE LOOP DETECTORS....	4-13

4.3.1	<i>Performance during free flow conditions</i>	4-13
4.3.2	<i>Performance during congested conditions</i>	4-15
4.3.3	<i>The suspected pulse breakup rate</i>	4-16
4.4	SENSITIVITY OF THE ALGORITHM TO THE CHOICE OF THRESHOLD VALUES.....	4-17
4.5	PERFORMANCE OF THE PULSE BREAKUP DETECTION ALGORITHM.....	4-18
4.6	A BRIEF BEFORE AND AFTER STUDY OF LOOP DETECTOR SENSITIVITY.....	4-19
5	SUMMARY AND CONCLUSIONS	5-1
6	REFERENCES	6-1
APPENDIX A	LOOP DETECTOR SENSITIVITY	A-1
A.1	INTRODUCTION.....	A-1
A.2	IDENTIFICATION OF A LOOP DETECTOR WITH INCORRECT LOOP SENSITIVITY	A-3
A.2.1	<i>Daily median on-time test</i>	A-3
A.2.2	<i>Change of loop detector sensitivity over time</i>	A-5
A.3	CORRECTION OF MEASUREMENT ERRORS DUE TO INCORRECT LOOP DETECTOR SENSITIVITY AND DUAL LOOP SPACING	A-6
A.3.1	<i>Detector sensitivity at single and dual loop detectors</i>	A-6
A.3.2	<i>Dual loop detector spacing</i>	A-7
A.4	VALIDATION OF THE CORRECTION FACTORS	A-8
A.5	CONCLUSIONS	A-11
APPENDIX B	GROUND TRUTHING TOOL	B-1
APPENDIX C	SENSITIVITY OF THE SPLASHOVER DETECTION ALGORITHM WITH RESPECT TO ϵ	C-1
APPENDIX D	PERCENTAGE OF ADJUSTED RATE OF SUSPECTED SPLASHOVER RELATIVE TO SOURCE LANE	D-1
APPENDIX E	MEDIAN ON-TIME OF LOOP DETECTORS WITH GROUND TRUTH DATA	E-1
APPENDIX F	DETAILED RESULTS FROM THE EARLIER METHODOLOGIES TO IDENTIFY LOOP DETECTORS WITH SPLASHOVER	F-1
APPENDIX G	SPEED TRENDS OF THE GROUND TRUTH DATA IN CONGESTED CONDITIONS	G-1

1 INTRODUCTION

The development and deployment of Intelligent Transportation Systems (ITS) technologies provide a wide variety of opportunities for operating agencies to improve the capacity, reliability, and efficiency of the surface transportation system (Bertini and El-Geneidy, 2002). Ultimately most ITS systems rely on surveillance for collecting information on the state of the transportation system and this state is then used as input for active control measures to improve performance. A Freeway Management System (FMS) is one such example. An FMS is intended to improve safety, optimize the capacity of the freeway and provide a better level of service to motorists without the addition of more traffic lanes (Ontario MOT, 2008). A typical FMS acquires data from the roadway, processes these data to identify and respond to problems, and/or notifies operators and motorists of those problems (Hall and Persaud, 1989). The accuracy of incoming traffic data is critical to the FMS for responding efficiently and effectively to traffic conditions.

Loop detectors are the most common sensors used to collect the FMS traffic data. The loop detectors are effectively metal detectors embedded in the pavement (Coifman, 2001). A typical loop detector station will either have one or two loop detectors per lane, called single or dual loop detectors, respectively. Conventional single loop detectors can measure flow (the number of vehicles per unit time) and occupancy (the percent time the detector is occupied by vehicles during the sample). From the single loop detector measurements one can estimate average speed over a sample, but not measure it. Dual loop detectors overcome the speed estimation problem; they can measure individual vehicle speeds from the difference in arrival times at the two loops and the known loop separation. The measured individual speeds can then be used to calculate the average speed over a sample.

Data obtained from loop detectors are used for applications such as ramp metering (e.g., Papageorgiou et al., 1997; Hourdakis and Michalopoulos, 2002), incident detection (e.g., Payne and Tignor, 1978; Payne and Thompson, 1997; Williams and Guin, 2007), travel time prediction (e.g., Kwon et al., 2000; Coifman and Krishnamurthy, 2007), and vehicle classification (e.g., FHWA, 2001; Coifman and Kim, 2009). The performance of such applications greatly depends on the accuracy of the detector data, but data collected from loop detectors are prone to various errors caused by hardware and software

problems. Detector errors degrade the quality of detector data, and the impact of these errors will propagate to the subsequent measurements of flow, occupancy, and speed. In the end, the detector errors can affect the traffic control decisions and traveler information based on the detector's data. In an effort to improve the quality of detector data (and thereby the performance of an FMS), this research seeks to identify the presence of several detector errors that otherwise would go undetected and degrade performance.

1.1 Objectives of the study

There has been considerable research to automatically screen the quality of loop detector data and identify detector errors to improve data quality, as will be reviewed in the next section. Despite the previous research efforts to screen the quality of loop detector data, some significant detector errors have not received sufficient attention due to the difficulty of identifying their occurrence. This research develops algorithms to automatically identify two such detector errors that have remained elusive to identify: splashover, the false detection in one lane of a vehicle from an adjacent lane; and pulse breakup, when a single vehicle produces two or more pulses in its lane of travel even though it should register a single pulse¹. Both errors will lead to inaccurately high flow because upon each occurrence a single vehicle is counted two or more times. Splashover will lead to inaccurately high occupancy while pulse breakup will lead to inaccurately low occupancy measurements. As will be discussed in the next section, although some existing tests may respond to severe cases of splashover or pulse breakup, e.g., by detecting unfeasibly high flows, the existing body of tests in the literature is not responsive to the errors at lower levels. Of equal importance is the fact that generally the tests presented in the literature do not distinguish between splashover, pulse breakup, or any other error or event that could lead to an increased flow. Knowing the source of the overcounting is valuable for solving the problem, e.g., splashover is often due to the detector sensitivity being set too high while pulse breakup is often due to the detector sensitivity being set too low². It is necessary to clearly identify the source of these errors so as to find proper treatment to fix a loop detector exhibiting the given error, and the more precise information that the diagnostic tests can provide the better.

¹ This error is also commonly called "drop out" in reference to the fact that the detector drops out in the middle of a pulse. Pulse breakup is also one source of "chattering", denoting that the detector is changing states too rapidly.

² Though both problems can also arise from other causes, e.g., the physical loops being misaligned within the lane of travel.

The first objective of this study is to develop algorithms to identify (1) the presence of chronic splashover problems³ and (2) the presence of individual pulse breakup events. The algorithms are based on the nature of splashover and pulse breakup events at loop detectors revealed from concurrent video recorded ground truth data. The second objective of this study is to evaluate the performance of the developed algorithms at several loop detector stations. We use data collected from 15 loop detector stations (22 directional stations) with concurrent video ground truth data.

1.2 Background and literature review

There has been considerable research to automatically identify detector errors and screen the quality of freeway loop detector data. This section reviews the general approaches that we have found in the literature. In some cases there are numerous studies and we only present typical examples while in other cases there have only been one or two studies, in which case we discuss them all. Of course not all of the tests to automatically identify detector errors are well documented in the literature. This situation often arises when the tests are designed in-house by an operating agency (see Chen and May, 1987, for examples) or were developed by a consulting firm using proprietary tools. In fact, as noted by Coifman (1999), most operating agencies employ simple heuristics such as: "Do the loop sensor indicator lights come on as a vehicle passes?" "Is a given detector off-time unfeasibly short?" or simply, "Do the time series 30 second average flow and occupancy seem reasonable to the eye?"

The various methods have been developed at macroscopic and microscopic levels. Macroscopic tests embody the formalization of heuristics to check average measurements from a given sample period against statistical tolerance, while microscopic tests examine the individual vehicle actuations (i.e., the detector "pulses" when the detector turns "on" and "off") for each vehicle that passes over a loop detector. The macroscopic tests are more common in the literature because conventional traffic monitoring practice discards the microscopic data within the controller after aggregation to macroscopic metrics (e.g., flow, occupancy and average speed).

As representative examples of the macroscopic approach, Jacobson et al. (1990) introduced a macroscopic test setting limits for acceptable values of flow for a given occupancy. Their examples showed the test was effective for detecting some intermittent failures by the loop detectors, e.g., short pulses attributed to "hanging-off" by the authors. Cleghorn et al. (1991) presented several screening methods using macroscopic measurements. They claimed to have obtained a tighter upper bound than

³ The precise threshold for detectable chronic splashover problems depends on the traffic pattern in the two lanes, but as discussed in Chapter 3, the threshold is typically on the order of two or three percent of the passing vehicles splashing over.

Jacobson et al. from feasible flow-occupancy pairs to screen data from a single loop detector. Cleghorn et al. presented additional screening for dual loop detectors, first they compared the measurements between the upstream and downstream loop detectors, and second, they expanded the two-dimensional flow-occupancy feasible region to a three-dimensional speed-flow-occupancy “acceptable region”. There has been a renewed interest in macroscopic tests arising from several recent deployments of archived data systems that collect and store the real time data for subsequent performance monitoring and analysis. Two examples of such work are Turochy and Smith (2000) and Chen et al. (2003). Turochy and Smith (2000) developed a data-screening procedure that applies a critical threshold value on measurements such as occupancy and flow, as well as tests utilizing the relationships between speed, flow, and occupancy. Among the tests included in the procedure, a maximum hourly flow threshold test (e.g., 3,100 vehicles/lane/hr) was used to catch detector errors causing unreasonably high flow. Chen et al. (2003) developed a macroscopic error detection test using the time series of flow and occupancy measurements. Statistics computed over an entire day at each detector are used to differentiate between a “bad” and “good” detector with respect to various loop detector malfunctions, e.g., “sticking-on” after a given vehicle leaves the detection zone. The algorithm did not seek to find pulse breakup, but the authors suggested that an additional constraint, such as checking for consistently high flow, should be useful to detect loop detectors with these errors.

At the microscopic level, Chen and May (1987) may have been the first to use individual vehicle actuations, rather than the macroscopic measurements, to assess detector data quality. They examined the ratio of a detector’s average on-time to average on-time of all detectors at the loop detector station. This on-time ratio test provided an indication of detector status, e.g., sensitivity setting⁴. Chen and May found pulse breakup events and surmised that the breakups might be caused by the loop detector’s sensitivity setting being too low. In addition, they found unexpected detector actuations in their data reportedly due to lane change maneuvers over the loop detectors, splashover, and phantom actuations that did not appear to be due to any vehicles. Coifman (1999) presented a microscopic method utilizing the redundancy of a pair of loops to assess the performance of dual loop detectors and to identify detector errors; namely, that during free flow conditions the on-times for a given vehicle from each detector in the pair of loops should be virtually identical regardless of vehicle length. The method detected a chronic hanging-on problem and crosstalk⁵ problems. Coifman and Dhoorjaty (2004) developed eight detector validation tests using

⁴ The given loop detector installation in the pavement will impact how responsive the detector is to passing vehicles. To balance these physical variations, the loop sensor cards typically have a user selectable sensitivity setting. The given loop detector will yield poor performance if the sensitivity setting is not well matched to the physical loop’s responsiveness.

⁵ Crosstalk is an erroneous detection arising from electromagnetic coupling in the lead-in wires or the loop detector sensors.

microscopic data to identify various errors both at single and dual loop detectors. That work specifically classified errors into seven groups: the rising edge being premature, the falling edge being premature, the rising edge being delayed, the falling edge being delayed, pulse breakup, missed vehicle, and wrong detection. Some of these tests may catch the secondary impacts of pulse breakup without explicitly looking for breakup events (e.g., the feasible range of headway and on-time, or cumulative distribution of vehicle lengths). Neelisetty and Coifman (2004) developed a mode on-time test as one measure of loop detector performance and Coifman and Lee (2006) refined it. The test calculates the most common on-time over a day. Assuming most vehicles are free flowing passenger cars, this mode on-time should fall within a small range. The test indirectly detects an inappropriate loop detector sensitivity setting. Additionally, minimum on-time and maximum on-time tests were applied to catch extreme errors due to pulse breakup and the detector “sticking-on”. Coifman (2006a) re-implemented the mode on-time test, using the median on-time rather than the mode, and found similar results. Appendix A reviews the median on-time test. Cheevarunothai et al. (2007) developed an algorithm to improve the quality of dual-loop truck data so as to identify and correct detector problems such as pulse breakups, crosstalk, and a difference of sensitivity between the pair of loops in a dual loop detector. Pulse breakup detection simply used a short time headway as the indicator of a pulse breakup. When traffic is congested, the resulting short time headway due to a pulse breakup will frequently exceed the static thresholds used by Cheevarunothai et al. to find pulse breakup events.

1.3 Overview

The remainder of this document is organized as follows. Chapter 2 presents an overview of loop detectors, explaining how both the microscopic measurements (e.g., on-times) and macroscopic aggregations (e.g., flow and occupancy) are made. The chapter also presents the process of collecting and producing the ground truth data used for developing and validating the algorithms to identify splashover and pulse breakup errors. Since a splashover event could give rise to a pattern that looks like a pulse breakup event, the study develops the splashover detection algorithm first, then the pulse breakup detection algorithm second. Chapter 3 begins by reviewing the characteristics of splashover revealed from the ground truth data. Then, the splashover detection algorithm to identify a loop detector exhibiting chronic splashover problems is developed. The chapter closes with an evaluation of the algorithm at many detection stations. Chapter 4 introduces the nature of pulse breakup and the limitations of previous research on detecting pulse breakup. A pulse breakup detection algorithm is developed for single loop detectors. Once more, the chapter closes with an evaluation of the algorithm at many detection stations. Finally, Chapter 5 presents the conclusions of this research and recommendations for further research.

2 DATA DESCRIPTION

The chapter introduces the data sources used to develop the splashover and pulse breakup detection algorithms. First, the chapter reviews the pertinent details of single loop detector and dual loop detector operation, reviewing how both the microscopic measurements and macroscopic aggregations are made. Then, the focus of this chapter shifts to the ground truth data used to develop and validate the error detection algorithms.

2.1 Loop detector overview

Typically a loop detector consists of several turns of wire embedded in the pavement (the physical loop), connected via a lead-in cable to a sensor card in the controller cabinet. The sensor card looks for a change in the loop's inductance, indicating the presence (or absence) of a vehicle and reports the resulting state to the controller. As noted previously, there are two common types of loop detector deployments: single and dual loop detectors. Single loop detectors provide flow and occupancy, but cannot measure speed. Dual loop detectors provide all of the measurements available from single loop detectors as well as enabling direct speed measurement from the traversal time between the given pair of loops. The rest of this section presents methods to calculate measurements from both single loop detectors and dual loop detectors.

2.1.1 Single loop detectors

Figure 2.1 shows the time-space diagram of a vehicle passing over a single loop detector and at the bottom of the figure, the detector response. The detector response has two states: “off” indicating that there is no vehicle on the loop detector and “on” indicating that a vehicle is occupying on detection zone. The effective detection zone (DZ) indicates the area along the roadway in which the loop responds to the presence of vehicles. The size of the detection zone depends not only on the physical dimensions of the loop but also on the sensitivity of the loop detector (both due to the responsiveness of the detector installation and the sensitivity of the sensor card)⁶. The higher the sensitivity, the larger detection zone,

⁶ See Appendix A for further details about loop detector sensitivity.

and in any case the zone can potentially be larger or smaller than the physical loop itself. Typically a loop detector’s sensitivity is not known, so by extension, the exact size of the detection zone is not known.⁷ Note that throughout the remainder of this document, unless otherwise specified, “detection zone” is used to refer to the effective detection zone after accounting for these variables. As shown in Figure 2.1(b), a single loop detector records two transitions, “turning-on” and “turning-off” for each vehicle that passes over it (called a “rising transition” and a “falling transition”, respectively, in this document), yielding a “pulse” that represents the vehicle actuation. In the absence of detector errors, passage of a vehicle is manifest as a single pulse and each pulse corresponds to a vehicle. Of course detector errors can disrupt this one-to-one relationship, as will be discussed more below.

Aggregating many pulses together, flow, q_i , in sample period i is defined as the number of vehicles per unit time that pass over the given loop detector during the sample period and is given by Equation 2.1. In practice n_i is set to the number of pulses during the corresponding period. However, some detector errors can cause a discrepancy between the true vehicle count and measured pulse count, and thus, flow could be underestimated or overestimated.

$$q_i = \frac{n_i}{T} \tag{2.1}$$

where,

n_i = number of vehicles that pass the detector during sample period i ,

T = duration of the sampling period.

The duration during which the k -th vehicle occupies a loop detector is called the detector on-time, denoted OnT_k in this work, and is shown in Figure 2.1. Occupancy (occ_i), the total percentage of time the detector occupied by vehicles in sample i , is given by Equation 2.2. In practice OnT_k is the difference between the time of a falling transition and the time of the preceding rising transition. However, many detector errors can degrade the accuracy of this measurement, e.g., the aforementioned errors impacting flow. Because on-time takes the difference in times of two events, occupancy is subject to additional sources of potential errors, e.g., a high or low sensitivity of the loop detector will lead to a systematic error in occupancy. Note that the conventional fixed period sampling approach of Equations 2.1-2.2 also

⁷ Technically, a loop detector’s sensitivity also depends on the physical characteristics of the passing vehicle itself and its location relative to the loop. But measuring these variations are at present beyond the resolution of conventional loop detectors and as is commonly done in the literature, we focus on the average impacts.

introduces noise when OnT_k straddles the boundary between sample periods. The on-time is typically split proportionately between the two samples but the vehicle's passage only contributes to the flow in one sample or the other.

$$\text{occ}_i = \frac{\sum_{k \in i} \text{OnT}_k}{T} \quad (2.2)$$

Assuming vehicle lengths and speeds are uncorrelated, speed from a single loop detector is commonly estimated by Equation 2.3⁸: As shown in Figure 2.1, the effective vehicle length (L) includes the vehicle's physical length (L^P) and the length of the effective detection zone, i.e., $L = L^P + \text{DZ}$. Throughout the remainder of this document, unless otherwise specified, "vehicle length" refers to effective vehicle length. From Equation 2.1 and 2.2, flow (q_i) divided by occupancy (occ_i) corresponds to mean on-time in sample period i . If the true but unmeasured mean effective vehicle length, L_{mean} , for sample i is consistent with \tilde{L}_{mean} , then Equation 2.3 should provide a good estimate. However, this approach fails to account for the fact that length changes from vehicle to vehicle, and hence L_{mean} changes from sample to sample. As noted in Coifman et al. (2003), if the discrepancy between L_{mean} and \tilde{L}_{mean} is large, the inconsistency will lead to a poor estimate of speed.

$$\hat{v}_i = \frac{\tilde{L}_{\text{mean}} \times q_i}{\text{occ}_i} \quad (2.3)$$

where,

\hat{v}_i = estimated space mean speed of sample period i ,

\tilde{L}_{mean} = assumed constant mean effective vehicle length.

A new aggregation methodology to estimate speed from a single loop detector was introduced in Coifman et al. (2003) to improve the consistency between assumed constant vehicle length and on-times, as shown in Equation 2.4. The median on-time is less sensitive to outliers in the sample, such as from long vehicles, compared to the mean on-time, so the true but unmeasured L_{median} should generally be more stable than L_{mean} from sample to sample. Indeed, as shown in Coifman et al. (2003), Equation 2.4 greatly

⁸ See, e.g., Coifman (2001) for a derivation of this commonly used estimation.

reduces the speed estimation errors relative to Equation 2.3. In this research we use Equation 2.4 to estimate speeds from single loop detectors.

$$\hat{v}_i = \frac{\tilde{L}_{\text{median}}}{\text{median}(\text{on-time}_i)} \quad (2.4)$$

where,

$\text{median}(\text{on-time}_i)$ = median of all on-times observed in sample period i ,

$\tilde{L}_{\text{median}}$ = assumed constant median effective vehicle length.

2.1.2 Dual loop detectors

A dual loop detector consists of two loop detectors spaced a fixed distance apart (typically on the order of 20 ft). The dual loop detector provides all of the measurements available from single loop detectors, while also overcoming the need to estimate speed. For this speed measurement, when a vehicle passes over a dual loop detector the upstream detector is activated and then the downstream detector. Figure 2.2 shows the time-space diagram of a vehicle passing over a dual loop detector and the detector responses. In the absence of detection errors, a passing vehicle gives rise to a single pulse at each of the loop detectors and a pulse at one loop detector should be uniquely matched to a single pulse at the other. In reality there will be unmatched pulses and the process of finding the matches is called “pulse matching”. Pulse matching may be as simple as matching a pulse at the downstream detector to the most recent pulse at the upstream detector⁹ or it may include many complicated steps to ensure a unique one-to-one match. After pulse matching, Figure 2.2(b) shows the measurements at a dual loop detector when a vehicle passes over it, where RT_u and RT_d denote the times of the rising transitions, FT_u and FT_d denote the times of the falling transitions of the pulses (subscripts denote which loop detector, u/d for upstream/downstream). OnT_u and OnT_d indicate the on-time that the given loop detector was occupied by a vehicle. Dual loop traversal time (TT_r and TT_f) is defined as the difference between the rising transitions, i.e., $TT_r = RT_d - RT_u$, or the falling transitions, i.e., $TT_f = FT_d - FT_u$, between upstream and downstream loop detection zones.

Speed is calculated from the effective loop spacing (denoted L_D in the figure) and traversal time that it takes for the vehicle to travel from the upstream loop detector to the downstream loop detector via

⁹ Potentially allowing an upstream pulse to be matched to several downstream pulses or giving rise to an unfeasibly fast speed.

Equation 2.5. The space mean speed for a sampling period is taken from a harmonic average of individual vehicles' speeds.

$$\begin{aligned} v_r &= \frac{L_D}{TT_r} \\ v_f &= \frac{L_D}{TT_f} \end{aligned} \tag{2.5}$$

2.2 Data sources

2.2.1 Loop detector data

Individual vehicle actuation data were collected from the 65 loop detector stations in the Columbus Metropolitan Freeway Management System (CMFMS) (Coifman, 2006a), sampled at 240 Hz. These stations include 658 mainline loop detectors and are shown in Figure 2.3. In detail, the 46 detector stations on the I-70/I-71 corridor were installed during the Phase I deployment of the CMFMS, completed in 2001. These stations include 390 mainline loop detectors. Another 19 loop detector stations were installed on SR 315, I-270, I-70, and I-670 during the Phase II deployment of the CMFMS, completed in 2006. These Phase II stations include 268 mainline loop detectors. In addition to the Phase II loop detector stations, another six detector stations were equipped with RTMS. Roughly 90% of Phase II detector stations have dual loop detectors, while only 35% of the Phase I detector stations have dual loop detectors. But the Phase I detector stations are at a much higher density than the Phase II stations. In most of the Phase I corridor there is one dual loop detector station every mile, with two single loop detector stations between the dual loop detector stations.

2.2.2 Ground truth data

This research uses microscopic loop detector data with concurrent video ground truth to develop and validate the various algorithms to identify detector errors. The task of collecting and extracting the ground truth data consists of the following steps: recording video of vehicles passing over the loop detector station and the concurrent detector actuations, digitizing the video, extracting the individual frames, synchronizing time between the loop detector data and video data, stepping through all of the loop

detector actuations individually, loading the specific frame corresponding to a given loop detector actuation, and manually classifying each detector actuation.¹⁰

Most of the video comes from the existing close circuit television (CCTV) traffic surveillance cameras in the CMFMS. At the time of the study there were 99 CCTV cameras in the CMFMS, with 74 of them adjacent to freeways¹¹. After reviewing the CCTV views, we found the set of cameras that provide good views across all lanes for one or both directions at one or more detector stations. The CCTV cameras were recorded with a videocassette recorder (VCR) in the Columbus Traffic Management Center (TMC). Several additional detector stations that are not readily viewed from the CCTV camera are included in the ground truth, in these cases a video camcorder was set up on an overhead bridge or the side of the freeway. Video was collected at a total of 15 detector stations (comprising 22 directional locations), the details of which are enumerated below. Figure 2.4 shows typical views (a) of station 56 from a CCTV camera, and (b) of station 41 eastbound from a video camcorder set up on an overpass (Woodcrest Rd in this case).

Both sources of video data were recorded in analog, thus the need for the digitizing step. The digital video was stored in Audio Video Interleave (AVI) format and the extracted images were stored in Joint Photographic Experts Group (JPEG) format at 30 frames per second. A purpose built software ground truthing tool with a graphical user interface (GUI)¹² was developed in MATLAB to semi-automate the process of generating ground truth data. The GUI interface can step through the detector data in a given lane and display both the time series detector data for a few seconds before and after the given actuation along with the frame corresponding to the actuation time (this GUI was inspired by VideoSync, Caltrans (2007)). If necessary, the user can step forward or backwards in time to review the vehicle. The tool allows the user to manually record types of vehicles and any detector errors from the direct comparison between concurrent detector and video data. The user indicates whether any errors were evident for the given actuation and if so, what the error was (pulse breakup; splashover; or other event such as a vehicle changing lanes). The GUI also allows the users to classify the vehicle as:

¹⁰ Obviously this process will completely miss a vehicle that does not actuate the detectors. By definition, such errors cannot be found in the time series detector data. These extreme errors are beyond the scope of the present work since the vehicle does not register a single actuation much less two actuations it cannot be a splashover or pulse breakup event. However, at a few stations we also used an independent trigger from the video to catch vehicles that passed without any detector actuation and at these locations we found that it was rare that the detectors missed a vehicle completely.

¹¹ Personal discussion with *Matt Graf* in Ohio Department of Transportation (2008)

¹² See Appendix B for a more in depth discussion of the ground truthing tool

motorcycle, short vehicle (SV), medium vehicle (MV), or long vehicle (LV). In this work LV denotes multiple unit trucks, while SV denotes cars, vans, and pick-up trucks, all without a trailer. Vehicles not included in SV, LV, and motorcycles are classified as MV, including large vans, buses, most single unit trucks, and most SV pulling a trailer. For the sake of understanding vehicle classes adopted from the ground truth data, Table 2.1 shows how our vehicle classes map to the 13 FHWA axle-based vehicle classification scheme (adapted from TxDOT, 2010). As the user enters the classification, the GUI jumps to the next detector actuation in that lane. This process was repeated for each visible lane during the entire time period of collected video data.

Table 2.2 summarizes the concurrent video data used to generate the ground truth data in this research. Approximately 21 hours of directional traffic data were ground truthed from 37 different data sets, collected at 15 locations (comprising 22 directional locations) and an average of 3.3 lanes per set. A total of 78,785 detector actuations were manually ground truthed (in the absence of a detector error, there should be exactly one actuation per vehicle). Out of these data, 9 sets include congestion, spanning 4.5 hrs and 20,576 detector actuations. The stations were selected strictly on the basis of whether they were safely viewable; the specific dates and times were chosen arbitrarily to fit our availability, though in some cases prior to the video data collection we deliberately sought periods that typically exhibited recurring congestion.

Table 2.1, Our vehicle classification in the ground truth data, relative to the conventional FHWA axle-based vehicle classification scheme (adapted from Texas DOT, 2010)

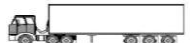
FHWA Vehicle Classification			Vehicle class in the study
Class Group	Examples	Description	
1		Motorcycle	Motorcycle
2 ^a		Passenger cars	Short vehicle
2 ^b		Passenger cars with 1 & 2 axle trailers	Medium vehicle
3 ^a		Pick-ups & vans	Short vehicle
3 ^b		Pick-ups & vans with 1 & 2 axle trailers	Medium vehicle
4		Buses	
5		2 axle single units	
6		3 axle single units	
7		4 or more axle single units	
8		4 or less axle single trailers	Long vehicle
9		5 axle single trailers	
10		6 or more axle single trailers	
11		5 or less axle multi-trailer	
12		6 axle multi-trailer	
13		7 or more axle multi-trailer	

Table 2.2, Information of concurrent video data used to generate the ground truth data.
 NB=northbound, SB=southbound, EB=eastbound, and WB=southbound.

Traffic conditions	Station number	Direction	Date	Number of lanes	Start time (hh:min)	End time (hh:min)	Duration of time (hh:min)
Free flow	2	NB	March 9, 2009	4	17:21	17:50	0:29
	3	NB	March 17, 2008	4	10:57	11:20	0:23
	3	SB	April 18, 2008	4	15:55	16:55	1:00
	3	NB	June 17, 2009	4	10:21	10:51	0:30
	3	SB	June 17, 2009	4	10:21	10:51	0:30
	4	NB	September 9, 2008	4(2)*	16:55	17:15	0:20
	4	SB	March 17, 2008	4	10:15	10:35	0:20
	6	NB	April 18, 2008	3	15:55	16:55	1:00
	9	NB	June 5, 2006	3	12:20	14:20	2:00
	9	SB	June 5, 2006	3	12:20	14:20	2:00
	9	NB	June 17, 2009	3	10:05	10:41	0:36
	9	SB	June 17, 2009	3	10:05	10:41	0:36
	15	NB	March 10, 2009	3	17:18	17:47	0:29
	18	NB	March 9, 2009	3	08:24	08:57	0:33
	19	NB	March 17, 2008	3	09:25	09:40	0:15
	31	NB	November 21, 2008	4	10:35	11:05	0:30
	38	EB	August 29, 2008	3	15:05	15:25	0:20
	38	WB	September 9, 2008	4	12:05	12:25	0:20
	41	EB	September 9, 2008	2	11:00	11:35	0:35
	43	EB	September 2, 2008	3	08:50	09:15	0:25
	43	WB	September 2, 2008	3	08:50	09:15	0:25
	56	EB	September 3, 2008	3	16:40	17:25	0:45
	56	WB	November 21, 2008	3	09:00	09:40	0:40
56	WB	June 17, 2009	3	09:33	10:03	0:30	
102	EB	March 10, 2009	3	17:05	17:20	0:15	
104	EB	March 17, 2008	3	16:00	16:10	0:10	
104	WB	March 12, 2009	3	17:00	17:18	0:18	
104	EB	June 26, 2009	3	13:14	13:29	0:15	
Congested	3	NB	March 21, 2008	4	16:35	16:50	0:15
	3	NB	April 18, 2008	4	15:55	16:55	1:00
	4	NB	September 9, 2008	4(2)*	17:15	17:55	0:40
	9	SB	April 7, 2008	3	07:50	08:10	0:20
	41	EB	March 12, 2009	2	16:40	17:06	0:26
	43	EB	March 12, 2009	3	17:07	17:48	0:41
	56	WB	September 3, 2008	3	16:40	17:25	0:45
	102	EB	March 10, 2009	3	16:46	17:05	0:19
104	EB	March 17, 2008	3	16:10	16:20	0:10	

*Two out of four lanes at station 4 northbound were not operational while the video data were collected.

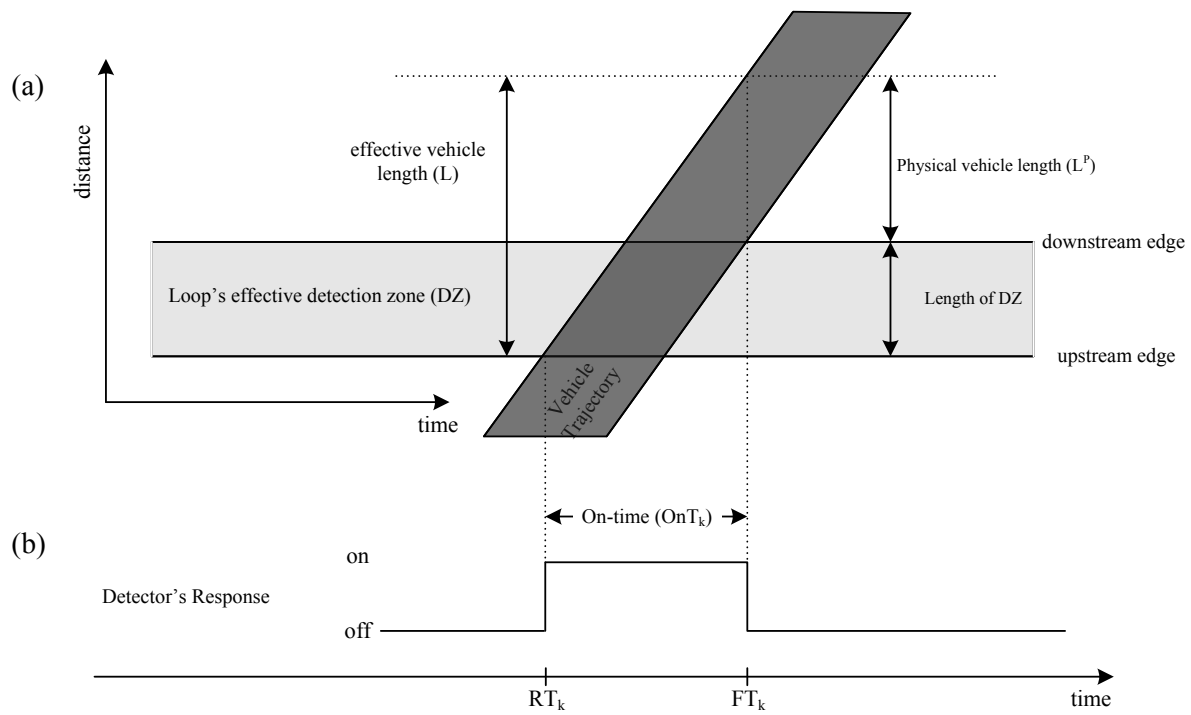


Figure 2.1, A vehicle passing over a single loop detector, (a) effective detection zone and vehicle trajectory in time space plane and (b) the associated turn-on and turn-off time (adapted from Coifman and Dhoorjaty, 2004).

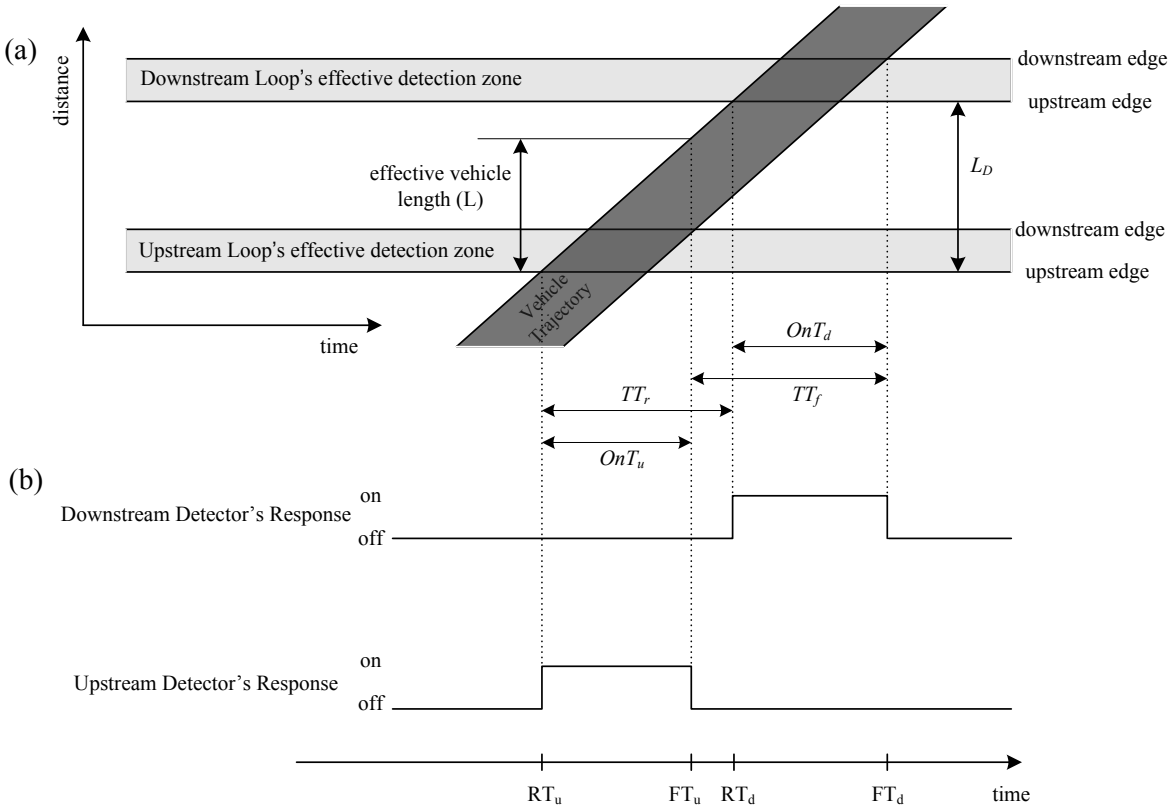


Figure 2.2, A vehicle passing over a double loop detector, (a) the two detection zones and vehicle trajectory in the time space plane and (b) the associated turn-on and turn-off times at each detector. Adapted from Coifman and Dhoorjaty (2004).

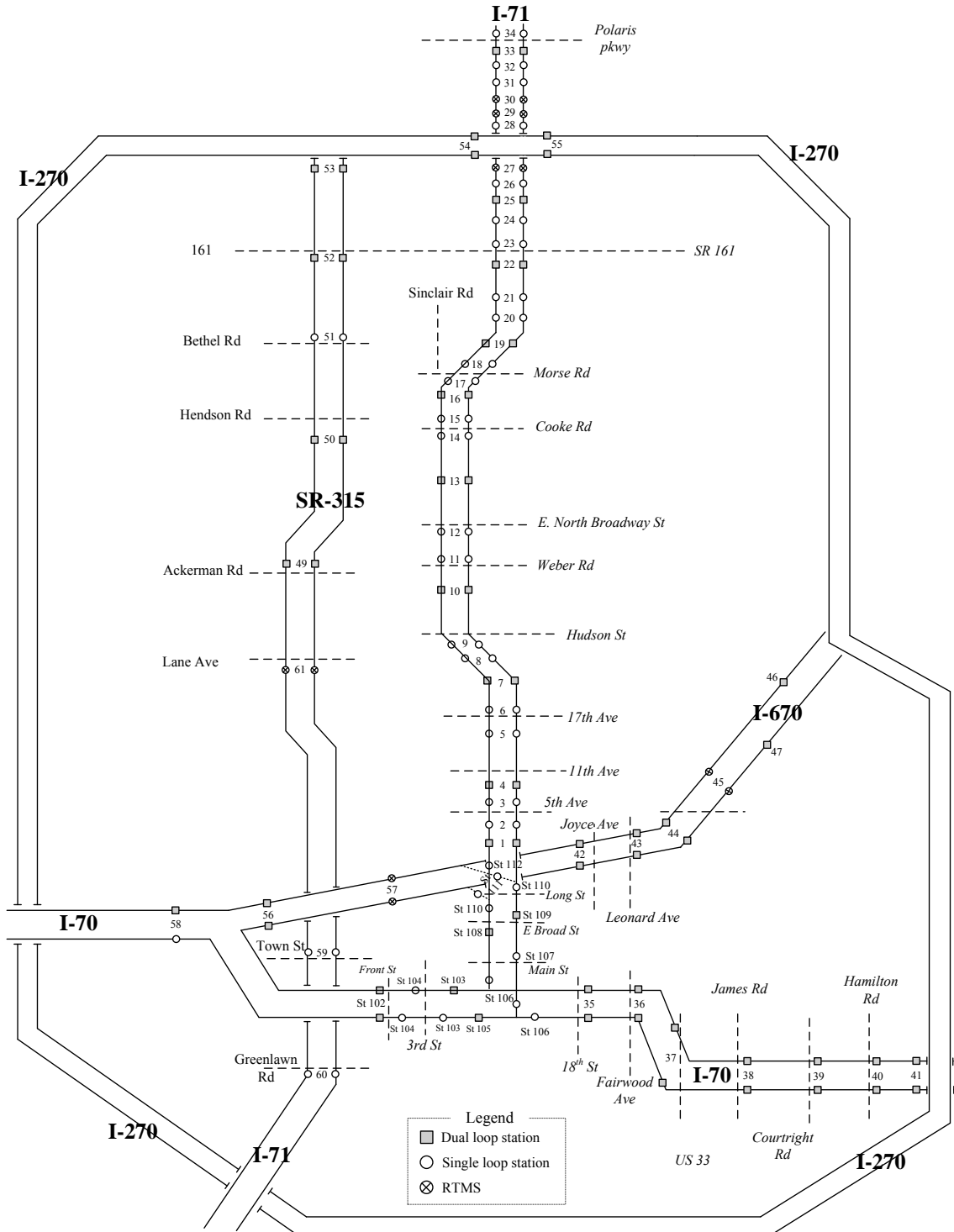


Figure 2.3, A schematic showing the locations of the detector stations in the CMFMS.

(a)



(b)



Figure 2.4, Sample camera views, (a) from a CCTV camera at station 56, and (b) from a video camcorder mounted on an overhead bridge near station 41.

3 AN ALGORITHM TO IDENTIFY DETECTORS EXHIBITING CHRONIC SPLASHOVER

Splashover is the erroneous detection in one lane of a vehicle from an adjacent lane. Typically, when this error occurs the loop detectors in two neighboring lanes record the same vehicle at roughly the same time.¹³ If not caught, the splashover of one vehicle will likely be recorded as two distinct vehicles that almost simultaneously passed over two adjacent loops. The resulting double count can lead to inaccurate measurements, e.g., higher flow and occupancy, and in general a splashover event degrades the accuracy of the loop detector data. The splashover problem has not received much attention in previous research due to the difficulty of identifying its occurrence, i.e., any given splashover event is usually indistinguishable from the non-error event of two vehicles passing the detector station at the same time. According to the Traffic Detector Handbook (Klein et al., 2006) splashover usually occurs when the sensitivity level of a loop detector is set too high or a loop detector is too close to an adjacent lane. While the handbook offers some advice for fixing this problem, it does not offer characteristics of detector data with splashover or a means of detecting the presence or absence of splashover in the detector data.

First, this chapter examines the nature of splashover from loop detector data with concurrent video-recorded ground truth data. Next it presents an algorithm to automatically find detectors exhibiting

¹³ Note that this work does not distinguish between different mechanisms that would lead to an erroneous detection in one lane of a vehicle from an adjacent lane. Unless otherwise noted, all such events are collectively referred to as "splashover" in this work. Though technically there are different mechanisms that can yield the same error in the data stream. True splashover event occurs when an other-lane vehicle passes through the fringes of the detection zone in the source-lane, causing the source-lane loop detector to actuate. Some forms of crosstalk can yield a similar erroneous actuation, but it is due to electromagnetic coupling in the lead-in wires or the loop detector sensors. Using just the pulse stream from the loop detectors it is impossible to distinguish between these two sources, but the result is the same, a vehicle in one lane is erroneously detected in another lane. Both problems require a technician to visit the controller, but once the technician is there, an additional step may be necessary to determine which problem is the source of the errors.

chronic splashover problems.¹⁴ The chapter closes with an evaluation of the algorithm at many detection stations.

3.1 *The nature of splashover*

Consider the hypothetical example of a splashover event on a two-lane freeway in Figure 3.1. The time-space diagram shows a vehicle passing in lane 2. A schematic of the roadway is shown coincident with the distance axis. For this vehicle the lane of travel has a larger detection zone, DZ_2 than the splashover lane, DZ_1 . The resulting pulses from both lanes are shown below, coincident with the time axis. The loop detector in lane 1 erroneously responded to this lane 2 vehicle for an on-time denoted OnT_1 while the valid actuation in lane 2 had an on-time of OnT_2 . In general, the resulting double count can lead to inaccurate measurements, e.g., higher flow and occupancy. A loop detector's sensitivity is inversely proportional to the square of the distance to the vehicle (Klein et al., 2006). So typically DZ_1 for the splashover event should be smaller than DZ_2 for the valid vehicle actuation. Thus, a pulse arising from splashover in one lane should usually be bounded by the valid pulse from the vehicle in its lane of travel, e.g., the pulses at the bottom of Figure 3.1 and we call these *suspected splashover events*. But as will be discussed shortly, a difficulty arises because any given splashover event in the data stream is usually indistinguishable from the non-erroneous, *valid concurrent actuations* of two vehicles passing the detector station at the same time.

To verify the preceding hypothetical examples of splashover, we use loop detector data with concurrent video-recorded ground truth data, as per section 2.2. Figure 3.2 shows three examples of actual splashover in lane 1 at a single loop detector station (station 104 eastbound). Figure 3.2(a) shows the pulses from all three lanes as the detectors respond to vehicles (throughout this example lane 1 is at the bottom and lane 3 is at the top). According to the concurrent video frames, Figure 3.2(b-d), all three of the pulses in lane 1 were erroneous. First, in Figure 3.2(b), a vehicle passing in lane 2 is also recorded in lane 1 in the absence of any vehicles in lane 1. We term this event a “*unique splashover*” because it only involved one vehicle. In contrast, Figure 3.3(c-d) both show examples where the on-time of a short vehicle in lane 1 are extended due to splashover from lane 2 (in both cases the on-times are roughly twice as long as they should be for the given lane 1 vehicle). We term events like these as “*combined splashover*” because an otherwise unique splashover merged with a valid actuation. This distinction between the two types of splashover appears to be novel, when splashover is discussed in the literature it

¹⁴ From the algorithm we only expect lane pairs with chronic splashover problems (typically greater than about 2% of actuations) will be identified. In other words, a pair of lanes that have occasional splashover events will not be found.

is usually limited to what we are calling unique splashover. We are not aware of any references to combined splashover. The difference between the two forms depends simply on whether or not a concurrent vehicle happens to be in the target lane. Since the time gaps between vehicles are typically much larger than the on-times during free flow, unique splashover is more common in free flow traffic.

From 10 min of video at this station we observed 164 vehicles in lane 1 and 347 in lane 2. Reviewing the loop detector data for lane 1, all of the lane 1 vehicles were detected, as well as 92% of the lane 2 vehicles via splashover¹⁵. Of these actual splashover events, 273 are unique splashover and 45 are combined splashover. In terms of macroscopic measurement errors, flow in lane 1 would be over-counted by the number of unique splashover events (66% in this case). While the combined splashover events do not impact flow, both types of splashover will lead to an erroneous increase in occupancy via Equation 2.2 because the detector reports that it is on for a longer cumulative time (i.e., $\sum \text{OnT}_1$) than it is actually occupied by vehicles.

Figure 3.3(a) plots the on-time for the erroneous splashover events seen in lane 1 versus the given vehicle's valid on-time seen in lane 2, the vehicle's lane of travel (i.e., OnT_1 versus OnT_2 in the notation from Figure 3.1). The dashed line shows the set of points where the two on-times are equal. As expected, unique splashover errors tend to fall below the reference line while most of the combined splashover errors fall above the reference line. Figure 3.3(b-c) tabulate the cumulative distribution function (CDF) of the difference of on-times between the two lanes for unique splashover and combined splashover, respectively. A negative value indicates that the splashover on-time is shorter than that of the valid pulse.

For unique splashover events the on-time difference ranges between $-13/60$ and $+3/60$ seconds. About 90% of the unique splashover pulses have shorter on-times in lane 1 than the corresponding valid pulses in lane 2, while the on-times of the remaining unique splashover events are little longer than the on-times from the corresponding valid pulses in the other lane. According to the concurrent video data, the difference of on-times appears to be related to the location of vehicles in lane 2 relative to the detection zone of lane 1. For example, Figure 3.4 shows a video frame corresponding to the case where the difference of on-times between valid detection and splashover is (a) $+1/60$ seconds, (b) $-5/60$ seconds, and (c) $-11/60$ seconds. The closer the vehicle is to the lane line in this figure, the more positive the on-time difference. These trends are typical of those observed throughout this sample.

¹⁵ We deliberately chose station 104 eastbound for this example because it had the highest rate of splashover among the 94 lane pairs studied and it happened to offer a concise example illustrating both unique splashover and combined splashover.

For a combined splashover events the on-time difference ranges between $-6/60$ and $+24/60$ seconds. About 90% of combined splashover pulses in lane 1 have longer on-times than the corresponding valid pulses in lane 2. The remaining four combined splashover events have a shorter on-time than the corresponding valid pulses in lane 2. According to the concurrent video data, these four combined splashover events occurred when a short vehicle in lane 1 and a long vehicle in lane 2 passed over two adjacent loop detectors at roughly same time. Figure 3.5 shows an example of a combined splashover with a shorter on-time than the valid detection in lane 2. In this case it appears that the splashover event from lane 2 completely bounds the valid pulse in lane 1.

The pulse from each detector actuation is defined by a rise time (RT) and fall time (FT). Comparing these across the two lanes, the difference in rising transition times (DRTT) and the difference in falling transition times (DFTT) between a splashover pulse in lane 1 and the valid pulse in the vehicle's lane of travel, lane 2, are used to quantify the characteristics of splashover. Figure 3.6(a) illustrates the various relationships between DFTT and DRTT. The plane is divided into four regions (numbered I to IV, counterclockwise from top right) with boundaries at zero seconds on both axes. Hypothetical examples of the relationship are shown between the splashover pulse in lane 1 and the valid pulse in lane 2 for each region. So if the lane 1 pulse begins before the lane 2 pulse, the result will fall to the left of the vertical division line (region II or III), otherwise it will fall to the right of the division line (region I or IV). One would expect most unique splashover events from lane 2 to lane 1 to be like Figure 3.1 and fall in region IV, while the combined splashover events should fall in regions I and III. Using the data from Figure 3.3, Figure 3.6(b) shows the relation of DFTT and DRTT between each splashover actuation in lane 1 and the corresponding valid detection in lane 2 at station 104 eastbound. Within each region the brackets tally the total number of observations of [unique splashover, combined splashover] seen. As expected, 86% of unique splashover events (236 out of 273) fall in region IV. The concurrent video data reveals that the unique splashover observed in Region II occurred when the lane 2 vehicle traveled much closer to the boundary with lane 1 than the vehicles observed in Region IV. Since a loop detector's sensitivity is inversely proportional to the square of the distance to the vehicle (Klein et al., 2006), typically the detection zone for the splashover actuation (DZ_1 in Figure 3.1) should become larger and the detection zone for valid vehicle actuation (DZ_2 in Figure 3.1) should become smaller as a lane 2 vehicle gets closer to the lane boundary. Meanwhile, 82% of combined splashover events are observed in Region I (18 out of 45) and III (19 out of 45). Not surprisingly, the concurrent video data reveal that for the combined splashover events in region I a vehicle in lane 2 causing splashover is followed by a vehicle in lane 1 (e.g., Figure 3.2(c)), while in region III a vehicle in lane 1 is followed by a vehicle in lane 2 causing splashover (e.g., Figure 3.2(d)). Combined splashover events in region II and region IV usually occurred when two

vehicles passed over loop detectors at roughly same time. In this case, about 76% of all splashover events are bounded by the valid pulses from the vehicle's actual lane of travel (e.g., Figure 3.1), consistent with the fact that unique splashover is more frequent than combined splashover in free flow traffic. These results are typical of the ground truth data from other stations with splashover during free flow conditions. These relationships are the starting point for developing the splashover detection algorithm in the next section.

3.2 Development of an algorithm to identify loop detectors with splashover

As seen in Figure 3.6, a splashover pulse is usually bounded by the valid pulse from the actual lane of travel. This feature of splashover is used as the starting point for the splashover detection algorithm. A pair of loop detectors in adjacent lanes is selected for testing; one loop is arbitrarily taken as the "source lane", and for the test is assumed to provide an accurate record of vehicle actuations in that lane. The other loop is taken as the "target lane," and is evaluated as to whether or not it may be recording splashover pulses in response to vehicles in the source lane. The algorithm checks each pulse in the source lane to see if it spans a pulse in the target lane (i.e., falling in region IV in Figure 3.6). Any time the check is true it is considered to be a suspected splashover event and added to the number of suspected splashover events (nSS), e.g., Figure 3.7(a) shows a hypothetical example where indeed the pulse in the source lane, s1, spans a pulse in the target lane, t1. So in this case t1 is suspected of arising from splashover and is added to nSS. The algorithm repeats the process over all pulses in the source lane for the data set (in this study the duration of the ground truth video sequence). The roles of the lanes are exchanged and the process is repeated, then it is repeated for every other pair of adjacent lanes at the station. So like Lang and Coifman (2006), the present work uses the temporal relationships between different detectors to identify errors.

The first two rows of Table 3.1 summarize the actual splashover number (ASn) from the ground truth data and nSS from the algorithm for each pair of adjacent lanes at station 104 eastbound. The three loop detectors at the station have a total of four adjacent lane pairs. First consider the case with lane 2 as the source and lane 1 the target: ASn is 318 and the algorithm reported nSS is 240 in lane 1 from vehicles in lane 2. In this case, all 240 of nSS turn out to be actual splashover events, but in general any given suspected splashover event could be valid concurrent actuations as two vehicles pass simultaneously in adjacent lanes. The rest of the lane pairs have no actual splashover events in this case but the algorithm found a positive nSS for every pair of lanes. According to the concurrent video, all suspected splashover events between lane 2 and lane 3 arise from valid concurrent actuations, but suspected splashover events

with source lane 1 and target lane 2 arise both from valid concurrent actuations in the adjacent lanes and from lane 2 vehicles splashing over to lane 1 and falling into region II in Figure 3.6 (which then appears to be region IV when lane 1 is used as the source lane). Clearly nSS alone is not sufficient to differentiate between lane pairs with and without splashover. The situation is further complicated by the fact that it is not uncommon for a vehicle changing lanes over a detector station to actuate the loop detectors in both lanes, i.e., a detector error of a slightly different nature (see, e.g., Coifman, 2006b). As such, occasional splashover or lane change maneuver errors are within normal tolerance of conventional loop detector stations and such intermittent errors are below the target resolution of the present work.

3.2.1 Expected number of false positives

The task of detecting splashover is complicated by the fact that one cannot differentiate between a given splashover event and valid concurrent actuations using just the detector data. Instead, we estimate the expected number of valid concurrent actuations, i.e., the expected number of false positives (EnFP) in nSS. If vehicle arrivals are independent in the two lanes and there were no splashover events, the frequency of the non-error, valid concurrent actuation events between the two lanes depends on the demand in each of the lanes. When all arrivals in the source lane are shifted by a small time offset of a few seconds relative to the target lane's clock, the demand in the two lanes does not change and in most cases the time-shifted vehicle arrivals in the source lane remain independent of the un-shifted vehicle arrivals in the target lane. So the expected number of valid concurrent actuation events from the target lane for the time-shifted source lane pulse train and the original source lane pulse train is the same if there are no splashover events, but the offset will eliminate the possibility that the given target pulse arose from the same vehicle that caused the given source pulse. Formalizing the process to derive a Conservative Expected number of False Positives (EnFP^C), like nSS before, any time a pulse in the time-shifted source lane pulse train spans a pulse in the target lane then EnFP^C for this lane pair is incremented by one. For example, Figure 3.7(b) revisits the data from Figure 3.7(a), only now it shows the arrival s1 in the source lane shifted by ϵ .¹⁶ In the absence of splashover events, the probability that s1 spans a pulse in the target lane should be the same whether or not it is time-shifted, but any target lane pulses falling within the shifted s1 could not have arisen from the same vehicle that caused s1. In this case, target lane pulse t3 begins within the time-shifted window from the source lane pulse but it is not spanned by the time-shifted pulse, since t3 ends after the time-shifted s1 it would not contribute to EnFP^C. This conservative expected number of false positives is listed in the third row of Table 3.1 and the difference between nSS and EnFP^C

¹⁶ This report arbitrarily sets ϵ to five seconds. As shown in Appendix C, we repeated the analysis for ϵ set to each integer value from 1 to 10 seconds and found similar results.

is tabulated in the fourth row. While the difference is smaller than nSS, all lane pairs still exhibit positive values. Of course both nSS and EnFP^C are random variables with the same expected value, so in the absence of actual splashover events the latter will not always cancel the former. Furthermore, it is possible that the arrivals in adjacent lanes are not completely independent (e.g., drivers may momentarily slow down as they are overtaking a vehicle in an adjacent lane).

So we adopt more liberal definition for EnFP to ensure its expected value is slightly larger than that of nSS when there are no actual splashover events. Instead of requiring the entire pulse in the target lane to fall within the time-shifted source lane pulse, a target lane pulse will be counted in EnFP if the target pulse's rising edge is bounded by the time-shifted source lane pulse (i.e., regions I and IV in Figure 3.6). So pulse t3 in Figure 3.7(b) would contribute to EnFP. The results for the on-going example at station 104 are tabulated in the final two rows of Table 3.1. The liberal definition far outnumbers the suspected splashover that arose in the three lane pairs due to non-splashover events (negative numbers in the final row), but it does not outnumber the true splashover events from source lane 2 to target lane 1. Any lane pairs that have a positive value after subtracting EnFP from nSS are considered to be from a loop detector with splashover.

3.2.2 The adjusted rate of suspected splashover

To illustrate the fundamental ideas, thus far the narrative in this section has talked about the numbers of events (ASn, nSS, and EnFP). The corresponding rate of these events is more practical to work with. We define the Actual Splashover Rate (ASR), Rate of Suspected Splashover events (RSS), and the Expected Rate of False Positives (ERFP) relative to the total pulses in the source lane, N, as follows,¹⁷

$$ASR = \frac{ASn}{N}; RSS = \frac{nSS}{N}; ERFP = \frac{EnFP}{N} \quad (3.1)$$

This process of reducing RSS by ERFP to account for valid concurrent actuations is formalized in Equation 3.2, which is termed Adjusted Rate of Suspected Splashover (ARSS). The primary information from the test is the sign of ARSS, indicating whether RSS exceeds ERFP, i.e., a positive ARSS during free flow traffic is an indicator of chronic splashover. The magnitude of ARSS provides a coarse measure of confidence, but not with sufficient precision for diagnostics since the rate of two vehicles passing in

¹⁷ Note that these rates are all relative to the total number of pulses rather than the total number of vehicles. In practice one could not exclude all of the extra pulses in the source lane arising from splashover (and any other detector errors) without an independent ground truth process.

adjacent lanes simultaneously depends on demand in both lanes, and thus, the magnitude of ARSS is not in itself a fair measure of comparison between lanes (especially if N inadvertently includes many non-vehicle pulses due to a detector error in the source lane). When splashover is found, the underlying hardware or software error needs to be fixed. Often the necessary fix could be as simple as adjusting the loop sensor card's sensitivity setting. However if a fix is not feasible, any applications using the data must recognize that the data contain errors.

$$ARSS = \max \left(\frac{\sum_{i=1}^n \sum_{j=1}^m (P_{ij} - Q_{ij})}{N}, 0 \right) \quad (3.2)$$

where,

$$P_{ij} = \begin{cases} 1, & \text{if } RT_i^S \leq RT_j^T \leq FT_i^S \text{ \& } RT_i^S \leq FT_j^T \leq FT_i^S \\ 0, & \text{otherwise} \end{cases}$$

$$Q_{ij} = \begin{cases} 1, & \text{if } RT_i^S + \varepsilon \leq RT_j^T \leq FT_i^S + \varepsilon \\ 0, & \text{otherwise} \end{cases}$$

and

ARSS= adjusted ratio of suspected splashover between source lane and target lane,

N = total number of pulses in the source lane,

M = total number of pulses in the target lane,

i = i-th pulse in the source lane (i=1, 2, ..., n),

j = j-th pulse in the target lane (j=1, 2, ..., m),

P_{ij} = suspected splashover of pulse j in the target lane matched to pulse i in the source lane (i.e., contribution to RSS),

Q_{ij} = non-splashover of pulse j in the target lane matched to pulse i shifted by the constant delay in the source lane (i.e., contribution to ERF),

ε = constant delay for shifting a pulse in the source lane, set to five seconds in the presented results,

RT_i^S = i-th pulse rising transition time in source lane,

FT_i^S = i-th pulse falling transition time in source lane,

RT_j^T = j-th pulse rising transition time in target lane,

FT_j^T = j-th pulse falling transition time in target lane.

Of course the AARS calculation assumes that a given target and source lane have roughly the same detector sensitivity level. This sensitivity depends on the hardware installation and the settings of the loop sensor cards. If the sensitivity in the target lane is significantly greater than the source lane, it is possible to see an inversion, e.g., most unique splashover events in target lane 1 from source lane 2 fall in region II instead of region IV of Figure 3.6. In which case the algorithm will detect the splashover in the lane pair, but attribute it to the wrong lane.¹⁸

3.3 Optimal application periods

As speeds decrease due to congestion, ERF_P will increase simply because the source lane vehicles reside over the loop detectors for a longer on-time. Since chronic splashover usually arises due to a hardware fault and is non-transient, the present work is meant to be applied during (predominantly) free flow conditions.

There are many ways to ensure predominantly free flow traffic conditions. As noted previously, in this study the period was determined by the duration of the ground truth video sequence. In practice, one can use the macroscopic measures from the detectors to ascertain when conditions are free flowing and then apply the algorithm over several hours within one or more of these periods each day. One could also use time of day, e.g., when evaluating the Columbus detectors without ground truth (not shown), we have found that applying the tests daily during the mid-day period (9:00-15:00) yields good performance.

The free flow restriction will not increase the possibility of a false detection. Though it is possible that some errors may become more pronounced during congestion, e.g., if drivers tend to shift their lane position over the detector in response to vehicles in other lanes. Such a situation can easily arise on a curve, drivers may tend to travel close to the inside lane line if there are no vehicles there, but be more conservative when there is a vehicle in the inside lane. So the algorithm may miss some of the lane pairs exhibiting splashover if the events occur primarily during congestion. If coverage during congestion proves desirable, one might be able to use a rate derived from EnFP^C and examine the distributions of RSS and ERF_P^C sampled over many days.

¹⁸ Fortunately, most such cases of sensitivity errors can be detected via the median on-time test as presented in Appendix A if one wants to ensure that a detected splashover is not attributed to the wrong lane in the pair. In extreme situations when the majority of the pulses at a detector actually arise from splashover, at such an over-sensitive detector it may become difficult for the median on-time test alone to distinguish between low sensitivity and the dominant, erroneous short pulses from splashover. While we have yet to observe such a situation, in these cases the impacts should be readily evident in other metrics (e.g., conventional single loop detector speed estimation) or tests (e.g., Jacobson et al., 1990; or the combined results of our splashover test and median on-time during uncongested low flow periods).

3.4 Evaluation of the algorithm

A total of 21 directional ground truth data sets under free flow conditions from Table 2.2¹⁹ were employed for this evaluation. Four of these directional sets exhibited some degree of actual splashover events, while the remaining 17 data sets did not have any observed splashover events, as enumerated in Table 3.2. All of the congested data sets were excluded from the splashover study.

Reviewing the stations with actual splashover events in greater detail, the total pulses column in Table 3.3 tallies the number of pulses recorded by the loop detector during the period of concurrent video data collection at the given station, while the total vehicles column tallies the corresponding number of vehicles that traveled in the lane as seen in the video. The total number of actual splashover events is reported for the given lane where the vehicle was incorrectly detected (i.e., the target lane) as well as the subtotals for unique splashover and combined splashover. The total pulses do not always correspond to the sum of total vehicles and unique splashovers events, e.g., from the totals in the last row of the table, $3,758 - (3,177 + 473)$ leaves 108 extra pulses. The concurrent video showed that these remaining pulses are due to vehicles changing lanes and being counted in both lanes.²⁰ The source and target lanes giving rise to the splashover are shown in the second to the last column. The final column shows the ASR. For instance, target lane 3 at station 38 westbound has 115 unique splashover events and 2 combined splashover events, all of which are caused by vehicles traveling in source lane 2. So this lane pair has an ASR of $117/242$, equivalent to 48.3 %, as shown in the table.

Lane 1 at station 104 eastbound has the highest ASR (91.1%), and lane 2 at station 38 westbound has the lowest non-zero ASR (1.2%). There was a total of 537 actual splashover events from the four detector stations, 473 of which (88%) are unique splashover. So 473 out of 3,758 total pulses resulted from vehicles being counted a second time across these four stations, i.e., 12.6% over-counting due to splashover.²¹ As previously mentioned, while the combined splashover events do not impact flow, both types of splashover will lead to an erroneous increase in occupancy.

¹⁹ There are seven more directional ground truth sets under free flow conditions in Table 2.2. Of these, one is excluded because half of the detectors were not operational during the collection and the remaining six are used shortly for the after portion of the "Brief before and after study of loop detector sensitivity" in Sections 3.4.3 and 4.6.

²⁰ One might view these lane change maneuver errors as a milder manifestation of the splashover error. Furthermore, none of the four data sets with splashover exhibited any other extra non-vehicle pulses during the period of study, e.g., pulse breakup events, though some of the 17 other data sets did.

²¹ The total over-counting rate rises to 15.5% if one also includes the 108 vehicles counted in two lanes during lane change maneuvers.

3.4.1 Application and results

Table 3.4 presents the results of the splashover detection algorithm, ARSS from Equation 3.2²² applied to the loop detector data for the periods with ground truth. Note that all recorded pulses at a given detector, including any non-vehicle pulses due to detector errors, are used as input to the algorithm when generating the results reported in Table 3.4. Of the 94 adjacent lane pairs from 68 loop detectors at 15 loop detector stations, a total of seven lane pairs returned a positive ARSS. Five of these seven lane pairs exhibited actual splashover events (as per Table 3.3) while two did not, and the algorithm failed to identify two lane pairs with actual splashover events. Appendix E compares the daily median on-times at the seven adjacent lane pairs with actual splashover and verifies that the errors cannot be explained by an extreme difference of loop detector sensitivity. Employing the ground truth data from Table 3.3, the seven lane pairs that exhibited actual splashover are shaded in Table 3.4. The two lane pairs with actual splashover events that the algorithm failed to identify are target lane 2 from source lane 1 at both station 38 westbound and at station 41 eastbound. Looking at these two lane pairs in Table 3.3, they had a relatively small ASR, i.e., 1.2% in target lane 2 at station 38 westbound and 3.3% in target lane 2 at station 41 eastbound. In both cases the total pulses in the target lane was significantly greater than the total pulses in the source lane, i.e., the number of pulses in target lane 2 is more than 140% of source lane 1 in the station 38 westbound data set, and more than 150% in the station 41 eastbound data set, thereby increasing the chance of finding non-splashover events that contributed to ERFp. In the end, the RSS at each of these two lane pairs was exceeded by ERFp. These two cases represent the threshold of "chronic splashover" that the algorithm can detect. In contrast, target lane 3 at station 56 westbound also has a relatively low ASR (3.0%) but the algorithm correctly identifies this lane pair because the number of pulses in the target lane 3 is about 19% of source lane 2 and thus, the ERFp is small in this case.

Moreover, the algorithm correctly classified all but two detector pairs without splashover, the two errors being target lane 4 from source lane 3 at both station 2 northbound and station 31 northbound. Both of these failures occurred immediately upstream of two different lane drops where lane 4 ends. The nature of the traffic patterns upstream of a lane drop exasperates conditions for our algorithm. Relatively few drivers use a lane immediately upstream of when it drops, reducing ERFp. While those drivers that remain in lane 4 are seeking gaps to move over to lane 3 in anticipation of the pending lane drop. Such a vehicle is more likely to still be in lane 4 as they pass the detector station if there is a concurrent lane 3

²² For reference, the individual lane pair measurements underlying the calculations from Equation 3.2: N, nSS, and EnFP are presented in Appendix D.

vehicle precluding a convenient gap, i.e., violating our underlying assumption of independent arrivals in adjacent lanes and increasing RSS in the absence of splashover events.

3.4.2 A comparison of algorithm performance

To illustrate the fact that splashover may elude the existing error detection methodologies, we compare the performance of three earlier error detection methodologies (as reviewed in Section 1.2) against our algorithm using the same detector data sets that were used to generate Table 3.2. At each detector we implemented the following tests: Chen and May (1987), [C&M], which tabulates the percent of individual actuations with an off-time under 15/60 seconds; Jacobson et al. (1990), [JNB], which tabulates the percent of macroscopic data (20 second samples) outside of the combined acceptable thresholds on flow and occupancy; Turochy and Smith (2000), [T&S], which tabulates the percent of macroscopic data (30 second samples) with flow greater than 3,100 vehicles/hr; and our method (on each adjacent lane pair), [L&C], as described above. For each of the preceding tests we used the parameters and settings as given in the respective article. The earlier error detection methodologies were not specifically designed to identify a loop detector with splashover problems, but in theory the previous tests are capable of catching problems that arise from splashover errors. For example, the resulting double count due to unique splashover leads to inaccurate measurements, i.e., higher flow and occupancy, potentially allowing JNB or T&S to identify a loop detector with measurement errors via the macroscopic measurements. Meanwhile, C&M explicitly note that they found detectors exhibiting splashover. A unique splashover between valid pulses can lead to unexpected short off-time, potentially allowing C&M to identify a loop detector with splashover errors using their short off-time threshold.

We applied each of the three earlier error detection methodologies to all of the detectors with ground truth, thus effectively generating a separate table similar to Table 3.4 for each of the three earlier methodologies showing the results for each detector. For brevity, these tables are presented in Appendix F, we segregated the detectors into two groups, the 7 with actual splashover (now simply termed “splashover”), and the 61 without (termed “non-splashover”). Within each of these two groups (i.e., splashover and non-splashover detectors), for a given test we calculate the minimum (min), maximum (max), mean, and median values that were found by the test across all of the detectors in the group. These summary statistics are shown on Figure 3.8 and are tabulated in Table 3.5. Thus, in the case of L&C, the statistics simply summarize Table 3.4, e.g., the mean spalshover value is the mean of the seven shaded cells, and so forth.

One should not compare absolute values between methodologies since each test measures different features; rather, compare the relative values between splashover and non-splashover for a given

methodology as a gauge of the test's ability to differentiate between the two conditions. Only T&S and L&C have a near zero mean or median for the non-splashover detectors. But the difference between the splashover and non-splashover detectors is small for T&S across all four statistics. All four tests exhibit identical performance in terms of min. On the remaining three statistics, among the four tests L&C exhibits the largest relative difference between the splashover and non-splashover conditions. In fact, for mean and max, among the four tests L&C also exhibits the largest total (positive) difference between splashover and non-splashover. For the median JNB exhibits a slightly larger total difference between the two conditions compared to L&C. But because the median of the non-splashover detectors from JNB is so much larger, L&C has a larger relative difference for the median values. Unfortunately, JNB exhibits the undesirable feature that the max and mean from the non-splashover detectors is larger than the corresponding statistics of the splashover detectors, the only test to exhibit such an inversion. The general result that our method, L&C, offers the best performance at differentiating between the splashover and non-splashover detectors is not surprising since, as noted previously, the other tests were not specifically designed to identify splashover. But this example also illustrates the fact that splashover errors can easily go undetected using the existing suite of error detection methodologies.

3.4.3 Brief before and after study of loop detector sensitivity

This section seeks to illustrate the diagnostic power of the splashover test, namely whether it can be used to eliminate splashover problems. Klein et al. (2006) note that splashover usually occurs when the sensitivity level of a loop detector sensor card is set too high or the physical loop is too close to the lane line. The latter splashover errors require restriping the roadway or cutting new loop detectors to solve the problem. The former splashover errors due to the sensor card setting, however, can be easily resolved by reducing the sensitivity level of the sensor card. After completing Table 3.4, in most cases it was not known whether the actual splashover errors were due to the sensor setting or the loop placement in the lane. Two stations were selected for further investigation: station 104 eastbound with the highest ASR in Table 3.3 and station 56 westbound with the lowest ASR in Table 3.3 that yielded a positive ARSS (i.e., that was detected by the algorithm, as shown in Table 3.4).

Our team asked the operating agency (the Ohio Department of Transportation, ODOT) to reduce the sensitivity setting in lane 3 at station 56 westbound and lane 1 at station 104 eastbound. ODOT completed the changes on June 10, 2009 and reported the sensitivity level in lane 3 at station 56 westbound was reduced from "Normal" to "Low" and lane 1 at station 104 eastbound was reduced from "High" to "Low". A second round of video data was collected for each station in free flow conditions after the change: 30min (09:33 ~ 10:03) on June 17, 2009 from station 56 westbound and 15min (13:14 ~

13:29) on June 26, 2009 from station 104 eastbound. Table 3.6 shows a summary of the ground truth data at each station in free flow conditions before and after the change of a loop detector's sensitivity. After the sensitivity change no actual splashover events were found at either station. The splashover detection algorithm was then applied to the loop detector data after changing the loop sensor's sensitivity. After the change, the algorithm correctly labeled all of the lanes at those stations as being non-splashover, as shown in Table 3.7 (the format is comparable to before conditions included in Table 3.4).²³

²³ Obviously, a reduction in detector sensitivity should reduce the occurrence of splashover, while increasing the likelihood of pulse breakup and other errors. Pulse breakup is the topic of the next chapter and this point will be considered there.

Table 3.1, Application of the splashover detection algorithm to station 104 eastbound

Criteria of expected number of false positives	St 104 EB	[Source lane → Target lane]			
		Lane1 → Lane 2	Lane 2 → Lane 1	Lane 2 → Lane 3	Lane 3 → Lane 2
(A): Pulse	Actual splashover number (ASn)	0	318	0	0
	Number of suspected splashover (nSS)	32	240	7	35
	Conservative expected number of false positives (EnFP ^C)	10	14	6	24
	nSS - EnFP ^C	22	226	1	11
(B): Rising transition	Liberal expected number of false positives (EnFP)	61	60	47	74
	nSS - EnFP	-29	180	-40	-39

Table 3.2, The ground truth data sets used in this experiment. NB=northbound, SB=southbound, EB=eastbound, and WB=southbound.

the presence or the absence of splashover	Station number	Direction	Number of lanes	Date	Start Time (hh:min)	End Time (hh:min)	Duration of time (hh:min)
With splashover	38	WB	4	September 9, 2008	12:05	12:25	0:20
	41	EB	2	September 9, 2008	11:00	11:35	0:35
	56	WB	3	November 21, 2008	09:00	09:40	0:40
	104	EB	3	March 17, 2008	16:00	16:10	0:10
Without splashover	2	NB	4	March 9, 2009	17:21	17:50	0:29
	3	NB	4	March 17, 2008	10:57	11:20	0:23
	3	SB	4	April 18, 2008	15:55	16:55	1:00
	4	SB	4	March 17, 2008	10:15	10:35	0:20
	6	NB	3	April 18, 2008	15:55	16:55	1:00
	9	NB	3	June 5, 2006	12:20	14:20	2:00
	9	SB	3	June 5, 2006	12:20	14:20	2:00
	15	NB	3	March 10, 2009	17:18	17:47	0:29
	18	NB	3	March 9, 2009	08:24	08:57	0:33
	19	NB	3	March 17, 2008	09:25	09:40	0:15
	31	NB	4	November 21, 2008	10:35	11:05	0:30
	38	EB	3	August 29, 2008	15:05	15:25	0:20
	43	EB	3	September 2, 2008	08:50	09:15	0:25
	43	WB	3	September 2, 2008	08:50	09:15	0:25
	56	EB	3	September 3, 2008	16:40	17:25	0:45
	102	EB	3	March 10, 2009	17:05	17:20	0:15
104	WB	3	March 12, 2009	17:00	17:18	0:18	

Table 3.3, Summary of the ground truth data with splashover in free flow conditions. EB=eastbound, and WB=southbound.

Station number (Direction)	Lane number	Total pulses	Total vehicles	Actual splashover number (ASn)			Mechanism of splashover [Source lane → Target lane]	Actual splashover rate (ASR) [%]
				Total	Unique splash-over	Combined splash-over		
38 (WB)	1	172	172	0	0	0	-	-
	2	242	235	2	2	0	Lane 1 → Lane 2	1.2%
	3	206	90	117	115	2	Lane 2 → Lane 3	48.3%
	4	56	39	17	17	0	Lane 3 → Lane 4	8.3%
41 (EB)	1	337	274	53	39	14	Lane 2 → Lane 1	10.5%
	2	507	475	11	8	3	Lane 1 → Lane 2	3.3%
56 (WB)	1	345	340	0	0	0	-	-
	2	632	610	0	0	0	-	-
	3	121	84	19	19	0	Lane 2 → Lane 3	3.0%
104 (EB)	1	441	164	318	273	45	Lane 2 → Lane 1	91.1%
	2	349	347	0	0	0	-	-
	3	350	347	0	0	0	-	-
Total		3,758	3,177	537	473	64		

Table 3.4, Percentage of adjusted suspected splashover relative to source lane. Shaded cells indicate lane pairs with splashover verified from the ground truth data, and all of the non-shaded cells represent lane pairs that did not exhibit splashover in the ground truth data. NB=northbound, SB=southbound, EB=eastbound, and WB=southbound.

Condition	Station number	Direction	Adjusted rate of suspected splashover, ARSS [Source lane → Target lane]					
			Lane 1→ Lane 2	Lane 2→ Lane 1	Lane 2→ Lane 3	Lane 3→ Lane 2	Lane 3→ Lane 4	Lane 4→ Lane 3
Splashover	38	WB	0%	0%	41.3%	0%	6.8%	0%
	41	EB	0%	3.6%	-	-	-	-
	56	WB	0%	0%	2.2%	0%	-	-
	104	EB	0%	51.6%	0%	0%	-	-
Non-splashover	2	NB	0%	0%	0%	0%	0.6%	0%
	3	NB	0%	0%	0%	0%	0%	0%
	3	SB	0%	0%	0%	0%	0%	0%
	4	SB	0%	0%	0%	0%	0%	0%
	6	NB	0%	0%	0%	0%	-	-
	9	NB	0%	0%	0%	0%	-	-
	9	SB	0%	0%	0%	0%	-	-
	15	NB	0%	0%	0%	0%	-	-
	18	NB	0%	0%	0%	0%	-	-
	19	NB	0%	0%	0%	0%	-	-
	31	NB	0%	0%	0%	0%	0.9%	0%
	38	EB	0%	0%	0%	0%	-	-
	43	EB	0%	0%	0%	0%	-	-
	43	WB	0%	0%	0%	0%	-	-
56	EB	0%	0%	0%	0%	-	-	
102	EB	0%	0%	0%	0%	-	-	
104	WB	0%	0%	0%	0%	-	-	

Table 3.5, Comparison of the min, max, mean, and median results for splashover and non-splashover detectors

Method	Data	Min	Max	Mean	Median
C&M	Splashover	0.0%	7.7%	2.8%	2.5%
	Non-Splashover	0.0%	5.7%	1.2%	0.7%
	Difference	0.0%	2.0%	1.6%	1.8%
	Relative difference	-	26.4%	55.8%	71.2%
JNB	Splashover	0.0%	11.4%	5.3%	5.4%
	Non-Splashover	0.0%	87.9%	5.4%	1.5%
	Difference	0.0%	-76.6%	-0.1%	3.9%
	Relative difference	-	-673.9%	-1.3%	71.9%
T&S	Splashover	0.0%	4.0%	0.6%	0.0%
	Non-Splashover	0.0%	1.6%	0.0%	0.0%
	Difference	0.0%	2.4%	0.5%	0.0%
	Relative difference	-	59.0%	95.3%	-
L&C	Splashover	0.0%	51.6%	15.1%	3.6%
	Non-Splashover	0.0%	0.9%	0.0%	0.0%
	Difference	0.0%	50.7%	15.1%	3.6%
	Relative difference	-	98.2%	99.9%	100.0%

Table 3.6, Comparison before and after the change of a loop's sensitivity at station 56 westbound and 104 eastbound. Four of the loop detectors without splashover errors were not changed and they are shown with non-shaded cells.

Station number (Direction)	Lane number	Before			After			Date(duration) ["Before" data, "After" data]
		Level of sensitivity	Total pulses	Splash-over	Level of sensitivity	Total pulses	Splash-Over	
56 (WB)	1	Unknown	345	0	Unknown	234	0	[November 21, 2008 (40min), June 17, 2009 (30min)]
	2	Unknown	632	0	Unknown	446	0	
	3	Normal	121	19	Low	70	0	
104 (EB)	1	High	441	318	Low	136	0	[March 17, 2008 (10min), June 26, 2009 (15min)]
	2	Unknown	349	0	Unknown	435	0	
	3	Unknown	350	0	Unknown	401	0	

Table 3.7, Percentage of adjusted suspected splashover relative to source lane from stations where the loop detector sensitivity level was reduced. EB=eastbound and WB=westbound.

Station number	Direction	Adjusted rate of suspected splashover, ARSS [Source lane → Target lane]					
		Lane 1→ Lane 2	Lane 2→ Lane 1	Lane 2→ Lane 3	Lane 3→ Lane 2	Lane 3→ Lane 4	Lane 4→ Lane 3
56	WB	0%	0%	0%	0%	-	-
104	EB	0%	0%	0%	0%	-	-

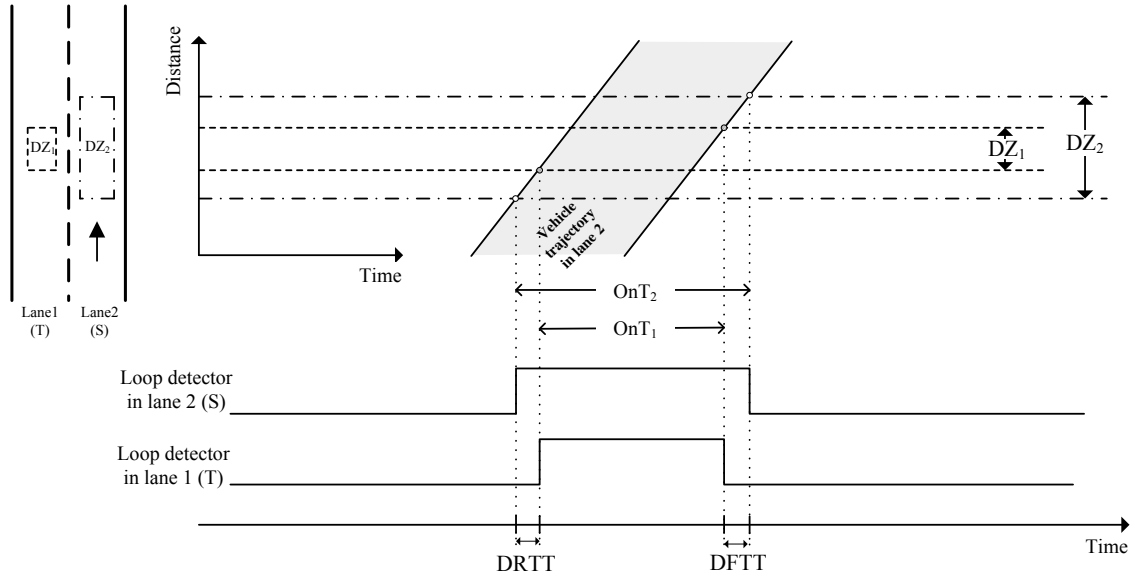


Figure 3.1, A hypothetical example of a splashover event from lane 2 to lane 1

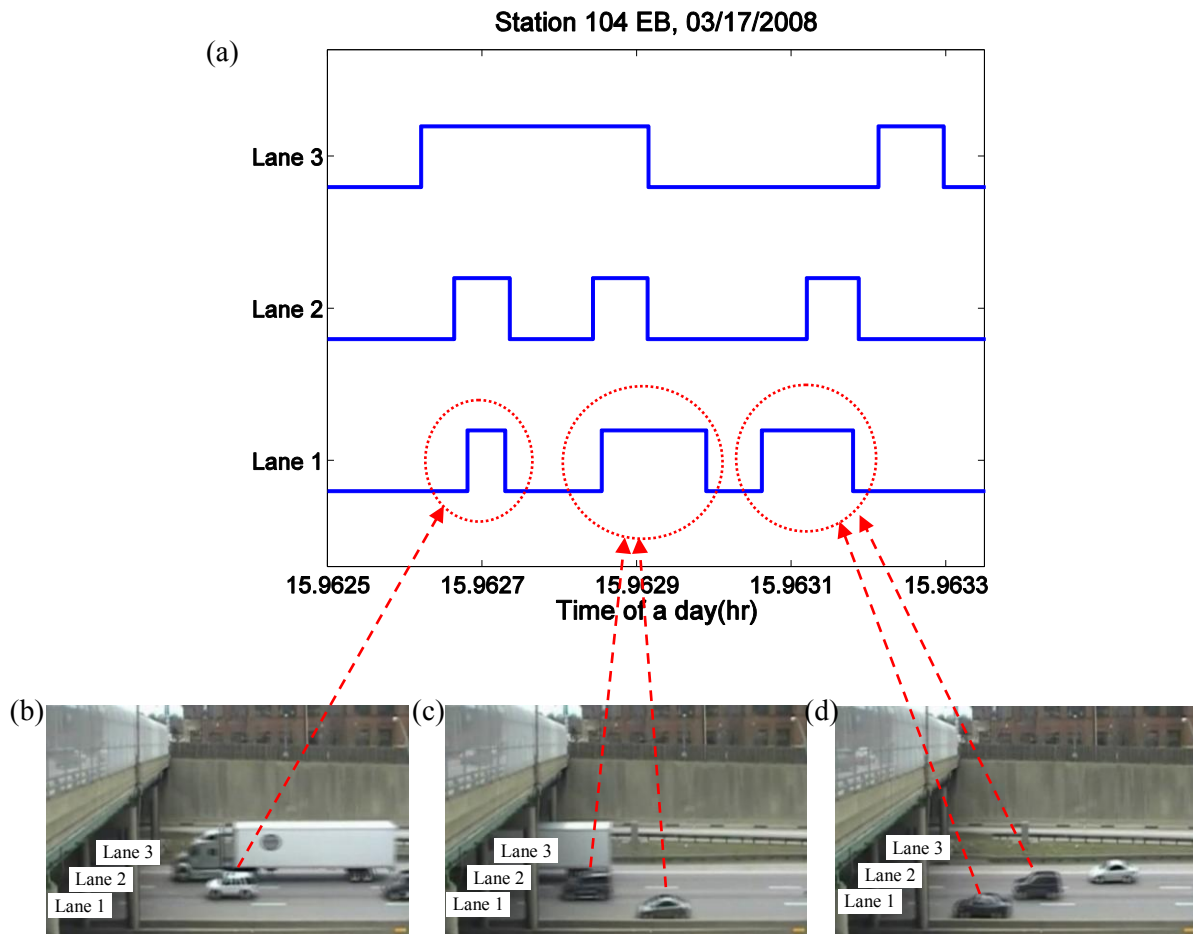


Figure 3.2, (a) A plot of transition pulses, and the corresponding video image at station 104 eastbound showing successively for the first through third pulses lane 1: (b) unique splashover, (c) combined splashover at the head end, and (d) combined splashover at the tail end.

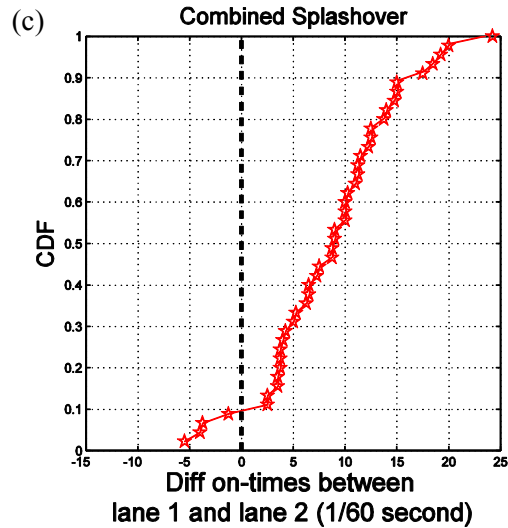
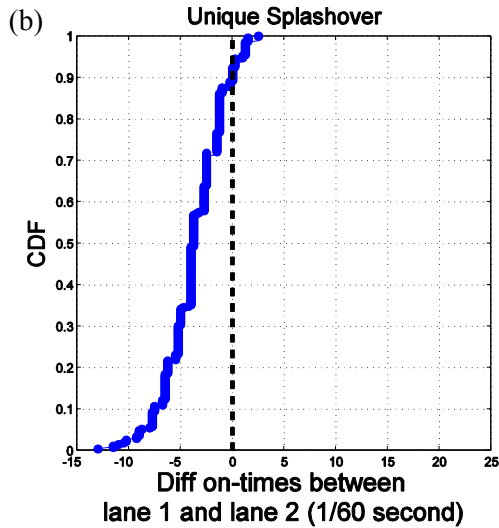
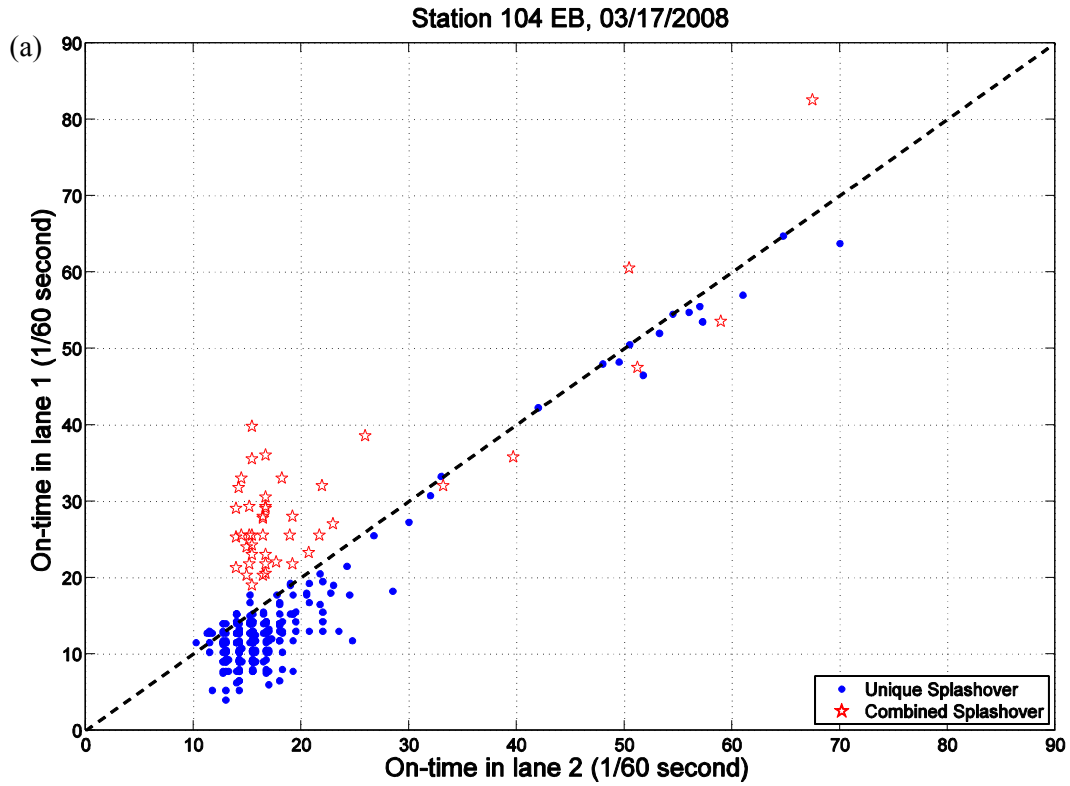


Figure 3.3, (a) A scatter plot of on-times in unique splashover events and combined splashover events at station 104 eastbound, splashover pulses in lane 1 and valid pulses in lane 2, (b) CDF of the difference of on-time in unique splashover and (c) combined splashover.

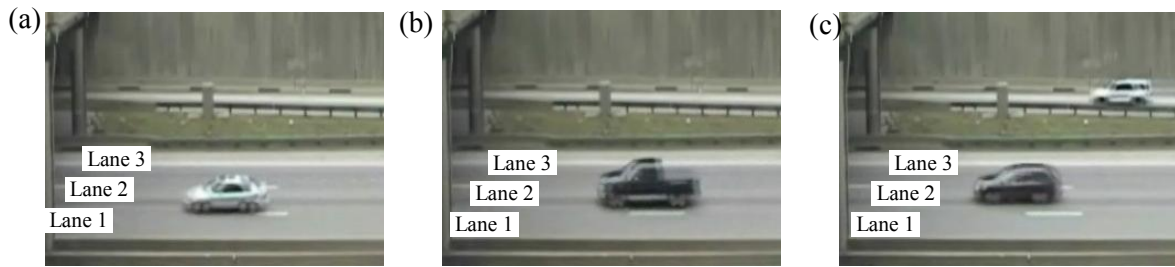


Figure 3.4, Three typical examples of unique splashover. The difference of on-time between a valid pulse in lane 2 and a splashover pulse in lane 1: (a) $+1/60$ seconds, (b) $-5/60$ seconds, (c) $-11/60$ seconds: generally the closer the lane 2 vehicle is to the lane line, the more positive the difference.



Figure 3.5, A video frame corresponding to the case where a pulse of a combined splashover bounds the pulse of the valid detection from lane 2. In this case, the difference of on-times is $-6/60$ seconds.

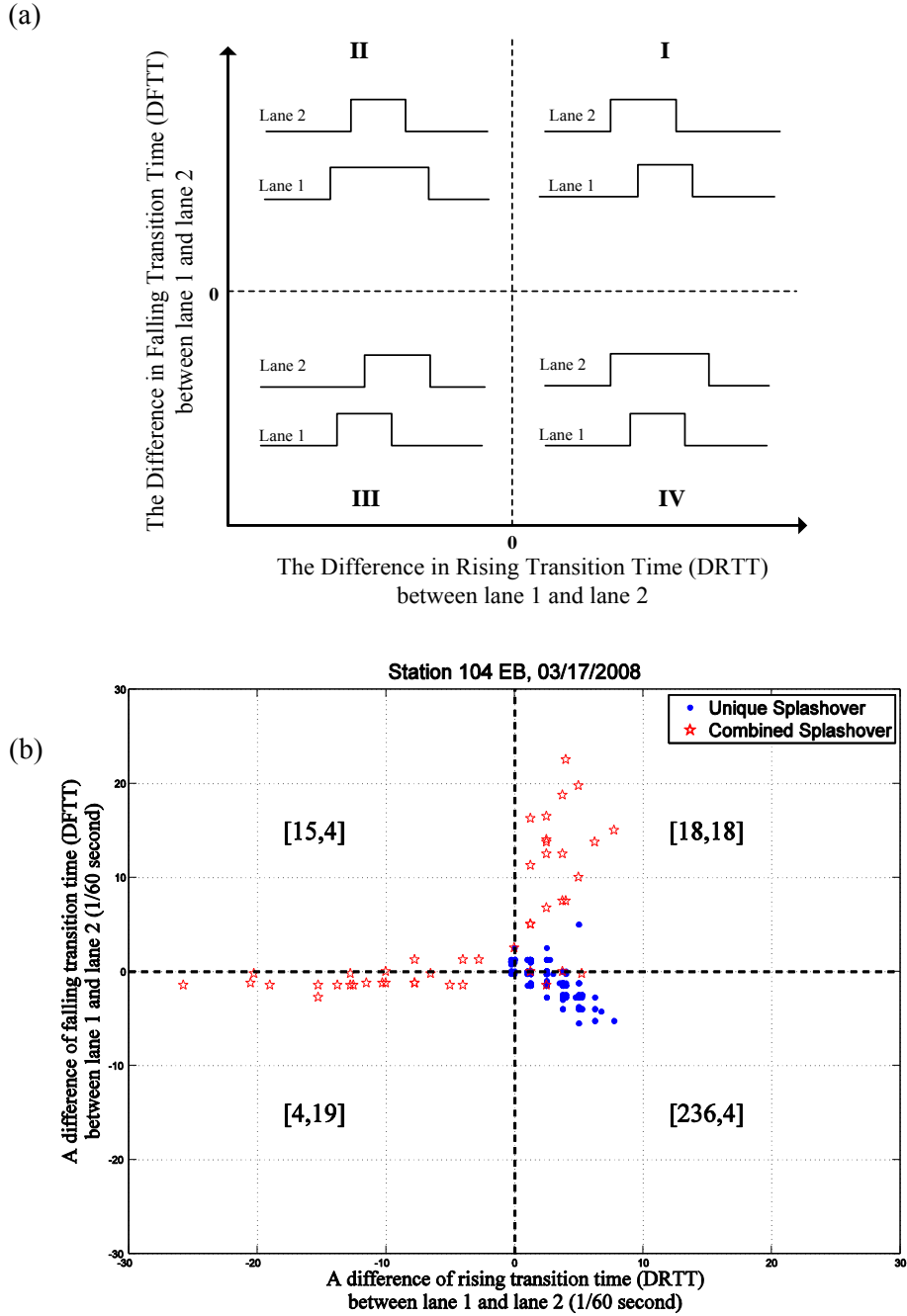


Figure 3.6, (a) The combined relationship between the difference in falling transition times and the difference in rising transition times: (lane 1 – lane 2) and (b) Scatter plot of the difference in rising and falling transition time for the splashover events from the ground truth data at station 104 eastbound, splashover pulses in lane 1 and valid pulses in lane 2. Within each region the brackets tally the total number of observations of [unique splashover, combined splashover].

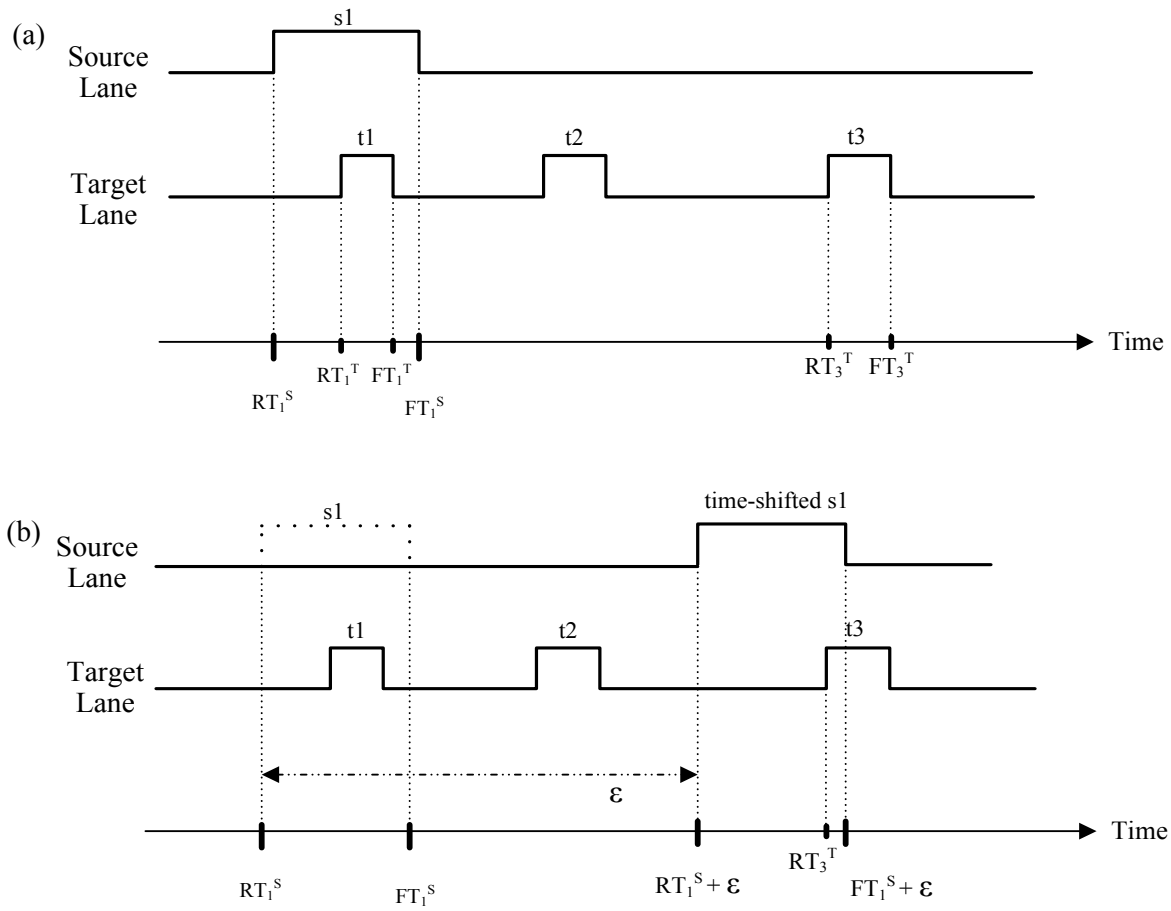


Figure 3.7, The splashover detection algorithm to select (a) a suspected splashover event and (b) the non-splashover events that contribute to the expected rate of false positives.

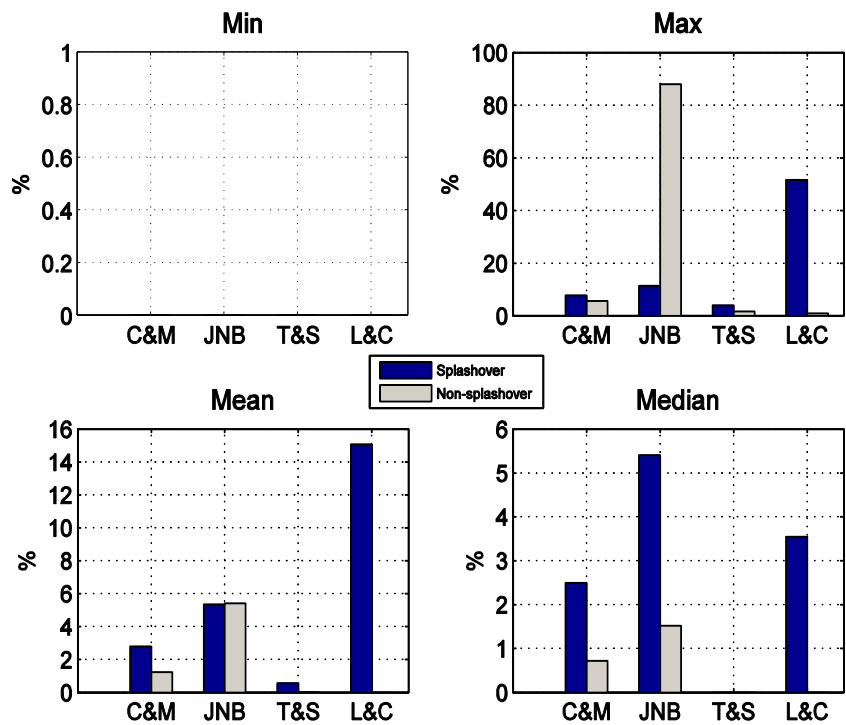


Figure 3.8, Bar charts comparing the min, max, mean, and median results for detectors with splashover and non-splashover from the four error detection methods, as applied to the data sets with ground truth data underlying Table 3.3. Note that vertical scales differ among the four plots

4 AN ALGORITHM TO IDENTIFY PULSE BREAKUP

Loop detectors record vehicle passages. When the detectors are operating properly the loop detectors(s) in the given lane of travel should record each passing vehicle as a single pulse (comprised of a rising transition and a falling transition). Sometimes, however, a detector "drops out" in the middle of a vehicle then "flickers" back on before the vehicle has departed the detection zone, and thus, when such *pulse breakup*²⁴ occurs, the vehicle is erroneously recorded as two or more pulses by the detector.

Pulse breakup most often occurs when multiple unit vehicles, (e.g., semi-trailer trucks or other vehicles pulling trailers), pass over a loop detector (Cheevarunothai et al., 2007). These vehicles exhibit a sharp increase in the height above the detector (e.g., at the rear of the semi-tractor²⁵) or some other large effective drop in ferromagnetic presence (e.g., at the trailer tow-bar) somewhere in the middle of the multiple units. Conventional loop sensor cards use discrete thresholds to determine whether or not the loop detector is occupied by a vehicle. If the deviation in the middle of a multiple unit vehicle is large enough to exceed the turn-off threshold, the sensor card will erroneously report the detector as being unoccupied, i.e., the detector will dropout. Often the rear axles or other features on the trailer have sufficient ferromagnetic presence to cause the sensor card to subsequently turn back on and register another pulse. An example of this error is evident in the comparison between the recorded loop detector data and concurrent video shown in Figure 4.1, in lane 2 at a single loop detector station (station 9 northbound). Figure 4.1(a) shows the pulses over a few seconds from all three lanes as the detectors respond to vehicles. In the absence of detector errors, a vehicle passage is manifested as a single pulse, so

²⁴ All three of these terms - "dropout", "flicker" and "pulse breakup" - are commonly used in the literature to refer to the same general phenomena provided the detector turns back on before the vehicle passes. For this work we will refer to all of these events as pulse breakup. Note, however, dropout is broader, also including dropout without return, a slightly different error that results in an erroneously short on-time but correct vehicle count. This section does not cover dropout without return. It is worth noting, however, that all detectors that we have seen exhibit dropout without return also exhibited pulse breakup, except when the detector sensor card was operating in "pulse mode". In pulse mode all pulses are suppose to be reported with the same fixed on-time. Note we use "operating in" rather than "set to" because occasionally a sensor card set to "presence mode" would report data as if set to pulse mode.

²⁵ Since a loop's sensitivity is inversely proportional to the square of the distance of the vehicle's undercarriage, loop detectors are more likely to dropout right after the tractor passes because the ground clearance abruptly jumps up to the bottom of the trailer.

without evaluation, the two pulses from lane 2 would be recorded as two distinct vehicles. However, Figure 4.1(b) presents a concurrent frame from the video, showing that the two pulses in lane 2 came from a single semi-trailer truck passing over the loop detector. For scale reference, immediately behind the truck a car is evident in lane 3 in both the plot and the image.

Figure 4.2 shows a hypothetical example of a semi-trailer truck's actuation breaking up into two pulses; both (a) in the time-space diagram, and (b) as recorded in the time-series detector data. The unobserved, actual on-time (OnT^A) denotes the period when the loop detection zone was physically occupied by the truck. However, OnT^A is divided into two distinct on-times (OnT_1 and OnT_2) and one off-time ($OffT_1$) because of the pulse breakup in the recorded data. The schematic on the left of the plot shows the truck's tractor and trailer at the instant the tractor leaves the detection zone. The length of the separate parts of the semi-trailer truck associated with the on-times and off-time are labeled on the schematic and shown on the time-space diagram. Initially the ground clearance of a typical semi-trailer truck is relatively small, the tractor is close to the ground (L_1^P , contributed to OnT_1), and then rises significantly under the trailer (L_X^P , contributed to $OffT_1$), only to come close to the ground once more with the trailer's axles (L_2^P , contributed to OnT_2). Given a vehicle's speed (V), the on-times and off-time in a pulse breakup can be expressed via Equation 4.1.

$$\begin{aligned}
 OnT_1 &= \frac{L_1^P + DZ}{V} = \frac{L_1}{V} \\
 OnT_2 &= \frac{L_2^P + DZ}{V} = \frac{L_2}{V} \\
 OffT_1 &= \frac{L_X^P - DZ}{V} = \frac{L_X}{V}
 \end{aligned} \tag{4.1}$$

If the pulse breakup error goes undetected, OnT_1 and OnT_2 will appear to be two short vehicles separated by the relatively brief $OffT_1$. This error will impact microscopic metrics, e.g., if the on-times are used to measure or estimate vehicle length, the resulting lengths from the two pulses (at best, L_1 and separately L_2) do not correspond to the vehicle's actual effective length ($L_1 + L_2 + L_X$); thus, degrading the performance of any subsequent length based vehicle classification methodology using the detector's data. In terms of the macroscopic metrics, the corresponding flow will be too high and occupancy will be too low. If there are only a few pulse breakup events in any given macroscopic sample, the impacts on flow and occupancy could easily be within the normal tolerance level necessary to accommodate different vehicles (e.g., as in the above example, a truck with pulse breakup might appear to be one car tailgating another). In such cases, while it might not be discernable from error free data, it will still impact subsequent controls, e.g., if occupancy is regularly 3% too low due to pulse breakup, a traffic responsive

ramp meter might turn on too late or provide too lenient metering. The pulse breakup may also impact the speed estimate from a single loop detector or speed measurement from a dual loop detector (Equation 2.3 – 2.5). The impact on average speed from any given pulse breakup event can be large if the pulse breakup causes a large error in the individual vehicle's apparent speed.

To address these problems, we develop an algorithm to identify the presence of individual pulse breakup events. Like the splashover algorithm, the algorithm is based on the nature of pulse breakup revealed from concurrent video recorded ground truth data. Previous efforts to identify pulse breakup have focused almost exclusively on the short off-times, but as will be shown momentarily, many errors omission and commission arise using the off-time alone. Like these earlier efforts, our algorithm begins with the short off-times, but then compares the on-times from the two successive pulses bounding a given short off-time. The algorithm employs several heuristic comparisons of the adjacent on-times with respect to traffic conditions to make the algorithm more robust to changing traffic conditions and the vehicle fleet composition.

The remainder of this chapter is organized as follows. First the previous research to detect pulse breakup events are reviewed. Next the characteristics of pulse breakup events are examined from loop detector data via concurrent video-recorded ground truth data. These characteristics are used to develop an algorithm to identify the presence of individual pulse breakup events at single loop detectors (or separately for each loop in a dual loop detector). Third the algorithm for pulse breakup events is tested over many detector stations with and without pulse breakup in the ground truth data. Fourth, performance of the algorithm is compared against previous algorithms from the literature. Finally the chapter closes with a brief before and after study of loop detector sensitivity.

4.1 Previous research related to pulse breakup

Reviewing the literature to place our work in context, there are few if any macroscopic detector validation tests that explicitly seek to catch detectors exhibiting low to moderate pulse breakup rates; though, many of the macroscopic tests will catch a detector exhibiting a high pulse breakup rate simply because these detectors report an unfeasibly high flow. Likewise, many of the existing microscopic tests may catch the secondary impacts of pulse breakup without explicitly looking for breakup events (e.g., the feasible range of headway and on-time, or cumulative distribution of vehicle lengths in Coifman and Dhoorjaty, 2004). There are two prior efforts that explicitly sought out pulse breakup events via microscopic data: Chen and May (1987) use a threshold of the time gap (i.e., the off-time) and Cheevarunothai et al. (2007) use the time headway between two successive pulses (i.e., the sum of a successive off-time and on-time). Both methods effectively use a short off-time as the indicator of a pulse

breakup. For example, Chen and May's method labels all off-times below 15/60 seconds as arising from pulse breakup.

Employing one of the ground truth data sets from Table 2.2, Figure 4.3(a) shows a CDF of off-times corresponding to pulse breakup events across all lanes during 2 hrs in free flow conditions at station 9 northbound on June 5, 2006. About 75% of the off-times arising from pulse breakup (231 out of 306 off-times) would be correctly labeled by Chen and May's threshold test. The largest off-time in Figure 4.3(a) is 20/60 seconds and such off-times are only 5/60 seconds longer than the threshold of pulse breakup used in Chen and May's method. While a pulse breakup usually results in a short off-time, a short off-time does not always correspond to pulse breakup. A short off-time can also arise due to tailgating and other vehicle maneuvers. Revisiting the same 2 hours of data from station 9 northbound, Figure 4.3(b) shows the CDF of off-times from all of the remaining pulses that were excluded from Figure 4.3(a) (i.e., all of the pulses that were manually verified from the concurrent video to be true and valid off-times). Among these non-pulse breakup events, about 0.4 % of the off-times (29 out of 7,248 off-times) would be erroneously labeled as pulse breakup by Chen and May's threshold test.

Unlike free flow traffic, the resulting off-time in a pulse breakup event during congestion will frequently exceed their static threshold used to find pulse breakup events because the dwell time over the detection zone becomes much larger. Once more employing one of the ground truth data sets, Figure 4.4(a) shows the CDF of off-times by lane during 1 hr in congested conditions at station 3 northbound on April 18, 2008. The off-times from pulse breakup events during congestion span a much larger range than their counterparts from free flow conditions. In this case three off-times exceed 1 second and only 20% of the off-times arising from pulse breakup (24 out of 116 off-times) fall below Chen and May's 15/60 seconds threshold. A larger off-time threshold should catch more pulse breakup events if they are present, but at the cost of more non-pulse breakup events being erroneously be labeled as pulse breakup events. Figure 4.4(b) shows the CDF of off-times from all of the remaining pulses that were excluded from Figure 4.4(a). If we set 60/60 seconds as a boundary of off-time in pulse breakup, most of the actual pulse breakup events fall within the new boundary (as shown in Figure 4.4(a)), but 21 % of the non-pulse breakup off-times (1,206 out of 5,686 off-times) would be erroneously labeled as pulse breakup.

Comparing Figures 4.3 and 4.4, it is clear that a static off-time threshold is insufficient to differentiate between pulse breakup events and valid actuations under all traffic conditions, e.g., the range of off-times arising from pulse breakup in congestion exceeds 1 second, which is longer than many valid free flow off-times. Furthermore, both of the figures show that the range of off-time arising from pulse breakup overlaps the range of valid off-times under the given traffic conditions. This overlap precludes

identifying all of the pulse breakup events even when using a threshold as a function of traffic speed. On the other hand, the figures also show that most of the pulse breakup off-times are shorter than most of the valid off-times. Employing these observations, the following section develops a pulse breakup detection algorithm to identify most (but not all) pulse breakup events in the microscopic, vehicle actuation pulse train.

4.2 Development of a new algorithm to identify pulse breakup

The pulse breakup detection algorithm is based on the nature of pulse breakup events revealed from the ground truth data. The development relies primarily on the 2 hrs in free flow conditions at station 9 northbound on June 5, 2006 (e.g., as seen in Figure 4.3). This single loop detector station has three lanes and each lane was processed individually. After generating the ground truth data at this station, 2,372 vehicles were observed from video in lane 1, 2,689 in lane 2, and 2,182 in lane 3. Upon merging these observations with the detector data, a total of 306 out of 7,243 vehicles (4%) exhibit pulse breakup. Of these pulse breakup events, 298 vehicles arise from multiple unit trucks (like Figure 4.1(b)), while the remaining 8 events arise from single unit trucks pulling trailers. All observed pulse breakup events in this data set consist of two pulses, and our algorithm focuses on identifying pulse breakup events consisting of two pulses²⁶. Like the earlier works, we begin with a simple off-time threshold, but then employ five heuristic comparisons of the adjacent on-times with respect to traffic conditions to refine the performance, namely:

- Dynamic off-time
- Ratio of on-times
- Ratio of off-time and preceding on-time
- 20th percentile off-time
- Maximum vehicle length

as defined in the following subsections. The algorithm is designed to work at both single loop detectors and individually at each loop in dual loop detectors, as such, it only uses metrics that can be collected at single loop detectors. If dual loop detectors are available, the method can easily be extended to use measured speed and further improve the performance.

²⁶ Although the focus is on pulse breakup events consisting of two pulses, if a pulse breaks up into more than two pulses the successive pairs of erroneous pulses are still likely to be caught by the algorithm. We rarely observed a vehicle breaking up into more than two pulses in the ground truth data sets, so given the lack of empirical data, we were unable to explicitly test these conditions.

4.2.1 Dynamic off-time

While Chen and May (1987) used a static short off-time threshold of 15/60 seconds, we begin with a more liberal static threshold, $\text{OffT}_{\text{FF_Threshold}}$, set to 20/60 seconds from the upper bound of the pulse breakup off-times in Figure 4.3(a). As seen in Figure 4.3, 20/60 seconds appears to do a good job of selecting pulse breakup events during free flow conditions (100% of the pulse breakup events have off-times less than or equal to 20/60 seconds), while catching only 1.5% false positives from the valid actuations (110 out of 7,248). However, as shown in Figure 4.4, the same threshold will do a poor job during congestion, missing most of the pulse breakup events (72%, 83 out of 116). As per Figure 4.4(b), if the off-time threshold were any larger it would start selecting a large number of non-pulse breakup events even in congestion. It reaffirms the fact that no static off-time threshold will yield satisfactory results across all traffic conditions.

Returning to Figure 4.2, given the off-time threshold in free flow conditions, $\text{OffT}_{\text{FF_Threshold}}$, the free speed, V_f , and size of the detection zone, DZ , there is some maximum physical gap, L_x^p that will be labeled as suspected of arising from pulse breakup, as per Equation 4.2.

$$L_x^p = V_f \times \text{OffT}_{\text{FF_Threshold}} + DZ \quad (4.2)$$

At some congested speed, V_c , this L_x^p will correspond to a larger off-time threshold, $\text{OffT}_{\text{C_Threshold}}$, via Equation 4.3.

$$\text{OffT}_{\text{C_Threshold}} = \frac{L_x^p - DZ}{V_c} \quad (4.3)$$

The off-time threshold in congested traffic conditions in Equation 4.3 can be rewritten as Equation 4.4.

$$\text{OffT}_{\text{C_Threshold}} = \frac{V_f}{V_c} \times \text{OffT}_{\text{FF_Threshold}} \quad (4.4)$$

In other words, the off-time threshold from L_x^p in congestion corresponds to the free flow off-time threshold multiplied by the ratio of V_f and V_c . As one would expect, the off-time threshold in congestion is greater than in free flow because speed in congestion is lower than free flow speed ($V_f / V_c > 1$). Speeds cannot be measured at single loop detectors, but we use Equation 2.4 to estimate speed, i.e., the assumed effective vehicle length divided by median on-time in the given sample (Coifman et al.,

2003).²⁷ Since the median speed in off-peak time periods should usually correspond to free flow speed, for this work we use 9 hr to 15 hr for the off-peak time period to estimate V_f .²⁸ A vehicle's speed in congested conditions (V_c) is estimated from the assumed effective vehicle length divided by the median on-time over a window of a fixed number of pulses (41 pulses in this study), centered on the subject pulse (Coifman et al., 2003). So, Equation 4.4 can be rewritten as Equation 4.5, where we use “OnT” and “OffT” to denote a single on-time or off-time, respectively, and “on-times” in the equations to denote a set of several OnT. As a result, the off-time threshold from Equation 4.5 of suspected pulse breakup events in congested conditions just depends on the median on-time over 41 successive pulses because the median on-time during off-peak time periods is nearly constant²⁹. Since the threshold depends on the prevailing traffic speed, we call it the “dynamic off-time”. An OffT is suspect if it is less than the threshold, rewriting the equation as such a test yields Equation 4.6.

$$\begin{aligned}
 \text{OffT}_{C_Threshold} &= \frac{\frac{\tilde{L}}{\text{median (on-times)}_{\text{off-peak time period}}}}{\frac{\tilde{L}}{\text{median (on-times)}_{41\text{pulses}}}} \times \text{OffT}_{FF_Threshold} \\
 &= \frac{\text{median (on-times)}_{41\text{pulses}}}{\text{median (on-times)}_{\text{off-peak time period}}} \times \text{OffT}_{FF_Threshold}
 \end{aligned} \tag{4.5}$$

$$\frac{\text{OffT}}{\text{median (on-times)}_{41\text{pulses}}} \leq \frac{\text{OffT}_{FF_Threshold}}{\text{median (on-times)}_{\text{off-peak time period}}} \tag{4.6}$$

²⁷ As noted in Coifman and Kim (2009), the median on-time breaks down if there are a large number of long vehicles (over 30% of the fleet). Though by 30% long vehicles just about every other method of estimating speed from single loop detectors also breaks down. In any event, none of the detectors in this study had such a high percentage of long vehicles.

²⁸ Transient events such as incidents or a snowstorm can negate this expectation of free speed in the middle of the day, but this problem can be addressed by taking the median over many days or weeks.

²⁹ Excluding low flow periods during the early morning, when the number of passenger vehicles drops but the number of trucks may remain high, as per Coifman (2001). As a result, the off-peak median in Equation 4.5 is intended to come from many hours if not all off-peak periods over 24hrs.

4.2.2 Ratio of on-times

Most of the observed pulse breakup events arose in the middle of semi-trailer trucks between the tractor and rear axles. So OnT_1 and OnT_2 in Figure 4.2 should be proportional to the length of the tractor and the trailer axles, respectively. The effective length observed for the tractor is typically longer than the effective length of trailer axles. Figure 4.5(a) shows the relation of on-times between the following pulse, OnT_2 , and the preceding pulse, OnT_1 , for the station 9 northbound pulse breakup events (recall that these data come from free flow conditions and in this case the pulses are known to arise from pulse breakup events). The dashed line shows the set of points where the two on-times are equal. In general, the preceding pulses in the pulse breakup events have a longer on-time than the following pulses. Capturing this observation in a metric, the ratio of on-times is used to select successive pulses that exhibit this relationship. Like the dynamic off-time above, the ratio is used rather than the difference because the ratio of on-times is impacted less by traffic speed, as will be discussed below. Assuming the vehicle speed is roughly constant between OnT_1 and OnT_2 , from Equation 4.1, the ratio of two successive on-times is related to the ratio of the corresponding effective vehicle length via Equation 4.7.

$$\frac{OnT_2}{OnT_1} = \frac{\frac{L_2}{V_2}}{\frac{L_1}{V_1}} \approx \frac{L_2}{L_1} \quad (4.7)$$

Figure 4.5(b) shows the CDF of the ratio of on-times between the two successive pulses in a pulse breakup from Equation 4.7. The on-time ratio ranges between 0.13 and 1.40. For about 99% of pulse breakup events the preceding pulses (OnT_1) have longer on-times than the following pulses (OnT_2). However, the ratio can give results in this range due to valid measurements as well, e.g., when a short vehicle follows a long vehicle.

Figure 4.6(a) shows the CDFs of the on-time ratio from Equation 4.7 for pulse breakup events and separately for successive non-pulse breakup events in the ground truth data at station 9 northbound. We seek to use Equation 4.7 to differentiate between pulse breakup and non-pulse breakup events using a threshold. While a threshold of 1 would capture 99% of the pulse breakup events, it would also capture 50% of the non-pulse breakup events. The on-time ratio threshold to identify pulse breakup events is chosen such that the suspected pulse breakup events include as many as actual pulse breakup events and as few as non-pulse breakup events as possible. To this end, for determining the on-time ratio threshold, we seek the point where the difference between the two CDFs is largest. Figure 4.6(b) shows the

difference between the two CDFs over the range from 0 to 2.5 at steps of 0.01. The peak is observed at 0.72 of on-time ratio and we take this as the threshold for the on-time ratio test, yielding Equation 4.8,

$$\frac{\text{OnT}_2}{\text{OnT}_1} \leq 0.72 \quad (4.8)$$

Of course the on-time ratio test is not meant to be applied alone. Figure 4.7 shows a scatter plot of intervening off-time versus on-time ratio for the pulse breakup events at station 9 northbound. The vertical dashed line shows the threshold of 0.72 from Equation 4.8 and horizontal dashed line shows the threshold of 20/60 seconds from Equation 4.6.³⁰ Roughly 94% (289 out of 306) of the pulse breakup events fall in the lower left quadrant, while only 0.1% (7 out of 7,248) of the non-pulse breakup events (not shown) fall in this same quadrant.

In Figure 4.7, the 8 single unit trucks pulling trailers are shown with a different symbol than the multiple unit trucks. Most of the single unit trucks pulling trailers exceed the on-time ratio threshold, but these vehicles typically exhibit a much shorter off-time (all below 10/60 seconds)³¹ compared to the multiple unit trucks with pulse breakup. If in addition to those successive on-times falling in the lower left quadrant of Figure 4.7, selecting all points that fall below a threshold of 6/60 seconds in Equation 4.6 (i.e., ignoring the on-time ratio while employing a more stringent off-time threshold), 50% of the pulse breakup events falling outside the quadrant are also caught. Moreover, since the smallest off-time from the non-pulse breakup data in this set is 8/60 seconds, the additional condition does not increase the number of non-pulse breakup events erroneously selected at this station.

4.2.3 Ratio of off-time and preceding on-time

Figure 4.8 shows a scatter plot of the off-time (OffT_1) and preceding on-time (OnT_1) for the pulse breakup events at station 9 northbound. The dashed dot line shows the set of points where the off-time and on-time are equal and the number of observations on each side of the line is shown on the plot. For the observed pulse breakup events, the on-time of the preceding pulse is generally greater than the off-time. Assuming the vehicle speed is roughly constant between OnT_1 and OffT_1 , from Equation 4.1, the ratio can be expressed via Equation 4.9,

³⁰ Since these data come from free flow, the dynamic off-time threshold would remain around 20/60 seconds for these data.

³¹ From the concurrent video, the pulse breakup events from single unit trucks pulling trailers occur at the trailer hitch, i.e., the smallest cross-section of the vehicle; however, the pulse breakup events from the multiple unit trucks typically occur at the end of the tractor, when the ground clearance suddenly increases.

$$\frac{\text{OffT}_1}{\text{OnT}_1} = \frac{L_x}{L_1} = \frac{L_x^p - DZ}{L_1^p + DZ} \quad (4.9)$$

As with the on-time ratio, Equation 4.9 just depends on the physical characteristics of the vehicle, not the traffic speed. Like the on-time ratio test, Figure 4.9(a) shows the CDFs of the ratio of off-time and the preceding on-time separately for the pulse breakup events and the non-pulse breakup events from station 9 northbound. The ratio of off-time and preceding on-time from pulse breakup events ranges between 0.12 and 1.65, while the ratio from non-pulse breakup events ranges between 0.35 and 62. Only 4% of non-pulse breakup events fall in the range exhibited by the pulse breakup events. Once more we seek the threshold ratio of off-time and preceding on-time at the point where the difference between the two CDFs is largest. Figure 4.9(b) shows the difference between the two CDFs over the range from 0 to 2.5 at steps of 0.01. The peak is observed at 1.2 and we take this as the threshold for the ratio of off-time and preceding on-time test, yielding Equation 4.10,

$$\frac{\text{OffT}_1}{\text{OnT}_1} \leq 1.2 \quad (4.10)$$

4.2.4 20th percentile off-time

As shown in Equation 4.6, the dynamic off-time in congestion depends on the median on-time over 41 successive pulses, centered on the current pulse. Usually speeds are stable enough for this constraint to hold, but under heavy congestion, speeds can change by more than 100% over a sample of 41 vehicles. So, the median on-time over 41 successive pulses is sometimes larger than the microscopic traffic conditions would dictate for the given vehicle. The large threshold of off-time due to large median on-time is more likely to erroneously select non-pulse breakup events and mark them as suspected pulse breakup events. To accommodate these errors, we exploit the fact that the off-time in a pulse breakup is usually shorter than the off-time between two successive vehicles. Or more formally, we assume that the off-time in a suspected pulse breakup should fall within the lowest 20% of off-times observed in the 41 successive pulses. For example, Figure 4.10(a) shows a CDF of off-time in 41 successive pulses during free flow conditions at station 9 northbound, highlighting the off-time in a pulse breakup at 19/60 seconds. This pulse breakup falls just below the 10th percentile of the distribution. Repeating this procedure for each pulse breakup at station 9 northbound, Figure 4.10(b) shows the CDF of the percentile of off-time of the pulse breakup events within their respective sample of 41 successive pulses. We can see that the off-time associated with the pulse breakup events is usually under the 20th percentile in the given sample of 41 successive pulses. From the congested data (station 3 northbound on April 18, 2008), we verify that the 20th percentile off-time also holds for congested conditions. The same procedure from Figure 4.10(b)

is repeated for the congested data and the result is shown in Figure 4.11. Of the 116 pulse breakup events observed in this data set, 112 of them fall within the 20th percentile in the given sample of 41 successive pulses. The four cases with higher percentile off-time occurred when the speed of the vehicle with pulse breakup is extremely low relative to the speeds of the remaining vehicles.³² Consequently, any event suspected of being a pulse breakup by the other tests but falling above the 20th percentile off-time for the given 41 pulses is no longer suspected of being a pulse breakup. The test is formalized in Equation 4.11.

$$\text{OffT}_1 \leq P_{20}(\text{off-times})_{41\text{pulses}} \quad (4.11)$$

4.2.5 Maximum vehicle length

When a pulse breakup occurs, using the notation in Figure 4.2, OnT^A should be at least equal to the sum of OnT_1 , OnT_2 and OffT_1 , denoted OnT^{sum} . For each suspected pulse breakup event that has passed all of the preceding tests, the product of estimated speed and OnT^{sum} yields an estimated vehicle length in the absence of a pulse breakup, i.e., as if OffT_1 never occurred. If the estimated vehicle length from OnT^{sum} is shorter than the maximum possible vehicle length, the event remains suspect of pulse breakup. Otherwise, if the resulting estimated vehicle length exceeds the maximum possible vehicle length, e.g., a short vehicle tailgating a long vehicle, the event is no longer suspected of pulse breakup. The estimated vehicle length for these suspected pulse breakup events can be calculated from the estimated individual vehicle speed multiplied by OnT^{sum} . As mentioned previously, the individual vehicle speed is estimated from the assumed effective vehicle length, \tilde{L} , divided by the median on-time for 41 successive pulses. Formalizing the test, a suspected pulse breakup is retained if Equation 4.12 is met and discarded otherwise.

$$\frac{\tilde{L}}{\text{median}(\text{on-times})_{41\text{pulses}}} \times \text{OnT}^{\text{sum}} \leq L_{\text{Threshold}} \quad (4.12)$$

To set maximum possible vehicle length, $L_{\text{Threshold}}$, we examined the effective vehicle length measured from dual loop detectors. Few vehicles should have true effective lengths over 85 ft, e.g., Figure 4.12 shows the distribution of measured vehicle length over the entire month of April, 2008, at a dual loop detector station, station 1 northbound and the maximum observed length is less than 85ft. However, a long vehicle's estimated length could be slightly longer than its actual length because a long vehicle's speed in free flow traffic may be slightly lower than the median speed. The median speed is expected to

³² This feature can cause violation of maximum vehicle length test that will be discussed shortly, i.e., the given estimated vehicle length is greater than the maximum vehicle length threshold due to high estimated speed and long measured on-time.

come from a passenger vehicle in Equation 2.4 but some locations have a different speed limit for trucks than for passenger cars, while in other locations passenger cars may be more likely to speed than trucks. So $L_{\text{Threshold}}$ is set to a conservative value of 100 ft, corresponding to an 85 ft long vehicle traveling at 55 mph but with an estimated speed of 65 mph. So if the estimated vehicle length from OnT^{sum} of a suspected pulse breakup is greater than 100 ft, the given event is no longer suspected of pulse breakup.

4.2.6 The pulse breakup detection algorithm for single loop detectors

Combining all of these tests into an algorithm to differentiate between pulse breakup events and non-pulse breakup events, Figure 4.13 shows the flow chart of the algorithm. To make the flowchart more intuitive, we replace OnT_1 , OnT_2 , and OffT with their relative descriptions within the given pair of pulses: “preceding on-time”, “following on-time” and “off-time”, respectively. The process consists of six steps. If two successive pulses satisfy the sequence of checks, these pulses are suspected of pulse breakup. Otherwise, these pulses are considered to be from separate vehicles and no pulse breakup is suspected between the pair. The process is repeated over all successive pulses in each lane. This algorithm is designed to work at single loop detectors, though obviously it could also be applied individually to each loop detector in a dual loop detector.³³

When a pair of successive pulses is labeled by the algorithm as a pulse breakup, the two pulses can be combined (OnT^{sum}) as an estimate of OnT^{A} to improve the accuracy of both the on-time and the vehicle count. While any detector should exhibit an occasional pulse breakup event, if these events are frequent, the algorithm can flag the detector as exhibiting suspicious behavior. In other words, if the number of suspected pulse breakup events retained by the algorithm is too large compared to the non-pulse breakup events, e.g., more than 1% of successive pairs of pulses are suspected of being pulse breakup by the algorithm³⁴, then a technician should be dispatched. Though as will be shown in Section 4.3, the algorithm exhibits better performance during free flow than it does during the more challenging congested conditions, so it is likely that such overall performance assessment would best be done during free flow periods.

³³ It should be clear, however, that the methodology can easily be extended to use measured speed from dual loop detectors to further improve performance of two steps: the dynamic off-time and the maximum vehicle length

³⁴ The threshold rate of suspected pulse breakup to flag the detector as exhibiting a detector error will be discussed in section 4.3.3, based on the stations without pulse breakup events.

4.3 Evaluation of the pulse breakup detection algorithm for single loop detectors

First, the algorithm from Figure 4.13 is applied to the 2 hr long development data set from station 9 northbound. Table 4.1 summarizes the performance of the algorithm on these data. The total pulses column tallies the number of pulses recorded by the detector during the video data collection. The actual pulse breakup column tallies the number of pulse breakup events seen from the ground truth data, while the suspected pulse breakup column tallies the number of events labeled by the algorithm as being pulse breakup events. The final three columns come from comparing the individual suspected pulse breakup events against the individual actual pulse breakup events. The success column counts the number of times that the algorithm correctly caught an actual pulse breakup, while the false positive column counts the number of times that the algorithm erroneously labeled a non-pulse breakup as a suspected pulse breakup event. Any actual pulse breakup events that were not included in the success column are counted in the false negative column, i.e., the algorithm failed to catch the given pulse breakup event. The algorithm correctly identifies 293 out of 306 actual pulse breakup events (96%) and it missed 13 actual pulse breakup events (4%). Three suspected pulse breakup events are false positives since they do not correspond to actual pulse breakup events. Two of the three false positive errors were due to tailgating. The other false positive error was due to a lane changing maneuver. The false positive errors found by the pulse breakup detection algorithm will be discussed in detail below.

4.3.1 Performance during free flow conditions

Moving now to the test data, Table 4.2 shows the 22 ground truthed data sets recorded during free flow conditions.³⁵ The data are sorted by those sets with and without pulse breakup. The data include 8 hr 20 min from 10 directional locations with pulse breakup (including the one development set) and 5 hr 12 min from 12 locations without pulse breakup. None of the locations with pulse breakup suffered from splashover, but four of the locations without pulse breakup did exhibit splashover, as indicated with an asterisk in the station number column. Much as was done for the development set in Table 4.1, all of the data sets from Table 4.2 were used to evaluate the performance of the pulse breakup detection algorithm for single loop detectors.

³⁵ Note, in the case of dual loop detectors, only the upstream loop detector is included in this evaluation of the single loop detector test.

The performance of the algorithm during free flow conditions is summarized in Table 4.3. The non-pulse breakup data are shown combined, and then repeated a second time, split between splashover and non-splashover stations. The pulse breakup data excluding the development data set, i.e., station 9 northbound, are also presented in the table. Detailed results from the stations with pulse breakup are presented in Table 4.4 and for stations without pulse breakup in Table 4.5. From Table 4.3, the algorithm correctly catches 677 out of 722 pulse breakup events (93.8%), thus our algorithm does not catch 45 pulse breakup events. From all of the data (i.e., both with and without pulse breakup), 78 out of 47,705 pulses (0.16%) are erroneously marked as suspected pulse breakup. From the pulse breakup data excluding a development data set, the algorithm correctly catches 384 out of 416 pulse breakup events (92.3%).

The last three columns of Table 4.3 through Table 4.5 tally the underlying reason whenever two valid successive pulses were erroneously marked as a suspected pulse breakup, i.e., a false positive error. As one might expect, “Tailgating” indicates two vehicles pass with a very small headway. In our algorithm, since the boundary of off-time in a pulse breakup during free flow conditions is assumed to be 20/60 seconds, given 65 mph in free flow speed and 6 ft for the size of the detection zone, the maximum L^P_x in Figure 4.2 attributed to causing dropout is 38 ft. So, if the gap distance between the following vehicle and the preceding vehicle is less than 38 ft, these vehicles may be erroneously labeled as suspected pulse breakup events by the algorithm and result in a false positive error. “LCM” (short for “Lane Change Maneuver”) indicates that at least one of the two pulses is generated from a vehicle changing lanes over the given loop detector³⁶. “Splashover” indicates that one of the two pulses was due to a splashover error from an adjacent lane (as per Chapter 3). Overall, the false positive errors due to splashover are 27 out of 78 (35%). At the four locations with splashover, splashover is the dominant cause of false positives, about 71% (27 out of 38). It is evidence that splashover problems can degrade the performance of the pulse breakup detection algorithm. Except for two loop detectors (lane 2 at station 38 westbound and at station 41 eastbound from Table 3.4), all of the stations and lanes exhibiting splashover in this set were previously labeled as stations with splashover in section 3.6. If loop detectors with splashover can be identified and fixed, obviously the false positive pulse breakup detection error arising from splashover will be reduced.

³⁶ Note that a vehicle changing lanes over a loop detector station may be recorded by loop detectors in two adjacent lanes, just one of the lanes, or neither lane, depending on the size of the detection zone in each lane. The LCM column in the tables just includes the first two cases, since the last case will not register any pulses and will not create a situation that may be suspected by the algorithm as being a pulse breakup.

4.3.2 Performance during congested conditions

Now moving to the more challenging congested conditions, Table 4.6 shows the nine ground truthed data sets recorded during congested conditions. Like the free flow conditions, the data are sorted by those sets with and without pulse breakup. The data include 2 hr 15 min from four directional locations with pulse breakup and 2 hr and 21 min from five locations without pulse breakup. None of the locations with pulse breakup suffered from splashover, but three of the locations without pulse breakup did exhibit splashover, as indicated with an asterisk in the station number column. For reference, the time series of speed from these locations are presented in Appendix G.

The performance of the algorithm during congested conditions is summarized in Table 4.7. Once more the non-pulse breakup data are shown combined, and then repeated a second time, split between splashover and non-splashover stations.³⁷ Detailed results from the stations with pulse breakup are presented in Table 4.8 and for stations without pulse breakup in Table 4.9. From Table 4.7, the algorithm correctly catches 157 out of 169 pulse breakup events (92.8%), thus 12 pulse breakup events are not caught by our algorithm. From all of the data (i.e., both with and without pulse breakup), 176 out of 20,576 pulses (0.86%) are erroneously marked as suspected pulse breakup. Overall the false positive errors due to splashover now account for only 27 out of 176 (15%), while the false positives due to tailgating are 127 out of 176 (72%). Compared to the performance of the algorithm in free flow conditions, the success rate has dropped by almost 2%, but remains above 92% and the false positive rate has increased by a factor of 5, i.e., increasing from 0.2% to 0.9%, but remains below 1%. In particular, false positive errors due to tailgating are much more frequent in congested conditions. As mentioned above, a false positive error due to tailgating indicates that the physical gap between two vehicles is under 38 ft, the maximum distance of L^P_X . In congested conditions, one should expect to see a shorter physical gap between two successive vehicles due to the lower speeds and this fact is reflected in the higher rate of false positive errors. Not all vehicles with a physical gap under 38 ft result in false positive errors, since the remaining tests in the algorithm will still successfully reject many of these cases.

One area of future research is this physical gap during congestion. Performance of the algorithm may be improved either by limiting it to median speeds above a certain threshold, or by handling the physical gap differently when speeds are low.

³⁷ Note that although station 3 northbound was used earlier for illustrative purposes during congestion, it was not used in deriving the parameters and settings. So unlike the free flow case, there was no development data for the congested case.

4.3.3 The suspected pulse breakup rate

The pulse breakup detection algorithm for single loop detectors was designed to identify individual pulse breakup errors and as shown in the above sections, and it exhibited fairly good performance identifying pulse breakup events both in free flow and in congested conditions. The rate of identified pulse breakup events can be used to flag the detector as exhibiting suspicious behavior if the number of suspected pulse breakup events found by the algorithm is too large compared to the non-pulse breakup events.

Again, we use the summary of the performance of the algorithm during free flow and congested conditions to examine loop detectors with pulse breakup, as shown in Table 4.10. The last four columns of Table 4.10 present the average actual pulse breakup rate, suspected pulse breakup rate, success rate, and false positive rate across all detectors. These rates are all relative to the total number of pulses. During free flow, the detectors that actually exhibit pulse breakup have much higher suspected pulse breakup rate than the non-pulse breakup detectors, by a factor of 4. During congestion, the detectors that actually exhibit pulse breakup still have a higher suspected pulse breakup rate than the non-pulse breakup detectors, but the difference between the two is very small. As discussed in section 4.3.2, false positive errors due to tailgating are much more frequent in congested conditions. So free flow conditions should be more robust to diagnose loop detectors with pulse breakup, compared to doing so during congested conditions.

To automatically identify loop detectors with chronic pulse breakup, we compare the suspected pulse breakup rate between loop detectors with pulse breakup and those without pulse breakup from free flow data. The loop detectors in Table 4.2 are segregated into two groups, the 29 with actual pulse breakup (now simply termed “pulse breakup”), and the 41 without (termed “non-pulse breakup”). The actual pulse breakup rate and suspected pulse breakup rate at each loop detectors are calculated, relative to the total number of pulses. As expected, a loop detector with pulse breakup has positive actual pulse breakup rate, while a loop detector without pulse breakup has zero actual pulse breakup rate. Figure 4.14 shows a scatter plot of actual pulse breakup rate and suspected pulse breakup rate from each loop detector during free flow conditions over a total 70 loop detectors. From the loop detectors with pulse breakup, the suspected pulse breakup rate and actual pulse breakup rate show a near linear relationship, with two exceptions, lane 4 at station 4 northbound and southbound, that deviate from the linear relationship having a positive actual pulse breakup rate, but zero suspected pulse breakup rate. In detail, both loop detectors have a single pulse breakup event, but no suspected pulse breakup events are found. Since both detectors had a relatively small number of total pulses, they exhibited a relatively high actual pulse breakup rate.

From the non-pulse breakup loop detectors, most (37 out of 41 loop detectors) have suspected pulse breakup rate under 1% and the remaining four loop detectors has suspected pulse breakup rate in a range of 1.3 % and 4.4%. Three out of the four loop detectors with the highest suspected pulse breakup rate from non-pulse breakup data had splashover problems that increased the false positive errors. Using a threshold of 1% rate of suspected pulse breakup events would catch 59% of the loop detectors that exhibited pulse breakup (17 out of 29 loop detectors). Those that are missed all exhibited an actual pulse breakup rate below 1.2%. The threshold would also correctly identify 90% of the non-pulse breakup loop detectors (37 out of 41 loop detectors), which increases to 97% among those without splashover (36 out of 37 loop detectors).

Finally, when applying the pulse breakup detection algorithm for single loop detectors in practice, during free flow the algorithm appears beneficial for differentiating between detectors with and without pulse breakup events. When congestion sets in, the algorithm continues to yield benefits at detectors with pulse breakup (as identified during free flow periods) but the increased rate of false positives at detectors without pulse breakup events begins to outweigh the benefits. Taking a conservative path, if a loop detector does not test positive for pulse breakup during free flow conditions (i.e., suspected pulse breakup rate is under 1%), it would likely be best to suppress the algorithm during congestion.

4.4 Sensitivity of the algorithm to the choice of threshold values

There are several parameters in the algorithm to identify pulse breakup in single loop detector data that were derived from one detector station (station 9 northbound) using only the 2 hr long development set. The preceding results are based on the assumption that the nature of pulse breakup events observed at the development location is similar to all of the detector stations. While it is not possible to test stations for which we do not have data, the assumption will be examined using the data with pulse breakup from the evaluation set enumerated in Table 4.2. This section examines the optimal threshold for the ratio of on-times between two pulses and the optimal threshold for the ratio of off-time and the preceding on-time in the algorithm, repeating the analysis from Figure 4.6 and Figure 4.9, but now using the entire free flow evaluation data set with pulse breakup from Table 4.2 (excluding the development set).

First the on-time ratio threshold is evaluated, holding the other parameters constant. The on-time ratio is stepped from 0.1 to 1.1 at increments of 0.01. The ratio is also set to infinity, i.e., the results of the algorithm excluding *the on-time ratio test* altogether. Figure 4.15 shows the evolution of the false positive error, the false negative error and the sum of the two errors. In general, as the on-time ratio increases, the false positive error increases, but the false negative error decreases. The sum of the two is minimized

when the on-time ratio threshold is between 0.72 and 0.76 (all of the tested values except 0.74). The original on-time ratio, 0.72, falls within this range.

Second the ratio of off-time and preceding on-time is evaluated, holding the other parameters constant. The ratio is stepped from 0 to 1.5 at increments of 0.1. The ratio is also set to infinity, i.e., the results of the algorithm excluding *the ratio of off-time and preceding on-time test* altogether. Figure 4.16 shows the evolution of the false positive error, the false negative error and the sum of the two errors. In general, as the ratio increases, the false positive error increases, but the false negative error decreases. The sum of the two is minimized when the ratio of off-time and preceding on-time threshold is between 1.2 and 1.3. The original ratio of off-time and preceding on-time, 1.2, falls within this range.

Finally, varying both the *on-time ratio*, and *the ratio of off-time and preceding on-time thresholds*, Figure 4.17 shows the resulting performance. The ratio of off-time and preceding on-time is varied from 0.7 to 1.5 at increments of 0.1, separated by the bold vertical dashed lines. Between each pair of bold dashed lines, the on-time ratio is varied between 0.69 and 0.78 at increments of 0.01. In total 90 combinations are tested, 10 values of the on-time ratio threshold and 9 values of the off-time ratio threshold. The sum of the two errors is minimized when the on-time ratio is between 0.72 and 0.76 (all of the tested values except 0.74) at the off-time ratio threshold of 1.2 and when the on-time ratio is between 0.71 and 0.75 (all of the tested values except 0.74) at the off-time ratio threshold of 1.3. The original on-time ratio, 0.72, and the ratio of off-time and preceding on-time, 1.2, falls within this range. These results suggest that the calibration from one location is transferable to the other locations in this study. Though it is possible that these results may still exhibit biases that are common across the entire Columbus Metropolitan Freeway Management System, so if such microscopic event data become available from other metropolitan areas, it would be advisable to test the calibration on those facilities as well.

4.5 Performance of the pulse breakup detection algorithm

We compared the performance of two earlier pulse breakup detection algorithms (from Section 4.1) against our algorithm [L&C] using the data underlying Table 4.2 and Table 4.6 (excluding the development data set). In previous studies, Chen and May (1987), [C&M], used a static threshold of the time gap (i.e., the off-time between two successive pulses) of 15/60 seconds, while Cheevarunothai et al. (2007), [CYN], used a static threshold of the time headway (the sum of a successive off-time and on-time) of 38/60 seconds. Both algorithms considered two successive pulses as a suspected pulse breakup if the metric (off-time for C&M or the time headway for CYN) is below the given threshold criterion. The performance of each algorithm is evaluated in terms of the number of success, false positive, and false negative, summed across all of the detectors with ground truth data, as shown in Table 4.11.

For detectors with pulse breakup in free flow conditions, the success column shows that our algorithm, L&C, caught 36% more pulse breakup events than C&M, and 38% more than CYN. As a direct result, our false negative rate was smaller, on the order of one quarter the size of either of the earlier methods. Our false positive rate was an 1/6 of C&M and 1/60 of CYN. For detectors without pulse breakup in free flow conditions, our false positive rate was 38% of C&M and 11% of CYN.

For detectors with pulse breakup in congested conditions, our algorithm caught more than three times as many pulse breakup events than C&M and more than 10 times as many as CYN. As a direct result, our false negative rate was an order of magnitude smaller in size compared to either of the earlier methods. Our false positive rate was roughly 5 times larger than C&M and identical to CYN. Compared to C&M, the 18 extra false positives by our algorithm is much smaller than the 108 extra successes. For detectors without pulse breakup in congested conditions, our false positive rate was 19% larger than C&M and 26% larger than CYN.

4.6 A brief before and after study of loop detector sensitivity

This section seeks to illustrate the diagnostic power of the test to correct pulse breakup problems. We selected two detector stations with many suspected pulse breakup events, namely station 3 (northbound and southbound) and station 9 (northbound and southbound). Our team asked the operating agency (the Ohio Department of Transportation, ODOT) to increase the detector sensitivity setting of all loop detectors at both stations. ODOT completed the changes on June 9, 2009 and reported that the sensitivity levels in all lanes at station 3 were increased from “Normal” to “High” and all lanes at station 9 were increased from “Low” to “High”. A second round of video data was collected for each station in both directions in free flow conditions after the change: 30 min (10:21 ~ 10:51) on June 17, 2009 from station 3 and 36 min (10:05 ~ 10:41) on June 17, 2009 from station 9. Table 4.12 shows the performance at each station relative to the ground truth data before and after the change of the loop detector sensitivity. All of the data come from free flow conditions. Note that we did not normalize for the different sample sizes before and after. After the sensitivity level of a loop detector with pulse breakup errors is set high, the pulse breakup errors disappeared at all of the loop detectors. However, at one detector (lane 1 at station 9 southbound) we overcompensated and went from suffering from pulse breakup to suffering from splashover.³⁸

³⁸ Obviously, an increase in detector sensitivity should reduce the occurrence of pulse break up, while increasing the likelihood of splashover and related errors.

Next, applying the pulse breakup algorithm for single loop detectors after the change, Table 4.13 shows that the pulse breakup algorithm had 27 suspected pulse breakup events that all turn out to be non-pulse breakup events, or roughly 0.3% of the total number of pulses from the 14 loop detectors. Lane 1 at station 9 southbound reports a relatively high number of suspected pulse breakup events. It is the only detector that the algorithm would suspect of pulse breakup after the sensitivity changes. As noted, all of the suspected pulse breakups are false positives at this detector, most of which turn out to arise from splashover errors. After making the change, the splashover detection algorithm discussed in Chapter 3 correctly classified this loop detector as exhibiting splashover and all of the other detectors being without splashover, as shown in Table 4.14. Excluding lane 1 at station 9 southbound, roughly 0.2% of the total number of pulses in Table 4.13 are suspected of pulse breakup.

Table 4.1, The performance of the proposed algorithm to identify pulse breakup events in the development set: free flow traffic conditions at station 9 northbound over 2 hrs

Station number (Direction)	Lane number	Total pulses	Actual pulse breakup	Suspected pulse breakup	Performance		
					Success	False positive	False negative
9 (NB)	1	2,386	6	8	6	2	0
	2	2,900	208	197	197	0	11
	3	2,277	92	91	90	1	2
Total		7,563	306	298	293	3	13

Table 4.2, Ground truth data collection dates and times from free flow conditions. The total recorded time of video data is 500 min from locations with pulse breakup and 253 min from locations without pulse breakup. NB=northbound, SB=southbound, EB=eastbound, and WB=southbound.

Status of data	Station number	Direction	Number of lanes	Date	Start Time (hh:min)	End Time (hh:min)	Duration of time (hh:min)
With pulse breakup	3	NB	4	March 17, 2008	10:57	11:20	0:23
	3	SB	4	April 18, 2008	15:55	16:55	1:00
	4	NB	4	September 9, 2008	16:55	17:15	0:20
	4	SB	4	March 17, 2008	10:15	10:35	0:20
	6	NB	3	April 18, 2008	15:55	16:55	1:00
	9	NB	3	June 5, 2006	12:20	14:20	2:00
	9	SB	3	June 5, 2006	12:20	14:20	2:00
	15	NB	3	March 10, 2009	17:18	17:47	0:29
	18	NB	3	March 9, 2009	08:24	08:57	0:33
	19	NB	3	March 17, 2008	09:25	09:40	0:15
Without pulse breakup	2	NB	4	March 9, 2009	17:21	17:50	0:29
	31	NB	4	November 21, 2008	10:35	11:05	0:30
	38	EB	3	August 29, 2008	15:05	15:25	0:20
	38*	WB	4	September 9, 2008	12:05	12:25	0:20
	41*	EB	2	September 9, 2008	11:00	11:35	0:35
	43	EB	3	September 2, 2008	8:50	9:15	0:25
	43	WB	3	September 2, 2008	8:50	9:15	0:25
	56	EB	3	September 3, 2008	16:40	17:25	0:45
	56*	WB	3	November 21, 2008	9:00	9:40	0:40
	102	EB	3	March 10, 2009	17:05	17:20	0:15
	104*	EB	3	March 17, 2008	16:00	16:10	0:10
	104	WB	3	March 12, 2009	17:00	17:18	0:18

*location that exhibited splashover

Table 4.3, Summary of the performance of the pulse breakup detection algorithm for single loop detectors during free flow conditions

During free flow conditions		Total pulses	Actual pulse breakup	Suspected pulse breakup	Performance			Reason of false positive		
Data					Success	False positive	False negative	Tailgating	LCM	Splashover
with pulse breakup (including development data)		34,401	722	693	677	16	45	12	4	0
without pulse breakup		13,304	0	62	-	62	-	12	23	27
Total		47,705	722	755	677	78	45	24	27	27
With pulse breakup (excluding development data)		26,838	416	397	384	13	32	10	3	0
without pulse breakup	with splashover	3,758	0	38	-	38	-	4	7	27
	without splashover	9,546	0	24	-	24	-	8	16	0

Table 4.4, Performance of the pulse breakup detection algorithm for single loop detectors from the data with pulse breakup during free flow conditions, by detector (in the case of dual loop detector stations only the upstream loop detector is used). NB=northbound and SB=southbound

Date	Station number (Direction)	Lane number	Flow (vehs/hr)	Total pulses	Actual pulse breakup	Suspected pulse breakup	Performance			Reason of False positive		
							Success	False positive	False negative	Tailgating	LCM	Splashover
March 17, 2008	3 (NB)	1	947	310	6	6	6	0	0	-	-	-
		2	1,287	420	23	21	21	0	2	-	-	-
		3	1,098	359	16	13	12	1	4	1	0	0
		4	513	168	2	2	2	0	0	-	-	-
April 18, 2008	3 (SB)	1	963	995	1	2	1	1	0	1	0	0
		2	1,743	1,806	9	9	9	0	0	-	-	-
		3	1,484	1,537	4	4	4	0	0	-	-	-
		4	1,100	1,139	2	3	2	1	0	1	0	0
September 9, 2008	4 (NB)	3	2,081	619	10	10	9	1	1	0	1	0
		4	427	124	1	0	0	0	1	-	-	-
March 17, 2008	4 (SB)	1	635	225	0	0	-	0	-	-	-	-
		2	1,464	523	19	18	18	0	1	-	-	-
		3	1,503	533	21	13	13	0	8	-	-	-
		4	240	83	1	0	0	0	1	-	-	-
April 18, 2008	6 (NB)	1	2,201	2,249	26	25	25	0	1	-	-	-
		2	1,922	1,962	58	55	55	0	3	-	-	-
		3	1,708	1,747	8	9	8	1	0	0	1	0
June 5, 2006	9 (NB)	1	1,195	2,386	6	8	6	2	0	1	1	0
		2	1,450	2,900	208	197	197	0	11	-	-	-
		3	1,140	2,277	92	91	90	1	2	1	0	0
June 5, 2006	9 (SB)	1	1,218	2,434	2	7	2	5	0	4	1	0
		2	1,482	2,964	21	22	20	2	1	2	0	0
		3	1,144	2,288	107	106	105	1	2	1	0	0
March 10, 2009	15 (NB)	1	2,333	1,173	5	3	3	0	2	-	-	-
		2	1,878	940	24	23	23	0	1	-	-	-
		3	1,795	899	11	8	8	0	3	-	-	-
March 9, 2009	18 (NB)	1	1,086	197	0	0	-	0	-	-	-	-
		2	1,248	227	13	13	13	0	0	-	-	-
		3	769	140	3	3	3	0	0	-	-	-
March 17, 2008	19 (NB)	1	733	186	0	0	-	0	-	-	-	-
		2	1,174	297	13	13	13	0	0	-	-	-
		3	1,163	294	10	9	9	0	1	-	-	-
Total			1,359	34,401	722	693	677	16	45	12 (75%)	4 (25%)	0 (0%)

Table 4.5, Performance of the pulse breakup detection algorithm for single loop detectors from the data without pulse breakup during free flow conditions, by detector (in the case of dual loop detector stations only the upstream loop detector is used). NB=northbound, EB=eastbound and WB=westbound

Date	Station number (Direction)	Lane number	Flow (vehs/hr)	Total pulses	Actual pulse breakup	Suspected pulse breakup	Performance			Reason of False positive		
							Success	False positive	False negative	Tailgating	LCM	Splashover
March 9, 2009	2 (NB)	1	1,345	628	0	2	-	2	-	1	1	0
		2	1,377	642	0	1	-	1	-	0	1	0
		3	1,128	526	0	1	-	1	-	0	1	0
		4	100	45	0	0	-	0	-	-	-	-
November 21, 2008	31 (NB)	1	245	124	0	0	-	0	-	-	-	-
		2	575	296	0	0	-	0	-	-	-	-
		3	430	220	0	3	-	3	-	1	2	0
		4	55	27	0	0	-	0	-	-	-	-
August 29, 2008	38 (EB)	1	1,483	355	0	1	-	1	-	1	0	0
		2	1,374	331	0	1	-	1	-	1	0	0
		3	682	164	0	1	-	1	-	1	0	0
September 9, 2008	38 (WB)	1	747	172	0	0	-	0	-	-	-	-
		2	1,024	242	0	0	-	0	-	-	-	-
		3	864	206	0	9	-	9	-	0	0	9
		4	247	56	0	0	-	0	-	-	-	-
September 9, 2008	41 (EB)	1	667	337	0	6	-	6	-	0	0	6
		2	1,000	507	0	2	-	2	-	2	0	0
September 2, 2008	43 (EB)	1	736	262	0	1	-	1	-	0	1	0
		2	1,172	419	0	0	-	0	-	-	-	-
		3	1,078	384	0	1	-	1	-	0	1	0
September 2, 2008	43 (WB)	1	1,401	500	0	0	-	0	-	-	-	-
		2	1,650	590	0	3	-	3	-	0	3	0
		3	1,242	444	0	2	-	2	-	0	2	0
September 3, 2008	56 (EB)	1	964	596	0	1	-	1	-	0	1	0
		2	1,243	771	0	4	-	4	-	3	1	0
		3	521	322	0	0	-	0	-	-	-	-
November 21, 2008	56 (WB)	1	548	345	0	0	-	0	-	-	-	-
		2	1,004	632	0	5	-	5	-	0	5	0
		3	193	121	0	1	-	1	-	0	0	1
March 10, 2009	102 (EB)	1	1,059	189	0	1	-	1	-	0	1	0
		2	1,766	320	0	1	-	1	-	0	1	0
		3	1,785	322	0	0	-	0	-	-	-	-
March 17, 2008	104 (EB)	1	2,164	441	0	11	-	11	-	0	0	11
		2	1,718	349	0	1	-	1	-	0	1	0
		3	1,723	350	0	3	-	3	-	2	1	0
March 12, 2009	104 (WB)	1	1,387	359	0	0	-	0	-	-	-	-
		2	1,605	415	0	0	-	0	-	-	-	-
		3	1,142	295	0	0	-	0	-	-	-	-
Total			927	13,304	0	62	-	62	0	12 (19%)	23 (37%)	27 (44%)

Table 4.6, Ground truth data collection dates and times from congested conditions NB=northbound, SB=southbound, EB=eastbound, and WB=southbound.

Status of data	Station number	Direction	Number of lanes	Date	Start Time (hh:min)	End Time (hh:min)	Duration of time (hh:min)
With pulse breakup	3	NB	4	March 21, 2008	16:35	16:50	0:15
	3	NB	4	April 18, 2008	15:55	16:55	1:00
	4	NB	4	September 9, 2008	17:15	17:55	0:40
	9	SB	3	April 7, 2008	07:50	08:10	0:20
Without pulse breakup	41*	EB	2	March 12, 2009	16:40	17:06	0:26
	43	EB	3	March 12, 2009	17:07	17:48	0:41
	56*	WB	3	September 3, 2008	16:40	17:25	0:45
	102	EB	3	March 10, 2009	16:46	17:05	0:19
	104*	EB	3	March 17, 2008	16:10	16:20	0:10

*location that exhibited splashover

Table 4.7, Summary of the performance of the pulse breakup detection algorithm for single loop detectors during congested conditions

During congestion		Total pulses	Actual pulse breakup	Suspected pulse breakup	Performance			Reason of False positive		
Data	Success				False positive	False negative	Tailgating	LCM	Splashover	
with pulse breakup		10,721	169	181	157	24	12	24	0	0
without pulse breakup		9,855	0	152	-	152	-	103	22	27
Total		20,576	169	333	157	176	12	127	22	27
without pulse breakup	with splashover	5,177	0	97	-	97	-	52	18	27
	without splashover	4,678	0	55	-	55	-	51	4	0

Table 4.8, Performance of the pulse breakup detection algorithm for single loop detectors from the data with pulse breakup during congested conditions. NB=northbound and SB=southbound

Date	Station number (Direction)	Lane number	Flow (vehs/hr)	Total pulses	Actual pulse breakup	Suspected pulse breakup	Performance			Reason of False positive		
							Success	False positive	False negative	Tailgating	LCM	Splashover
March 21, 2008	3 (NB)	1	1,712	404	4	2	2	0	2	-	-	-
		2	1,565	369	6	6	6	0	0	-	-	-
		3	1,628	387	10	10	10	0	0	-	-	-
		4	890	208	3	3	3	0	0	-	-	-
April 18, 2008	3 (NB)	1	1,799	1789	36	43	36	7	0	7	0	0
		2	1,628	1619	47	48	44	4	3	4	0	0
		3	1,490	1482	29	30	25	5	4	5	0	0
		4	866	920	4	5	3	2	1	2	0	0
September 9, 2008	4 (NB)	3	1,967	1201	12	11	10	1	2	1	0	0
		4	493	298	1	1	1	0	0	-	-	-
April 7, 2008	9 (SB)	1	2,230	758	0	2	-	2	-	2	0	0
		2	2,069	704	3	6	3	3	0	3	0	0
		3	1,712	582	14	14	14	0	0	-	-	-
Total			1,484	10,721	169	181	157	24	12	24 (100%)	0 (0%)	0 (0%)

Table 4.9, Performance of the pulse breakup detection algorithm for single loop detectors from the data without pulse breakup during congested conditions. EB=eastbound and WB=westbound

Date	Station number (Direction)	Lane number	Flow (vehs/hr)	Total pulses	Actual pulse breakup	Suspected pulse breakup	Performance			Reason of False positive		
							Success	False positive	False negative	Tailgating	LCM	Splashover
March 12, 2009	41 (EB)	1	2,104	935	0	32	-	32	-	11	6	15
		2	1,654	733	0	24	-	24	-	23	1	0
March 12, 2009	43 (EB)	1	2,031	1,417	0	14	-	14	-	12	2	0
		2	1,894	1,322	0	26	-	26	-	24	2	0
		3	1,682	1,174	0	13	-	13	-	13	0	0
September 3, 2008	56 (WB)	1	2,177	1,350	0	7	-	7	-	5	2	0
		2	1,887	1,171	0	16	-	16	-	7	9	0
		3	530	329	0	3	-	3	-	1	0	2
March 10, 2009	102 (EB)	1	961	171	0	0	-	0	-	-	-	-
		2	1,587	286	0	0	-	0	-	-	-	-
		3	1,699	308	0	2	-	2	-	2	0	0
March 17, 2008	104 (EB)	1	2,331	308	0	10	-	10	-	0	0	10
		2	1,544	204	0	0	-	0	-	-	-	-
		3	1,136	147	0	5	-	5	-	5	0	0
Total			1,706	9,855	0	152	-	152	-	103 (68%)	22 (14%)	27 (18%)

Table 4.10, Summary of the performance of the pulse breakup detection algorithm for single loop detectors during free flow and congested conditions

Traffic conditions	Data	Total pulses	Actual pulse breakup	Suspected pulse breakup	Performance			Actual pulse breakup rate	Suspected pulse breakup rate	Success rate	False positive rate
					Success	False positive	False negative				
Free Flow	with pulse breakup	34,401	722	693	677	16	45	2.1%	2.0%	2.0%	0.0%
	without pulse breakup	13,304	0	62	-	62	-	0%	0.5%	-	0.5%
Conge- sted	with pulse breakup	10,721	169	181	157	24	12	1.6%	1.7%	1.5%	0.2%
	without pulse breakup	9,855	0	152	-	152	-	0%	1.5%	-	1.5%

Table 4.11, Comparison of our proposed algorithm against two previous algorithms for detecting pulse breakup events

Traffic condition	Status of data	Method	Total pulses	Actual pulse breakup	Suspected pulse breakup	Performance		
						Success	False positive	False negative
Free Flow	Pulse breakup	C&M	26,230	416	364	283	81	133
		CYN			1,159	279	880	137
		L&C			397	384	13	32
	Non-Pulse breakup	C&M	13,912	-	162	-	162	-
		CYN			544	-	544	-
		L&C			62	-	62	-
Conge- tion	Pulse breakup	C&M	9,963	169	53	49	4	120
		CYN			36	14	22	155
		L&C			179	157	22	12
	Non-Pulse breakup	C&M	10,613	-	129	-	129	-
		CYN			122	-	122	-
		L&C			154	-	154	-

Table 4.12, Detector performance before and after increasing the loop detector sensitivity setting.
 NB=northbound and SB=southbound

Station number	Direction	Lane number	Before			After			Date (duration) ["Before" data, "After" data]
			Total pulses	Splash-over	Pulse breakup	Total pulses	Splash-over	Pulse breakup	
3	NB	1	310	0	6	479	0	0	[March 17, 2008 (23min), June 17, 2009 (30min)]
		2	420	0	23	687	0	0	
		3	359	0	16	595	0	0	
		4	168	0	2	324	0	0	
3	SB	1	995	0	1	409	0	0	[April 18, 2008 (60min), June 17, 2009 (30min)]
		2	1,806	0	9	831	0	0	
		3	1,537	0	4	611	0	0	
		4	1,139	0	2	397	0	0	
9	NB	1	2,386	0	6	657	0	0	[June 5, 2006 (120min), June 17, 2008 (36min)]
		2	2,900	0	208	784	0	0	
		3	2,277	0	92	624	0	0	
9	SB	1	2,434	0	2	803	68	0	[June 5, 2006 (120min), June 17, 2009 (36min)]
		2	2,964	0	21	908	0	0	
		3	2,288	0	107	673	0	0	
Total			21,983	0	499	8,782	68	0	-

Table 4.13, Summary of the pulse breakup detection algorithm performance on stations where the detector sensitivity was increased to reduce the number of pulse breakup events. NB=northbound and SB=southbound

Station number (Direction)	Lane number	Total Pulses	Actual pulse breakup	Suspected pulse breakup	Performance			Reason of False positive		
					Success	False positive	False negative	Tailgating	LCM	Splashover
3 (NB)	1	479	0	1	0	1	0	1	0	0
	2	687	0	2	0	2	0	2	0	0
	3	595	0	1	0	1	0	0	1	0
	4	324	0	0	0	0	0	-	-	-
3 (SB)	1	409	0	0	0	0	0	-	-	-
	2	831	0	0	0	0	0	-	-	-
	3	611	0	3	0	3	0	0	3	0
	4	397	0	2	0	2	0	2	0	0
9 (NB)	1	657	0	2	0	2	0	0	2	0
	2	784	0	1	0	1	0	1	0	0
	3	624	0	1	0	1	0	1	0	0
9 (SB)	1	803	0	9	0	9	0	3	0	6
	2	908	0	4	0	4	0	3	1	0
	3	673	0	1	0	1	0	1	0	0
Total		8,782	0	27	0	27	0	14	7	6

Table 4.14, Percentage of adjusted suspected splashover relative to source lane from stations where the detector sensitivity was increased to reduce the number of pulse breakup events. NB=northbound and SB=southbound

Station number	Direction	A ratio of adjusted suspected splashover, ARSS [Source lane → Target lane]					
		Lane 1→ Lane 2	Lane 2→ Lane 1	Lane 2→ Lane 3	Lane 3→ Lane 2	Lane 3→ Lane 4	Lane 4→ Lane 3
3	NB	0%	0%	0%	0%	0%	0%
3	SB	0%	0%	0%	0%	0%	0%
9	NB	0%	0%	0%	0%	-	-
9	SB	0%	0.2%	0%	0%	-	-

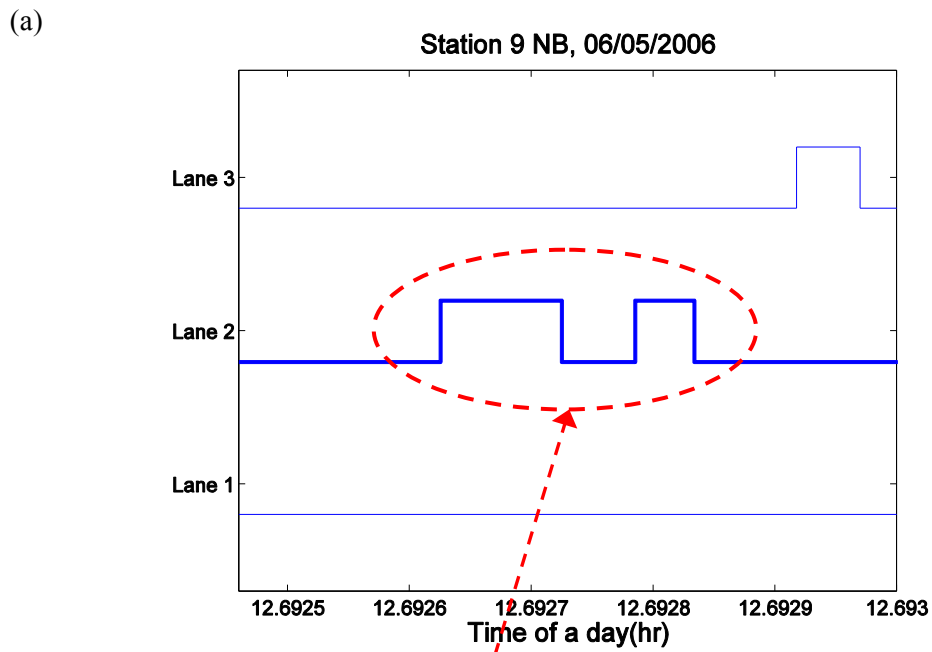


Figure 4.1, (a) A plot of transition pulses with pulse breakup recorded at station 9 northbound and (b) a concurrent video frame showing the two vehicles that gave rise to the three pulses.

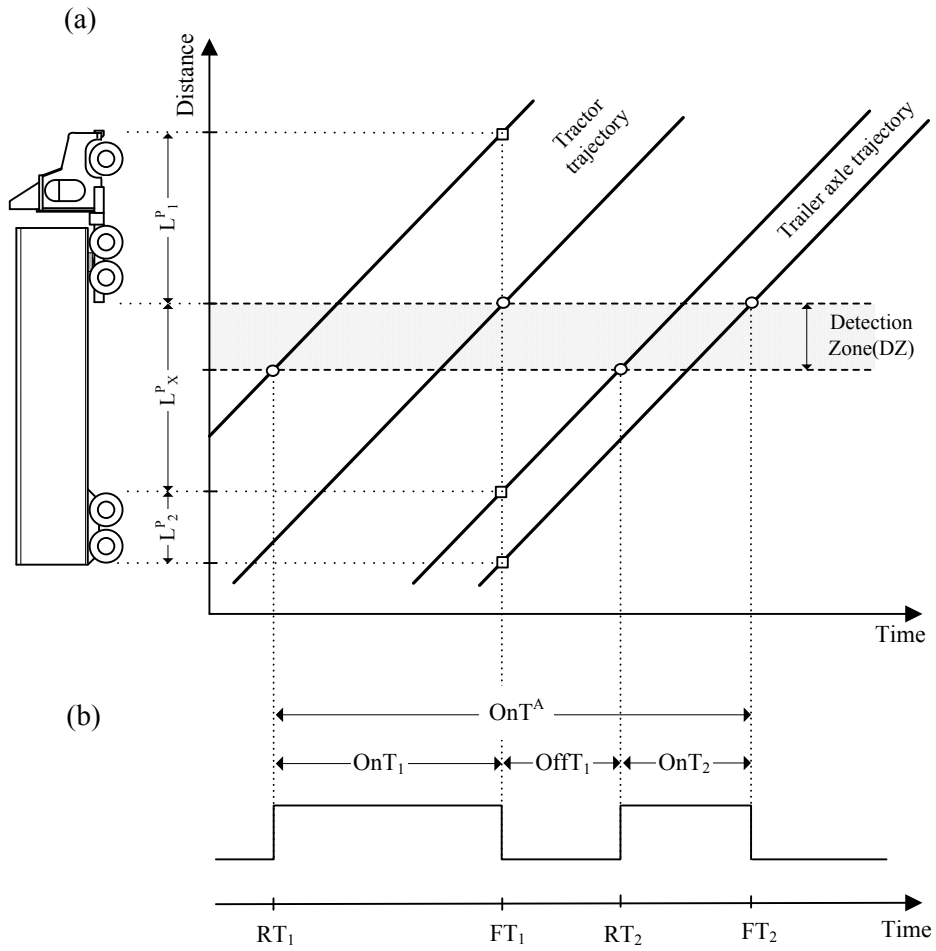


Figure 4.2, (a) a time-space diagram illustrating a hypothetical example of pulse breakups and (b) the associated detector's response

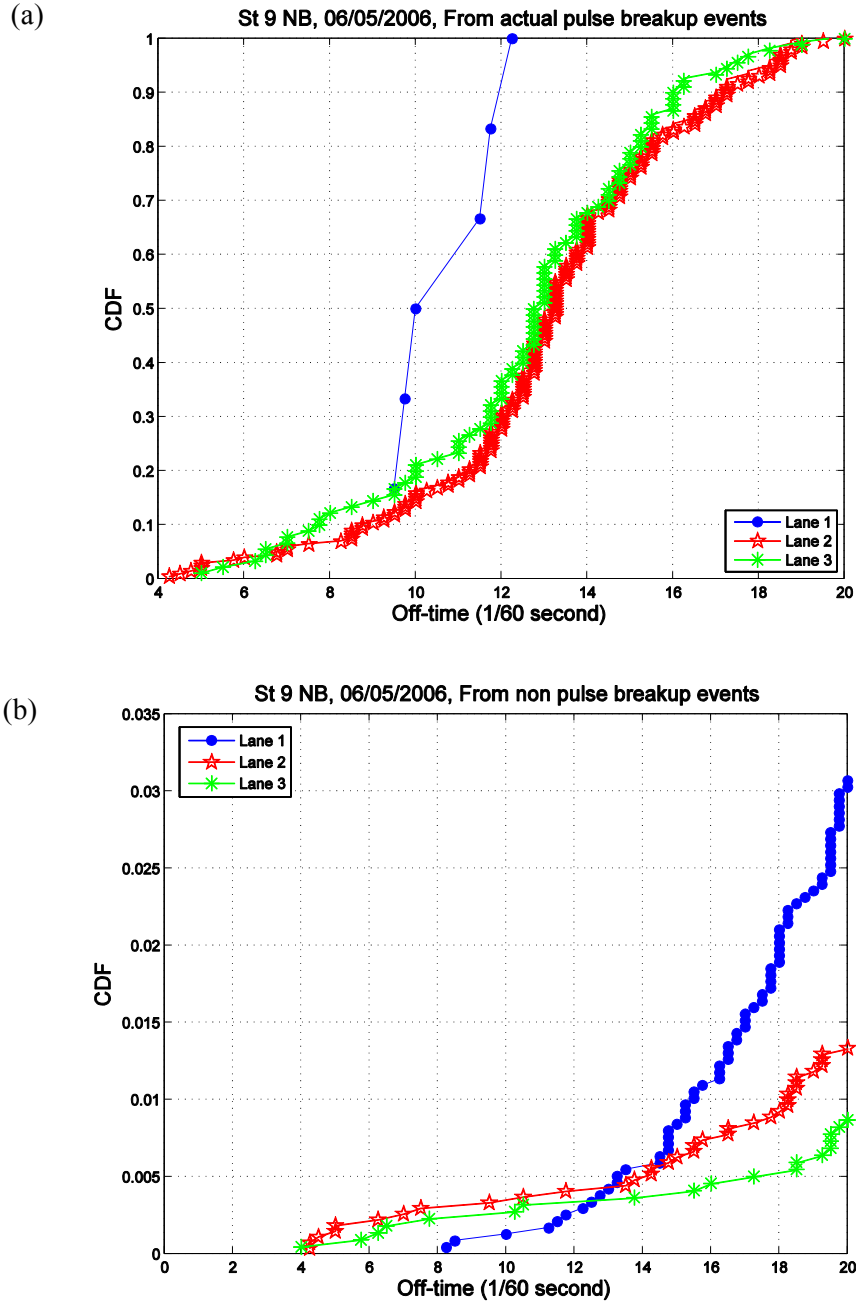


Figure 4.3, Station 9 northbound during 2 hr of free flow traffic (a) CDF of off-times from pulse breakup events by lane and (b) CDF of off-times from non-pulse breakup events after excluding pulse breakup events by lane. Note that the horizontal axis is the same scale between the two plots to facilitate comparison, but the vertical axis differs to highlight the details.

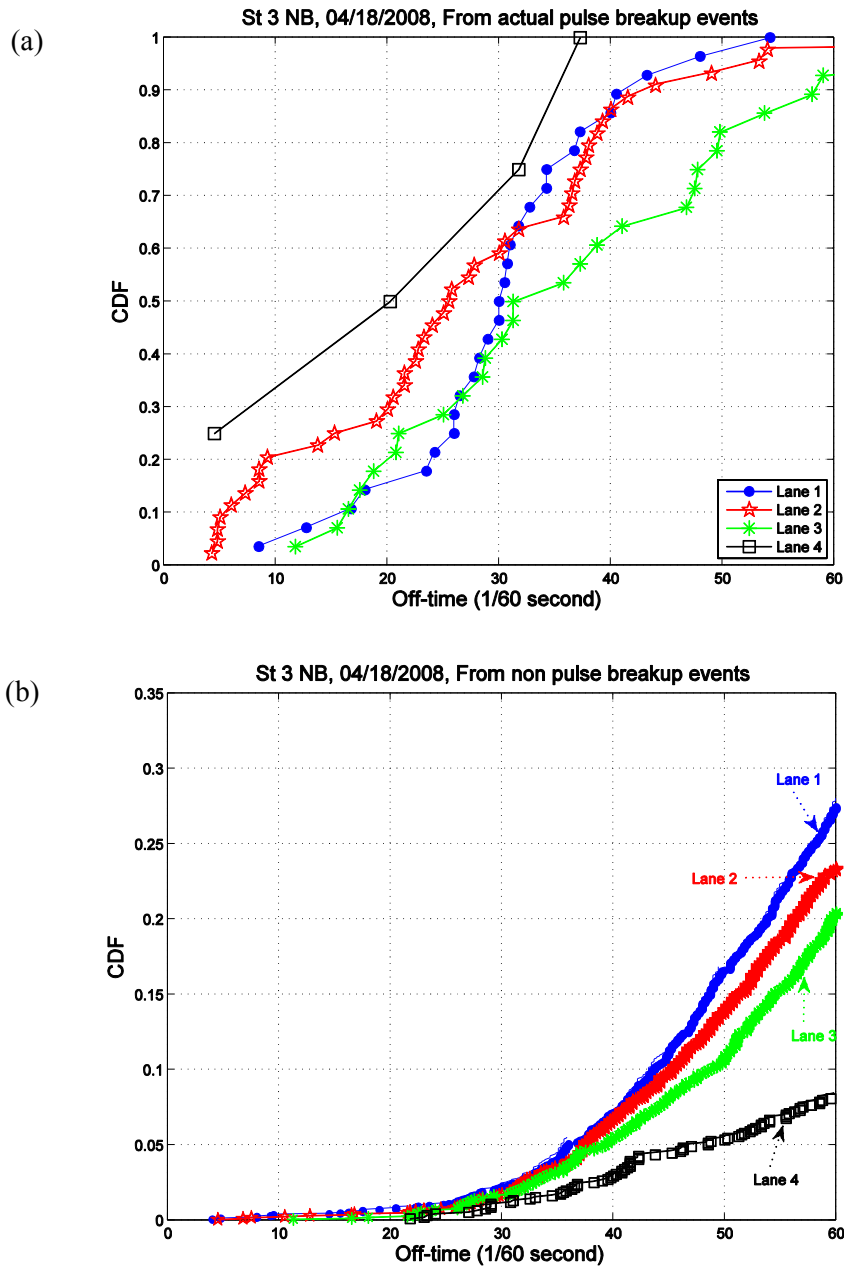


Figure 4.4, Station 3 northbound during 1hr of congested traffic (a) CDF of off-times from pulse breakup events by lane and (b) CDF of off-times from non-pulse breakup events after excluding pulse breakup events by lane. Note that the horizontal axis is the same scale between the two plots to facilitate comparison, but the vertical axis differs to highlight the details.

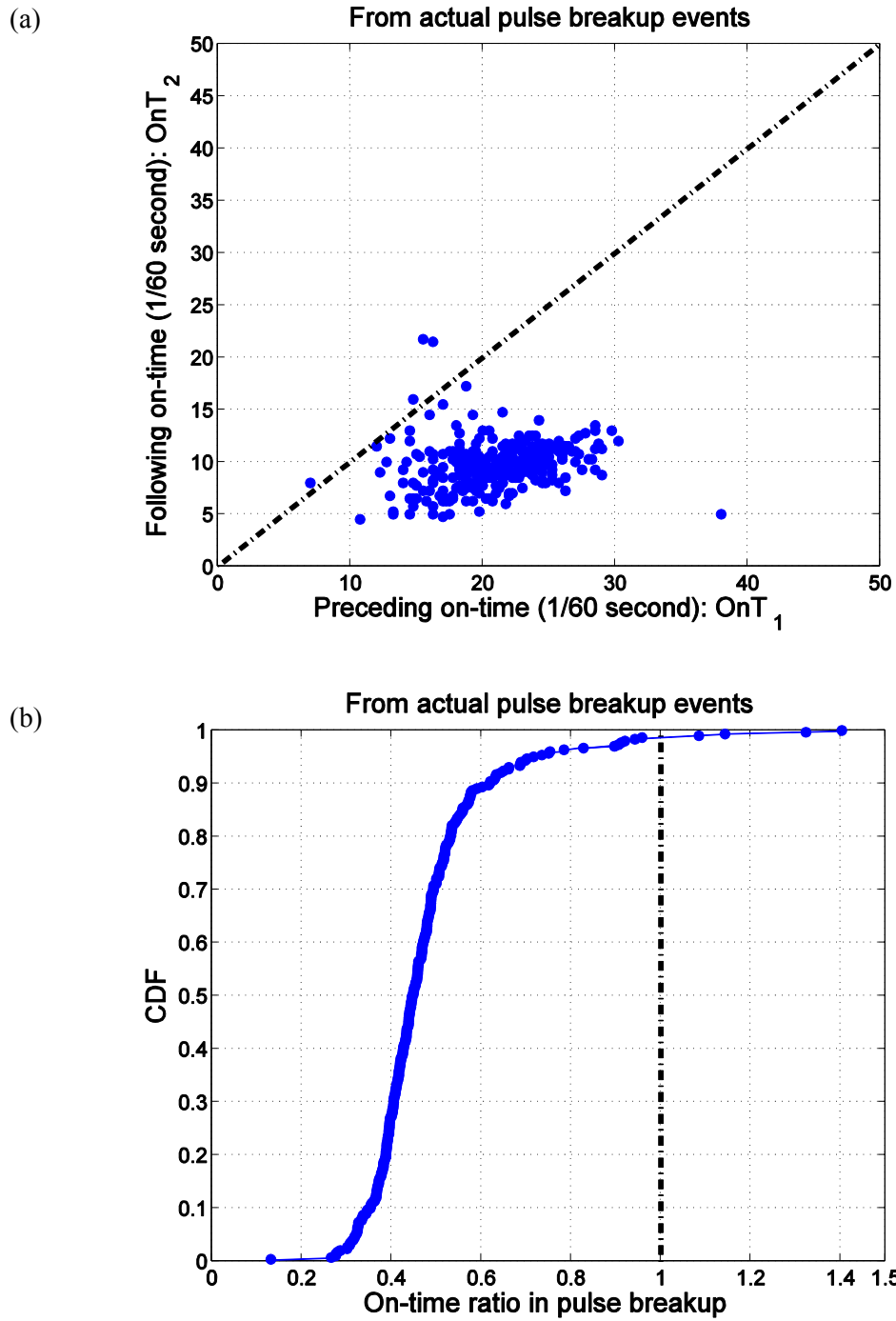


Figure 4.5, (a) A scatter plot of on-times between two pulses in pulse breakup event and (b) CDF of the on-time ratio in pulse breakup events.

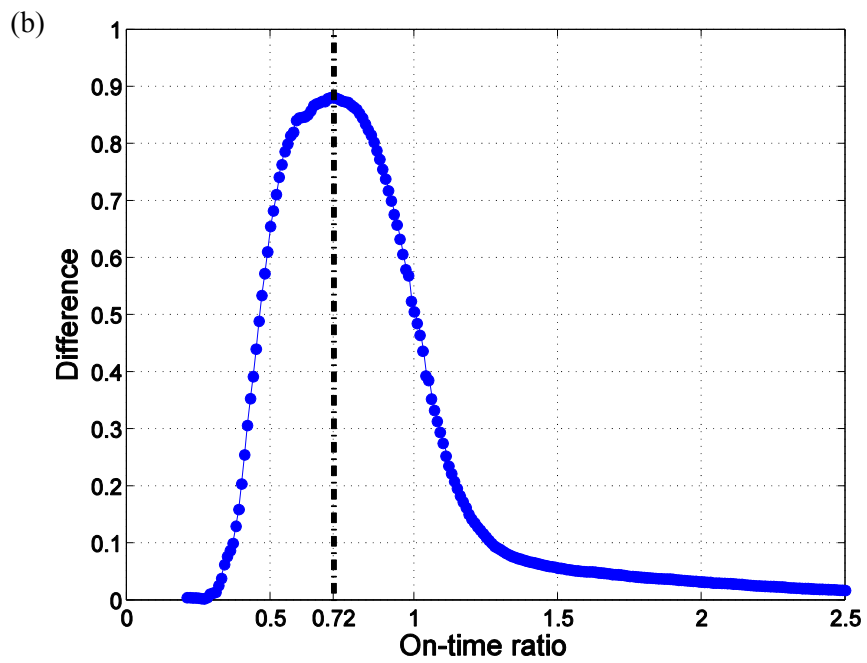
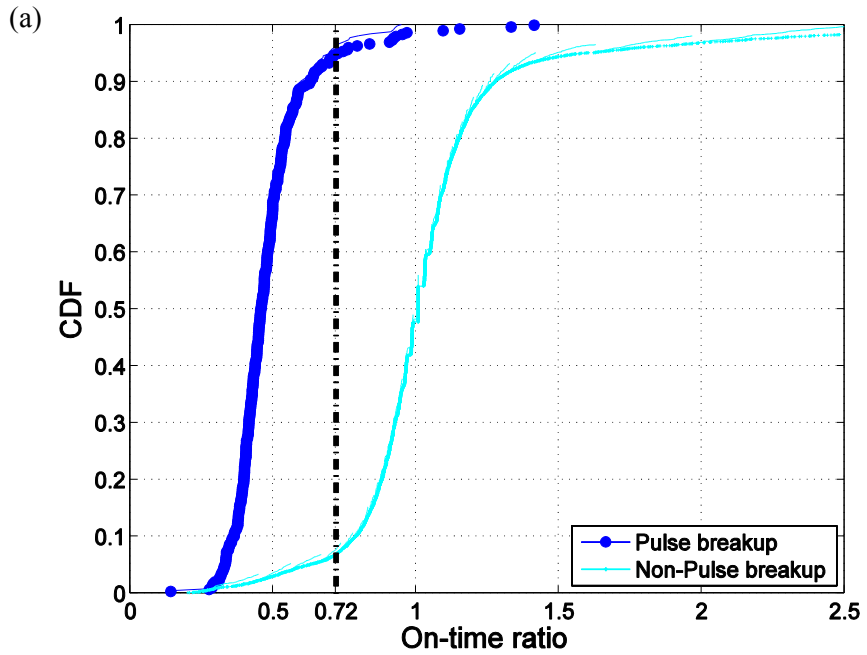


Figure 4.6, (a) CDF of the on-time ratio from pulse breakup events and separately from non-pulse breakup events and (b) the difference between two functions over the range of on-time ratio from 0 to 2.5.

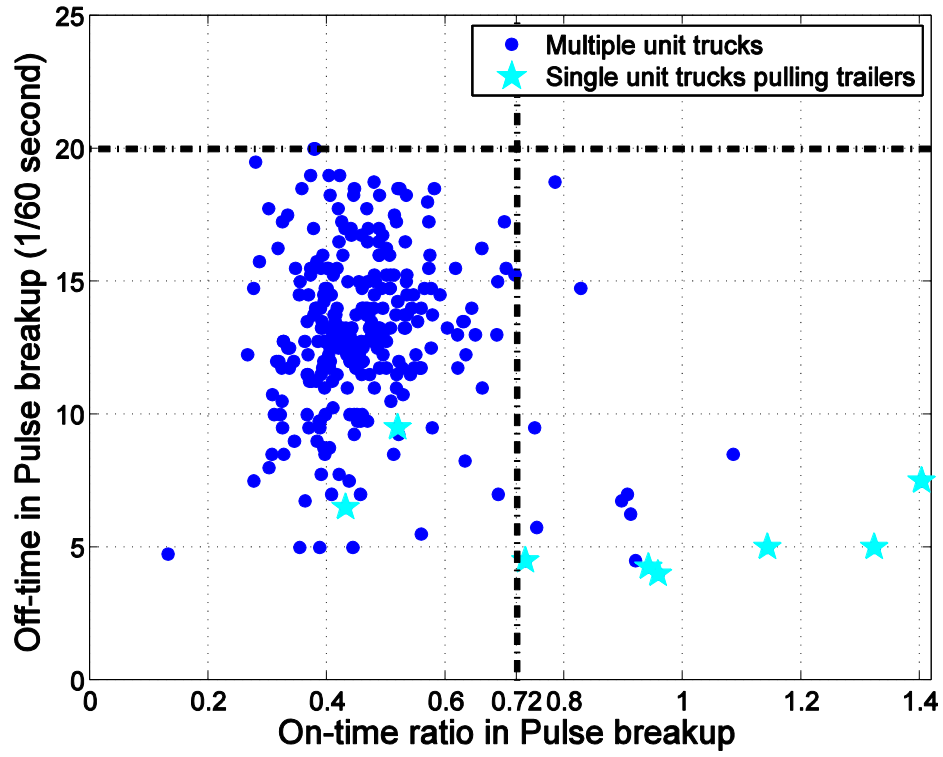


Figure 4.7, Scatter plot of off-time versus on-time ratio for pulse breakup events.

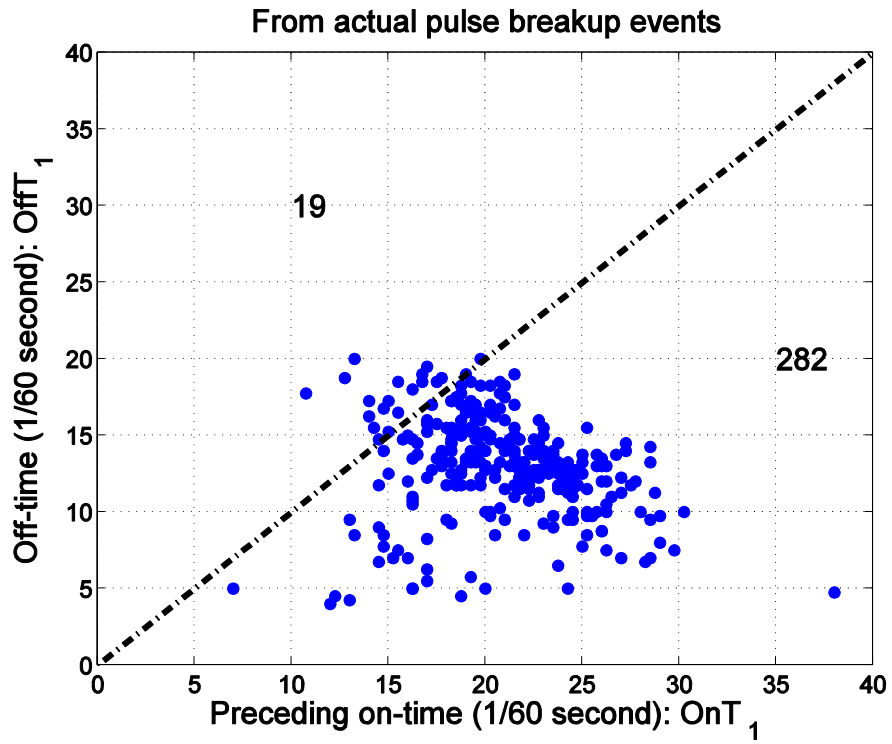


Figure 4.8, A scatter plot of off-time and preceding on-time of pulse breakup events at station 9 northbound.

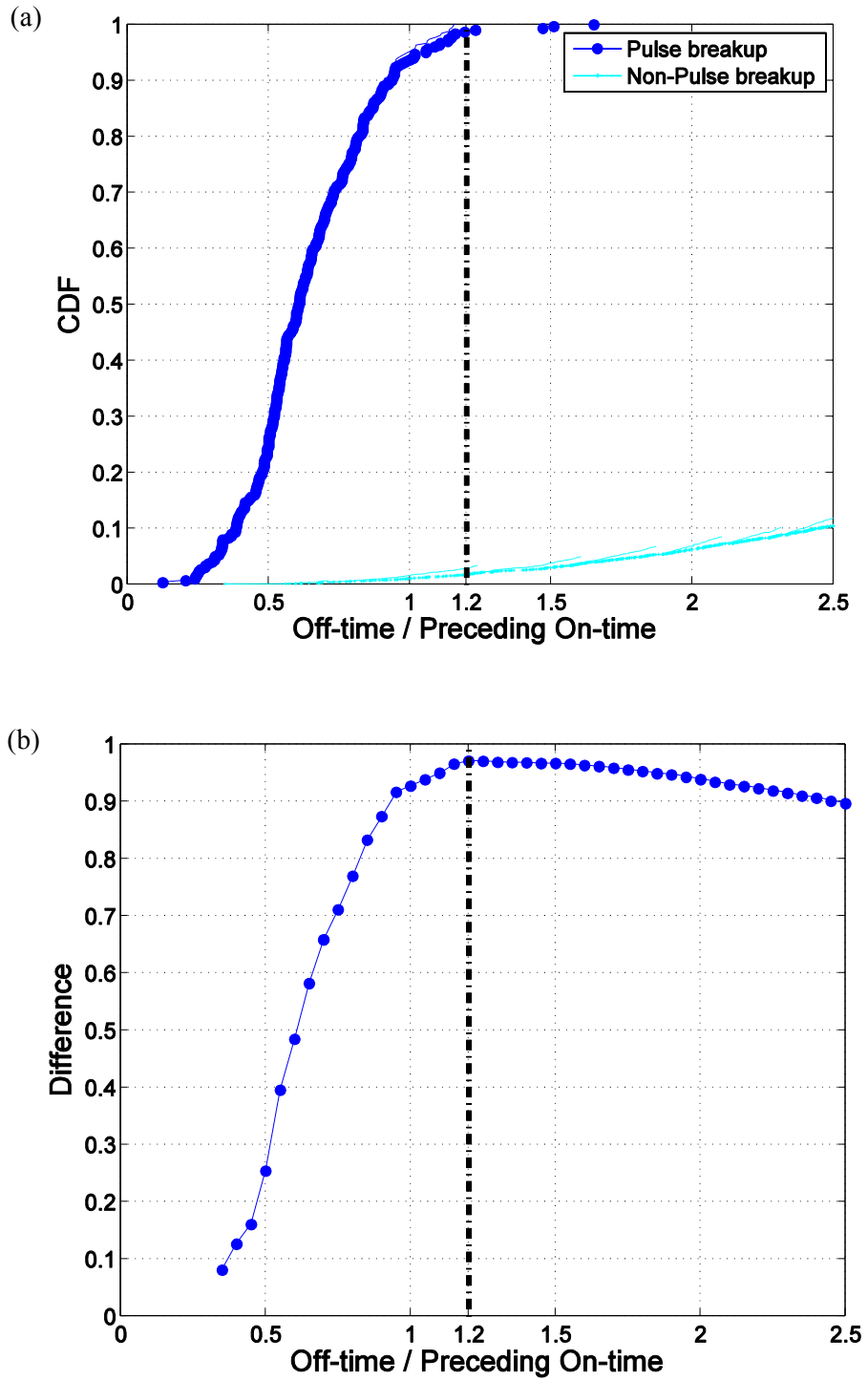


Figure 4.9, (a) CDF of the ratio of off-time and preceding on-time from pulse breakup events and separately from non-pulse breakup events and (b) the difference of two functions.

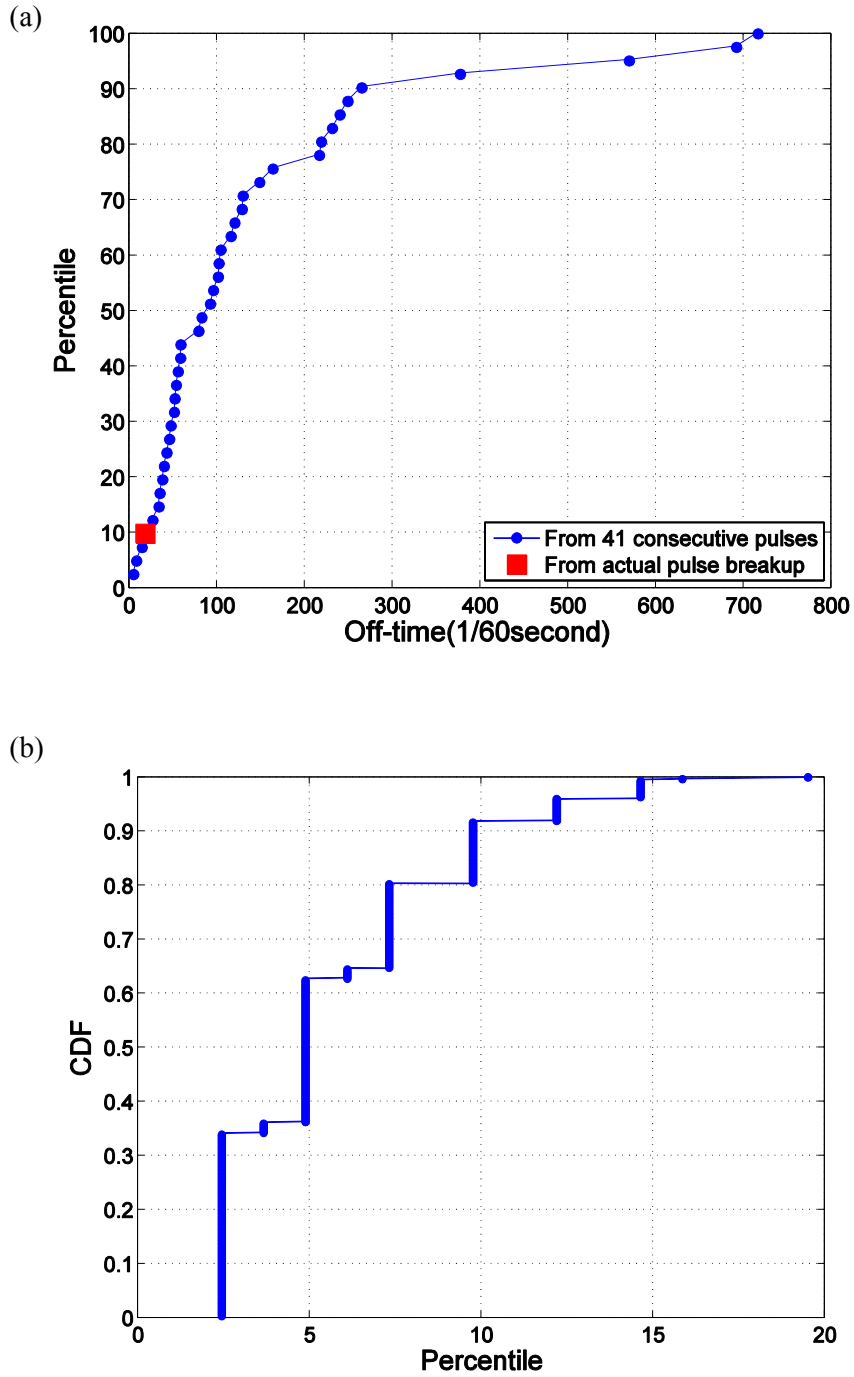


Figure 4.10, (a) CDF of off-time in 41 consecutive pulses in lane 2 at station 9 northbound during free flow conditions, including an actual pulse breakup with off-time of 18.5/60 seconds, falling at the 10th percentile. (b) A plot of the corresponding off-time percentile from each of the actual pulse breakup events at station 9 northbound .

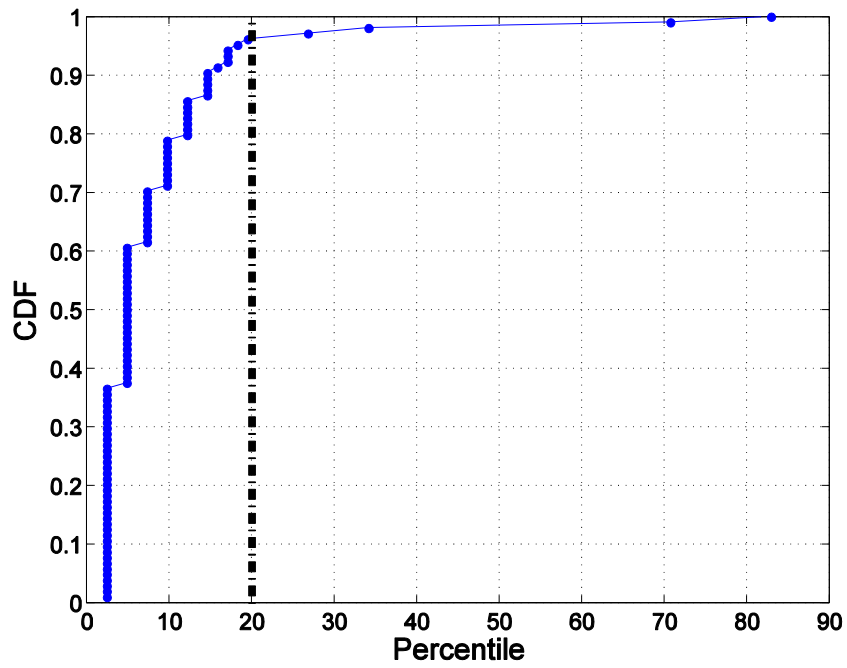


Figure 4.11, A plot of the corresponding off-time percentile from each of the actual pulse breakup events at station 3 northbound during 1hrs of congested conditions.

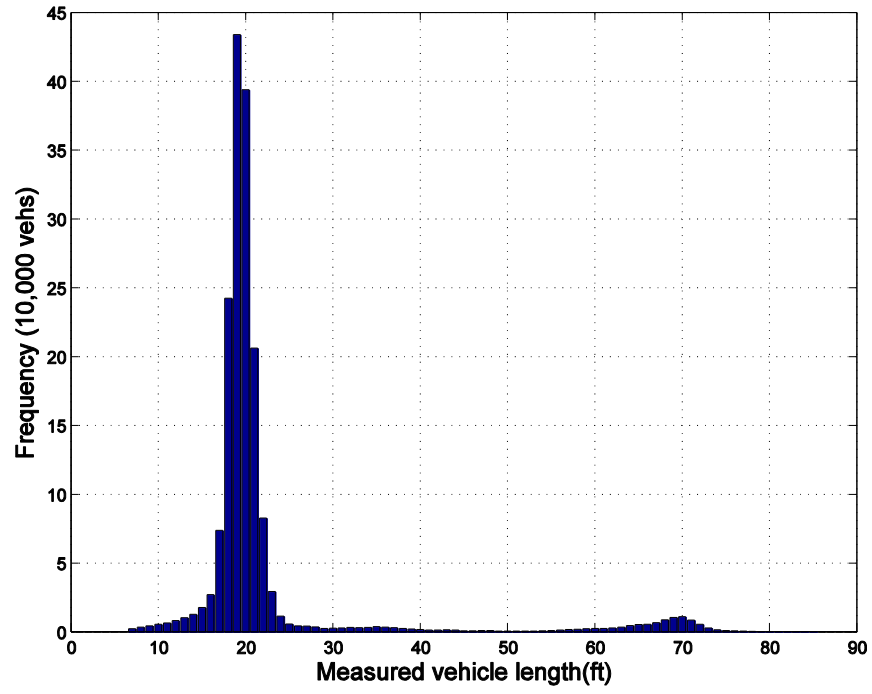


Figure 4.12, The distribution of measured vehicle length across all lanes at station 1 northbound over the entire month of April, 2008.

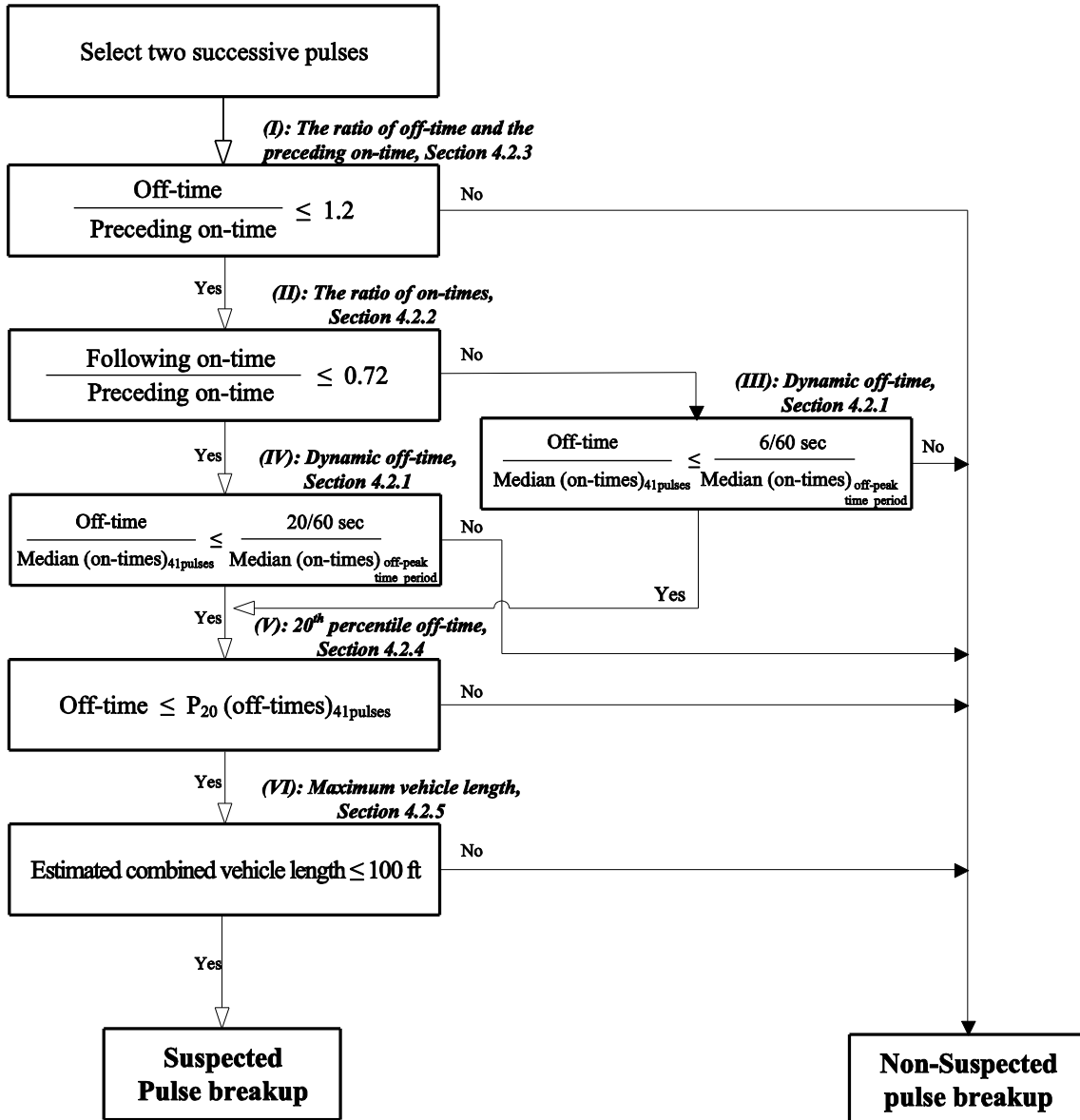


Figure 4.13, A flowchart of the algorithm to identify pulse breakup from a single loop detector.

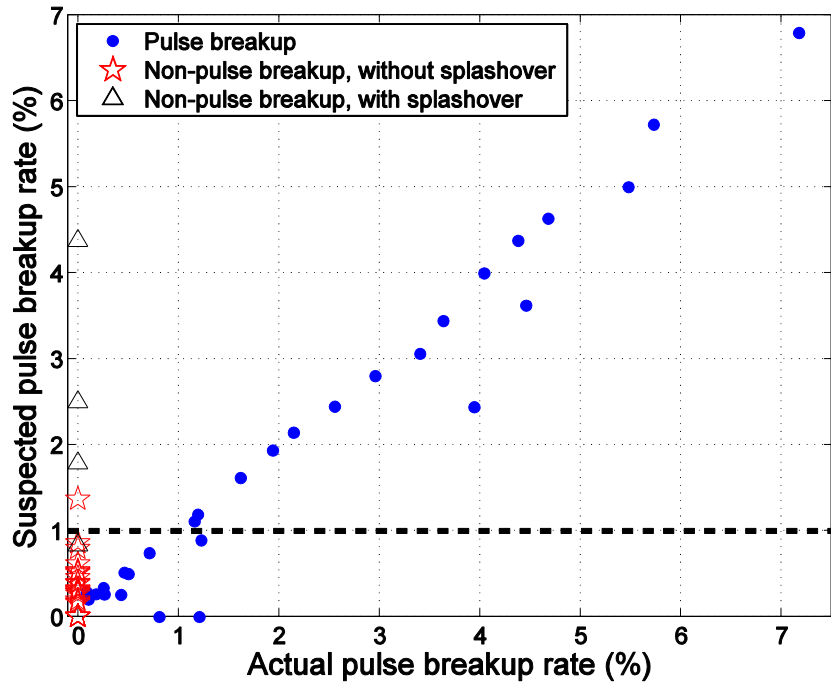


Figure 4.14, A scatter plot of suspected pulse breakup rate and actual pulse breakup rate over 70 loop detectors in free flow conditions.

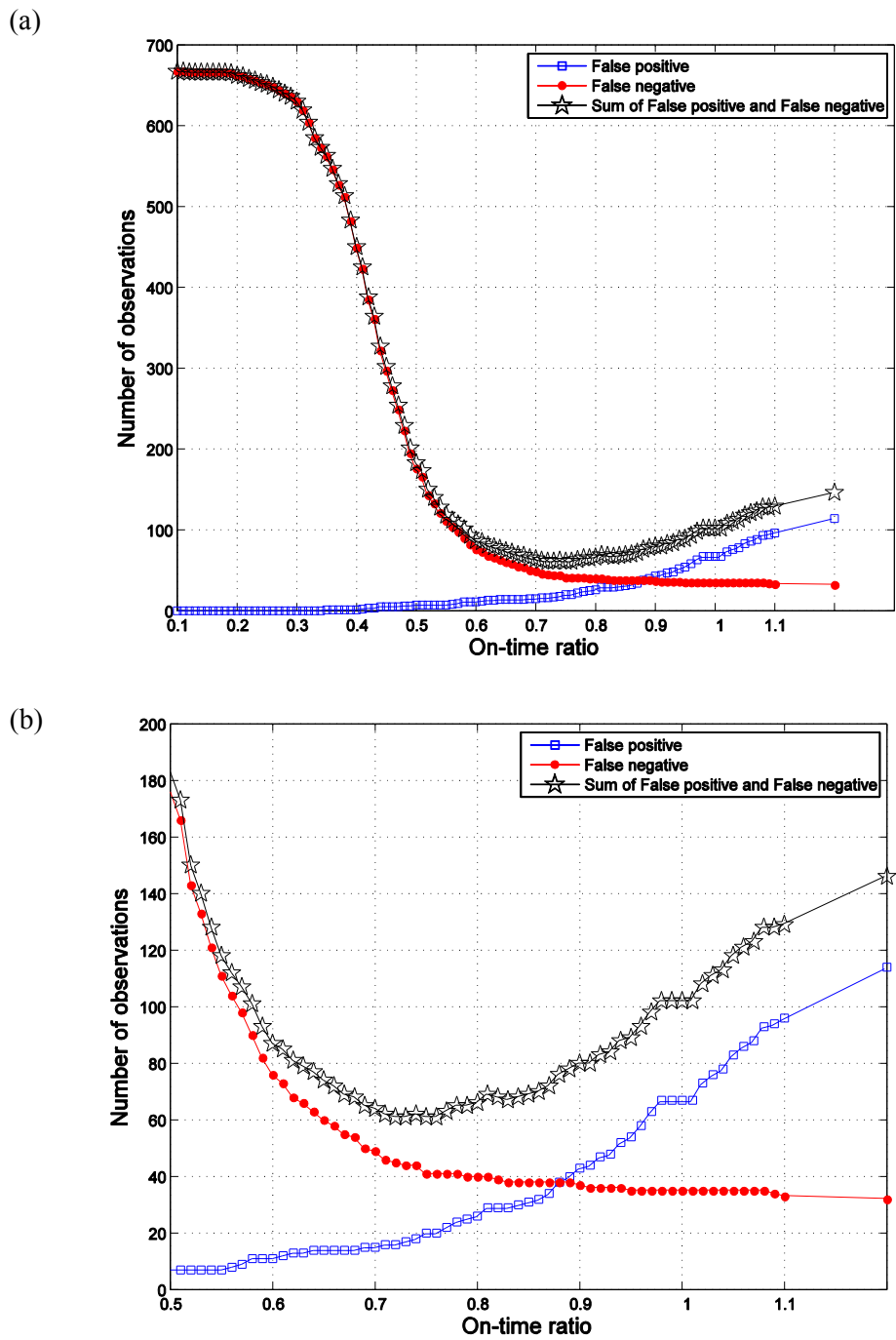


Figure 4.15, (a) Sensitivity analysis of the algorithm performance relative to the on-time ratio threshold, (b) detail of (a).

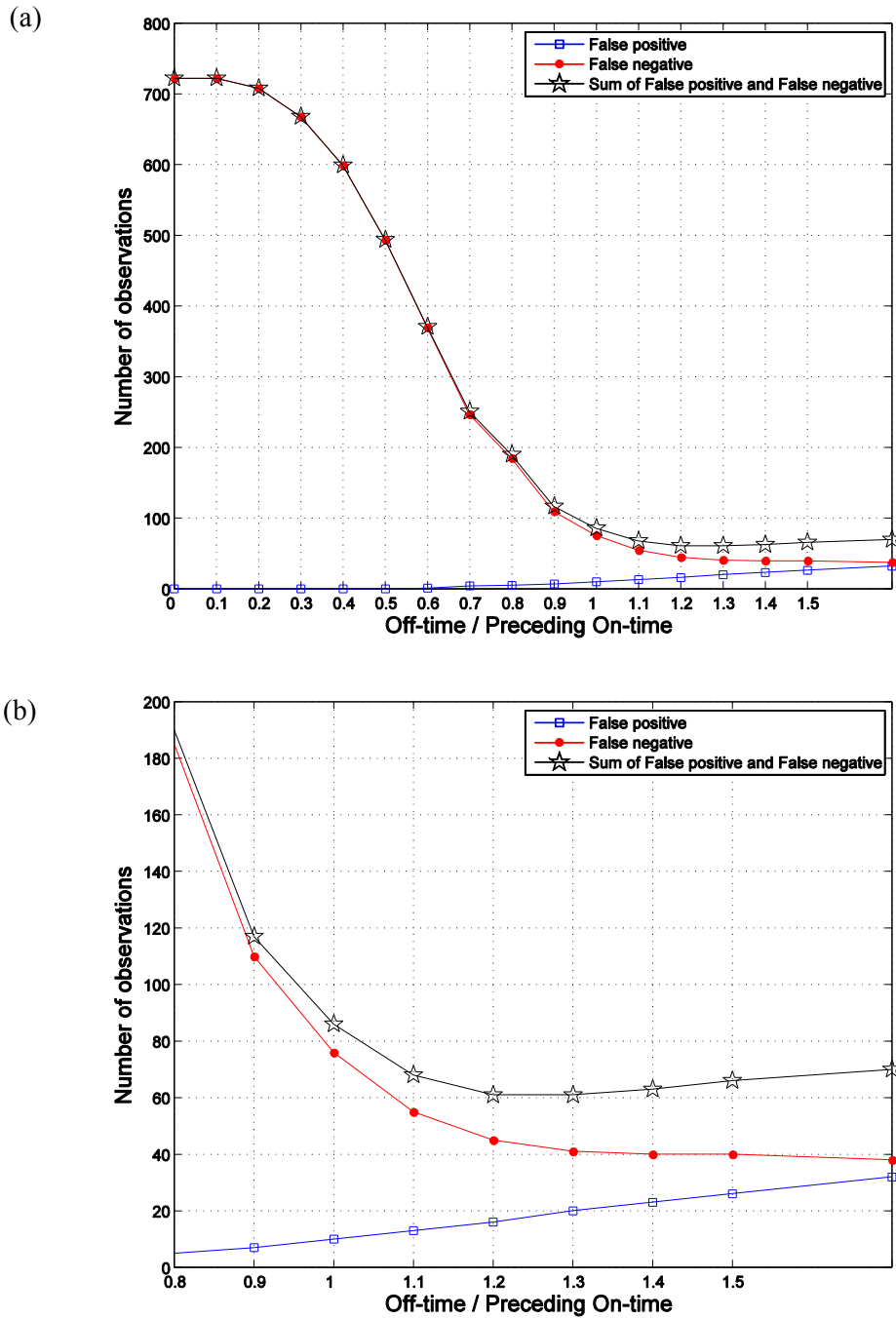


Figure 4.16, (a) Sensitivity analysis of the algorithm performance relative to the ratio of off-time and preceding on-time threshold, (b) detail of (a).

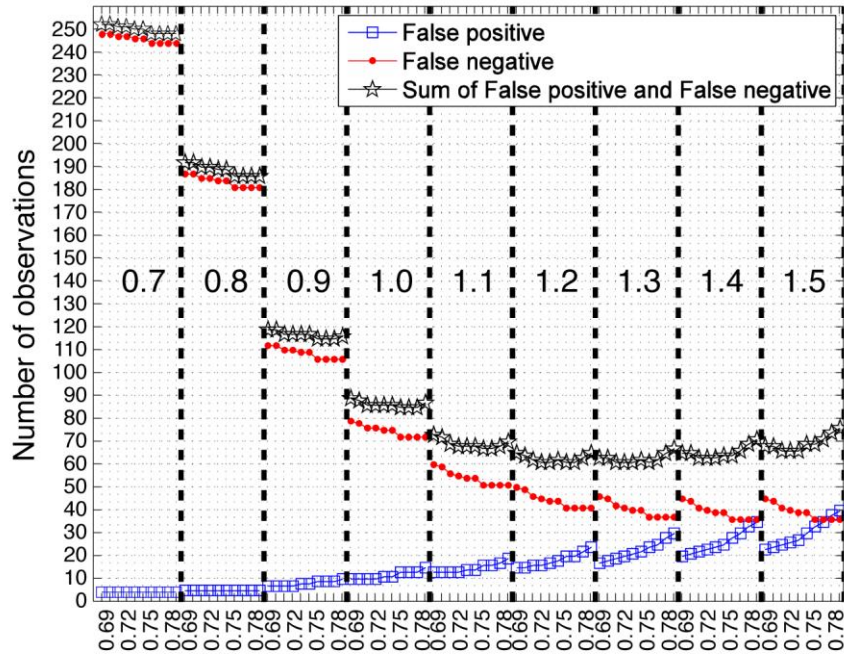


Figure 4.17, Sensitivity analysis of the performance of the algorithm relative to the combination of the on-time ratio threshold, and the ratio of off-time and preceding on-time threshold. The bold vertical delineations show the transition from one ratio of off-time and preceding on-time threshold to the next (indicated with large numbers on the figure), while the lighter vertical delineations show the steps between on-time ratio thresholds (indicated along the horizontal axis).

5 SUMMARY AND CONCLUSIONS

Data obtained from loop detectors are used for applications such as ramp metering, incident detection, travel time prediction, and vehicle classification. The performance of such applications greatly depends on the accuracy of the detector data, but data collected from loop detectors are prone to various errors caused by hardware and software problems. Detector errors degrade the quality of detector data, and the impact of these errors will propagate to subsequent measurements such as flow, occupancy, and speed from the loop detectors. In the end, data incorporating detector errors could affect the traffic control decisions and traveler information based on the detector's data.

There has been considerable research to screen the quality of loop detector data and to identify detector errors to improve data quality. However, some significant detector errors have not received much attention due to the difficulty of identifying their occurrence. This research focused on two such cases: splashover and pulse breakup. The microscopic tests developed herein are much more precise than the preceding macroscopic tests. Those older macroscopic tests generally can only detect large errors and they do not have sufficient resolution to distinguish between splashover, pulse breakup, or other sources of errors. Knowing the source of the overcounting is important for solving the problem, e.g., splashover is often due to oversensitive detectors while pulse breakup is often due to undersensitive detectors.³⁹

Since a splashover event could create a pattern that looks like a pulse breakup event, it could undermine the pulse breakup detection algorithm, thus, this work developed the splashover detection algorithm first, then the pulse breakup detection algorithm second. The algorithms were developed and evaluated using loop detector data with concurrent video recorded ground truth data. A total of 78,785 detector actuations were manually ground truthed from 37 different data sets collected at 22 different locations.

The splashover detection algorithm found loop detectors exhibiting chronic splashover problems. At the crux of our algorithm is the fact that the pulse from a unique splashover in the target lane is usually

³⁹ Though both problems could also arise from the physical placement of the detector being misaligned within the lane of travel.

bounded by a pulse of the valid vehicle detection in the source lane. The task is complicated by the fact that two concurrent vehicles in adjacent lanes can yield the same pattern in the time series detector data, even though it is not an error and it is not splashover. So the algorithm calculates the RSS and balances it with the ERF as a function of the observed traffic conditions to find loop detectors suspected of chronic splashover problems.

On a trial of 94 adjacent lane pairs from 68 loop detectors at 15 loop detector stations, the splashover algorithm correctly classified five out of the seven loop detectors that exhibited actual splashover, while the remaining two loop detectors that did not yield a positive response were below the threshold of the test, having a low ASR and a high ERF. Two out of 61 loop detectors that did not have actual splashover were erroneously labeled as having splashover. Both of these failures were just upstream of where the given lane drops. In each case the false positive arose due to a combination of low flow in the target lane and the fact that any driver that remains in the dropped lane past the detector is likely doing so because there is a concurrent vehicle in the through lane, thus violating our assumption that arrivals are independent in adjacent lanes. Next, the algorithm was compared against three existing error detection methodologies, and it exhibited the best performance differentiating between detectors with and without actual splashover problems. Finally, based on the results of the splashover test, two of the detectors identified as exhibiting actual splashover were subsequently adjusted and the change was shown to eliminate the splashover problem.

The pulse breakup detection algorithm was designed to identify individual pulse breakup events from vehicle actuation data. The algorithm started with the comparison of on-times from the two consecutive pulses bounding a given short off-time, and it improves the distinction between pulse breakup and non-pulse breakup events via several heuristic tests of the adjacent on-times with respect to the ambient traffic conditions. The algorithm for pulse breakup was tested over 68,281 actuations in both free flow and congested conditions collected at 15 detector stations (22 directional stations). From these data 834 out of 891 (94%) actual pulse breakup events were correctly identified as pulse breakup. The algorithm correctly caught over 92% of pulse breakup events under each condition tested in the evaluation datasets. In free flow traffic the success rate at detectors with pulse breakup is about five times larger than the false positive rate at detectors without pulse breakup. In congestion the algorithm remains beneficial at the detectors with pulse breakup, but the false positive rate increases at the non-pulse breakup detectors. So for the current form of the algorithm, it may be better to suppress the algorithm at a given detector during congestion if there is little evidence of pulse breakup at the detector during free flow. One area of future research is this physical gap during congestion. Performance of the algorithm

may be improved either by limiting it to median speeds above a certain threshold, or by handling the physical gap differently when speeds are low.

The rate of identified pulse breakups can be used as a measure of the detector's health, an important feature since the algorithm catches most, but not all of the breakup events. If the number of suspected pulse breakup events retained by the algorithm is too large compared to the non-pulse breakup events, i.e., more than 1% of suspected pulse breakup from the algorithm, a technician should be dispatched to fix the underlying hardware fault and thus, eliminate both the detected and undetected pulse breakup events.

The pulse breakup algorithm was compared against two previous algorithms and our work exhibited a higher success rate, lower total false positive rate, and lower false negative rate compared to the earlier algorithms. Based on the results of the pulse breakup algorithm, 14 detectors at two stations identified as exhibiting actual pulse breakup were subsequently adjusted and the change was shown to eliminate the pulse breakup problem (though at one detector we overcompensated and introduced a splashover problem).

While the focus is on microscopic data validation, the resulting improvements will propagate to the macroscopic metrics, e.g., by reducing over-counting errors in flow, under-counting errors in occupancy, and reducing speed measurement (or estimation) errors. If these results are typical, the improved detector calibration enabled by our research could lead to a very inexpensive means to improve the quality of loop detector data at existing loop detector stations. In the short term these algorithms could be incorporated into a field diagnostic tool to assess the performance of a given station, either by tapping into the data upstream of the controller, e.g., via the Case Global Technologies TMS 100⁴⁰, or running an alternate controller program for a day or two, e.g., Caltrans Log_I70. In the longer run, such tests should be incorporated into the standard controller software so that the controller can continually assess the health of the detectors. Ultimately the benefits of the research will be seen in various applications of loop detector data, e.g., length based vehicle classification, travel time estimation using vehicle reidentification, and traffic flow modeling.

While the focus of this study is loop detectors, the present work is likely applicable to emerging detectors as well, such as side-fire microwave radar detectors that seek to replace loop detectors. Most of these wayside mounted sensors emulate the operation of loop detectors. So, while the physical mechanism

⁴⁰ <http://www.caseglobaltech.com/tms100.shtml>, formerly called the InfoTek Wizard

of splashover and pulse breakup differs across the different detection technologies, the manifestation should be similar in the vehicle actuations.

6 REFERENCES

Bertini, R. L., and A. El-Geneidy. *Assessing the Benefits and Costs of ITS: Using Archived Advanced Traffic Management System Data to Evaluate ITS investments*. Kluwer Academic Publishers, 2002.

Caltrans. *VideoSync*. <http://www.dot.ca.gov/newtech/operations/videosync/index.htm>. Accessed January 3, 2010.

Cheevarunothai, P., Y. Wang, and N. L. Nihan. Identification and Correction of Dual-Loop Sensitivity Problems. In *Transportation Research Record: Journal of the Transportation Research Board*, No. 1945, Transportation Research Board of the National Academies, Washington, D.C., 2006, pp. 73-81.

Cheevarunothai, P., Y. Wang, and N. L. Nihan. Using Dual-Loop Event Data to Enhance Truck Data Accuracy. In *Transportation Research Record: Journal of the Transportation Research Board*, No. 1993, Transportation Research Board of the National Academies, Washington, D.C., 2007, pp. 131-137.

Chen, C., J. Kwon, J. Rice, A. Skabardonis, and P. Varaiya. Detecting Errors and Imputing Missing Data for Single Loop Surveillance Systems. In *Transportation Research Record: Journal of the Transportation Research Board*, No. 1855, Transportation Research Board of the National Academies, Washington, D.C., 2003, pp. 160-167.

Chen, L., and A. D. May. Traffic Detector Errors and Diagnostics. In *Transportation Research Record: Journal of the Transportation Research Board*, No. 1132, Transportation Research Board of the National Academies, Washington, D.C., 1987, pp. 82-93.

Cherrett, T., H. Bell, and M. McDonald. Traffic Management Parameters from Single Inductive Loop Detectors. In *Transportation Research Record: Journal of the Transportation Research Board*, No. 1719, Transportation Research Board of the National Academies, Washington, D.C., 2000, pp. 112-120.

Cleghorn, D., F. Hall, and D. Garbuio. Improved Data Screening Techniques for Freeway Traffic Management Systems. In *Transportation Research Record: Journal of the Transportation Research Board*, No. 1320, Transportation Research Board of the National Academies, Washington, D.C., 1991, pp. 17-23.

Coifman, B. Using Dual Loop Speed Traps to Identify Detector Errors. In *Transportation Research Record: Journal of the Transportation Research Board*, No. 1683, Transportation Research Board of the National Academies, Washington, D.C., 1999, pp. 47-58.

Coifman, B. Improved Velocity Estimation Using Single Loop Detectors. *Transportation Research: Part A*, Vol. 35, No. 10, 2001, pp. 863-880.

Coifman, B., S. Dhoorjaty, and Z. Lee. Estimating Median Velocity Instead of Mean Velocity at Single Loop Detectors. *Transportation Research: Part C*, Vol. 11, No. 3-4, 2003, pp. 211-222.

- Coifman, B., and S. Dhoorjaty. Event Data Based Traffic Detector Validation Tests. *ASCE Journal of Transportation Engineering*, Vol. 130, No. 3, 2004, pp. 313-321.
- Coifman, B. *The Columbus Metropolitan Freeway Management System (CMFMS) Effectiveness Study: Part 2 – The After Study*. Publication FHWA/OH-2006/19. FHWA, U.S. Department of Transportation, 2006a.
- Coifman, B. Vehicle Level Evaluation of Loop Detectors and the Remote Traffic Microwave Sensor. *ASCE Journal of Transportation Engineering*. Vol. 132, No. 3, 2006b, pp. 213-226.
- Coifman, B., and H. Lee. A Single Loop Detector Diagnostic: Mode On-Time Test. *Proc. of Applications of Advanced Technology in Transportation*, ASCE, August 13-16, 2006, Chicago, IL. pp. 623-628.
- Coifman, B., and S. Krishnamurthy. Vehicle Reidentification and Travel Time Measurement Across Freeway Junctions Using the Existing Detector Infrastructure. *Transportation Research: Part C*, Vol. 15, No. 3, 2007, pp. 135-153.
- Coifman, B., and S. Kim. Speed Estimation and Length Based Vehicle Classification from Freeway Single Loop Detectors. *Transportation Research: Part C*, Vol. 17, No. 4, 2009, pp. 349-364.
- Day, C. M., T. M. Brennan, M. L. Harding, H. Premachandra, A. Jacobs, D. M. Bullock, J. V. Krogmeier, and J. R. Sturdevant. Three-Dimensional Mapping of Inductive Loop Detector Sensitivity with Field Measurement. In *Transportation Research Record: Journal of the Transportation Research Board*, No. 2128, Transportation Research Board of the National Academies, Washington, D.C., 2009, pp. 35-47.
- Dixon, K.K., C. Wu, W. Sarasua, and J. Daniel. Posted and Free-Flow Speeds for Rural Multilane Highways in Georgia. *ASCE Journal of Transportation Engineering*, Vol. 125, No. 6, 1999, pp. 487-494.
- Federal Highway Administration. *Traffic Monitoring Guide*. Publication FHWA-PL-01-021. FHWA, U.S. Department of Transportation, 2001.
- Hall, F. L., and B. N. Persaud. Evaluation of Speed Estimates Made with Single-Detector Data from Freeway Traffic Management Systems. In *Transportation Research Record: Journal of the Transportation Research Board*, No. 1232, Transportation Research Board of the National Academies, Washington, D.C., 1989, pp. 9-16.
- Hamm, R.A. and D. L. Woods. Loop Detectors: Results of Controlled Field Studies. *ITE Journal*, Vol. 62, No. 11, 1992, pp 12-16.
- Hourdakis, J., and P. G. Michalopoulos. Evaluation of Ramp Control Effectiveness in Two Twin Cities Freeways. In *Transportation Research Record: Journal of the Transportation Research Board*, No. 1811, Transportation Research Board of the National Academies, Washington, D.C., 2002. pp. 21-29.
- Jacobson, L., N. Nihan, and J. Bender. Detecting Erroneous Loop Detector Data in a Freeway Traffic Management System. In *Transportation Research Record: Journal of the Transportation Research Board*, No. 1287, Transportation Research Board of the National Academies, Washington, D.C., 1990, pp. 151-166.
- Klein, L. A., M. K. Mills, and D. R. P. Gibson. *Traffic Detector Handbook*, Third Edition, FHWA-HRT-06-108, FHWA, U.S. Department of Transportation, 2006.
- Kwon, J., B. Coifman, and P. Bickel. Day-to-Day travel time trends and travel time prediction from loop detector data. In *Transportation Research Record: Journal of the Transportation Research Board*, No. 1717, Transportation Research Board of the National Academies, Washington, D.C., 2000, pp. 120-129.

- Lang, L and B. Coifman. Identifying Lane Mapping Errors at Freeway Detector Stations. In *Transportation Research Record: Journal of the Transportation Research Board*, No. 1945, Transportation Research Board of the National Academies, Washington, D.C., 2006, pp. 89-99.
- Neelisetty, S., and Coifman, B. Improved Single Loop Velocity Estimation in the Presence of Heavy Truck Traffic. *Proc. of the 83rd Annual Meeting of the Transportation Research Board*, Washington, D.C., 2004.
- Nihan, N. L., Y. Wang, and P. Cheevarunothai. *Improving Dual-Loop Truck (and Speed) Data: Quick Detection of Malfunctioning Loops and Calculation of Required Adjustments*. TNW2006-02 , Washington State Department of Transportation, Research Report, 2006.
- Ontario MOT (Ministry of Transportation). *Freeway Traffic Management Systems*. Government of Ontario. www.mto.gov.on.ca/english/traveller/trip/compass-ftms.shtml. Accessed on January 3, 2010.
- Papageorgiou, M., H. Hadj-Salem, and F. Middleham. ALINEA Local Ramp Metering Summary of Field Results. In *Transportation Research Record: Journal of the Transportation Research Board*, No. 1603, Transportation Research Board of the National Academies, Washington, D.C., 1997, pp. 90-98
- Payne, H. J., and S. M. Thompson. *Development and Testing of Operational Incident Detection Algorithms: technical report*, R-009-97. FHWA, U.S. Department of Transportation, 1997
- Payne, H. J., and S. C. Tignor. Freeway Incident-Detection Algorithms Based on Decision Trees with States. In *Transportation Research Record: Journal of the Transportation Research Board*, No. 682, Transportation Research Board of the National Academies, Washington, D.C., 1978, pp. 30-37.
- TxDOT (Texas Department of Transportation). *Traffic Data and Analysis Manual*. http://onlinemanuals.txdot.gov/txdotmanuals/tda/fhwa_vehicle_classification_figures.htm. Accessed January 2, 2010.
- Turochy, R.E., and B. L. Smith. New Procedure for Detector Data Screening in Traffic Management Systems. In *Transportation Research Record: Journal of the Transportation Research Board*, No. 1727, Transportation Research Board of the National Academies, Washington, D.C., 2000, pp. 127-131.
- Williams, B.M., and A. Guin. Traffic Management Center Use of Incident Detection Algorithms: Findings of a Nationwide survey. *IEEE Transactions on intelligent transportation systems*, Vol. 8, No. 2, 2007, pp. 351-358.

APPENDIX A LOOP DETECTOR SENSITIVITY

A.1 Introduction

When a vehicle passes over the physical loop, the ferromagnetic material in the vehicle lowers the loop's inductance. The sensor compares the loop's inductance against a threshold to establish the presence or the absence of a vehicle over a loop detector. The change in inductance depends on the physical loop's responsiveness as well as the spatial relationship between the vehicle and physical loop (e.g., the distance between a loop detector and the undercarriage of a vehicle and a ratio of the surface area of the loop and of the vehicle body, Day et al., 2009). The loop responsiveness is biased by the characteristics of the buried loop detector (e.g., the depth of the wires and design standards of the loop detector, Hamm and Woods, 1992), and pavement condition (e.g., pavement material, Cherrett et al., 2000; and temperature, Nihan et al., 2006). A loop sensor typically has a user selectable sensitivity setting to control for the wide range of feasible loop responsiveness that bias the inductance change. The higher the user sets the sensitivity level, the more readily the sensor will detect a vehicle, i.e., the larger the detection zone. In conventional practice, however, it is difficult to know the physical loop's responsiveness, which in turn makes it difficult to select the appropriate sensitivity setting on the sensor. A loop detector will yield poor performance if the sensitivity setting is not well matched to the physical loop's responsiveness. Such errors in turn degrade the detector's data, e.g., underestimated or overestimated speed due to the discrepancy of the expected effective vehicle length and the actual effective vehicle length. These errors will degrade the performance of the traffic control decisions and traveler information based on the detector's data.

Reviewing the literature, there have been a few investigations of the loop detector sensitivity from individual vehicle actuations. Chen and May (1987) examined the ratio of a detector's average on-time relative to the average on-time of all detectors at the detector station. This on-time ratio test provided an indication of a detector's status (e.g., sensitivity setting) relative to the other detectors at the station. But because of the relative comparison, if all of the loop detectors have a similar sensitivity setting error, Chen and May's test should fail to catch it. They explicitly considered detector sensitivity in two tests, first they showed that the sensitivity setting will bias aggregate occupancy measurements and noted the

importance of tuning all of the detectors in a corridor to the same bias (implicitly assuming that the responsiveness would be similar across all of the physical loops at the different stations). Second, they sought to eliminate detector dropouts in the middle of long vehicles by increasing the sensitivity, though the magnetometers used in the test continued to dropout even at high sensitivity. Neelisetty and Coifman (2004) developed a mode on-time test as one measure of loop detector performance and Coifman and Lee (2006) refined it. The test is applied individually to each loop in each lane and the mode on-time is found over 24 hrs. Assuming that most vehicles indeed have an effective length between 18 and 22 ft, and allowing a large range of acceptable free flow speeds (40 mph to 82 mph), they expected that the mode on-time should fall between 11/60 and 16/60 seconds. If the 24 hr mode on-time from a detector is outside the expected range, they surmised a detector error (e.g., incorrect loop's sensitivity) or transient event (e.g., severe weather or a major incident). Some efforts have sought to leverage the redundant measurements in a dual loop detector, e.g., Coifman (1999) compared the on-times between the upstream and downstream detectors in a given lane to look for discrepancies, which in turn would reveal a sensitivity error at just one of the detectors in the pair. But like Chen and May (1987), it would not catch an error that impacted both detectors similarly. Cheevarunothai et al. (2006) extended these ideas, after comparing the paired loop's on-times like Coifman (1999), they used the measured speed and on-time to measure effective vehicle lengths. They compared the observed distribution of lengths against an expected distribution of short vehicle lengths. If the two distributions differed by too much, the detector was suspected to be in error, either due to an inappropriate sensitivity or an inaccurate spacing between dual loops.

Most of these earlier studies simply sought to identify detectors with chronic problems, without explicitly focusing on detector sensitivity. Measurement errors from incorrect sensitivity have not received sufficient attention. This appendix addresses the problem directly, developing a method to identify and often negate the impact of such sensitivity errors. The approach is then transposed to dual loop detectors to identify and correct for inaccurate spacing between the paired detectors.

The remainder of this section is organized as follows; first, we develop a means to quantify detector sensitivity and show how the sensitivity can change over time. Then a methodology is developed to correct for unexpected sensitivity errors at a single loop detector. This same approach is extended to also correct for errors in the assumed effective spacing at dual loop detectors. The method is then validated against concurrent velocity measurements from a GPS equipped probe vehicle. Finally, we present our conclusions.

A.2 Identification of a loop detector with incorrect loop sensitivity

Our method begins by re-implementing the 24 hr mode on-time test (Coifman and Lee, 2006) to instead use the daily median on-time. But we go much further, focusing the effort explicitly on detector sensitivity, then we validate the results using independent measurements, develop correction factors to accommodate sensitivity errors, extend to dual loop detector spacing, and examine trends over years. This study uses the I-71 corridor in Columbus, Ohio. The corridor is 14 miles long, with dual loop detector stations roughly every mile and usually two single loop detector stations between successive dual loop detector stations. The facility is fairly unique because all of the stations report the individual vehicle actuations to the traffic management center, rather than discarding the individual measurements immediately after the controller calculates q , occ and average speed. Much of this section focuses on tests that can be applied at single loop detectors, in which case, at the dual loop detectors we will arbitrarily select the upstream detector and approach it as if it were a single loop detector. Obviously both loops in the dual loop detectors are used for the spacing analysis.

A.2.1 Daily median on-time test

Each on-time measurement at a loop detector depends on the effective vehicle length, L , and vehicle speed, v , via Equation A.1. The effective vehicle length is the sum of the physical length of the vehicle and the size of the detection zone. The latter depends on the loop responsiveness and the sensor sensitivity. If the sensitivity setting matches the physical loop's responsiveness the detection zone will correspond to the length of the physical loop (6 ft for the detectors used in this section, but different operating agencies use different loop sizes).

$$\text{on-time} = \frac{L}{v} \tag{A.1}$$

Although speed and length vary from vehicle to vehicle, over a 24 hour period at a typical detector, most of the vehicles should be free flowing and the majority should be passenger vehicles. Thus, over 24 hr of a day, the median on-time (termed the *daily median on-time*) at a loop detector should usually correspond to the effective length of a passenger vehicle at free flow speeds. In the US passenger vehicles are typically on the order of 14 ft long, so after adding in the physical length of the loop, the effective length should be on the order of 20 ft (e.g., Coifman and Lee (2006) found approximately 90% of the individual effective vehicle lengths observed at one dual loop detector station fell between 18 and 22 ft). While the free flow speed depends on several factors, e.g., road geometry, access points and characteristics of the lanes (Dixon et al., 1999), for the purposes of this work the free flow speed does not need to be known precisely, it can either be estimated from the posted speed limit or measured with a

radar gun. The daily median on-time should fall in a small range, e.g., assuming that most effective vehicle lengths indeed fall in the 18 to 22 ft range and drivers usually obey the posted speed limit in free flow conditions, the daily median on-time should fall between 13/60 and 16/60 seconds at 55 mph and between 11/60 and 14/60 seconds at 65 mph (alternatively, one could employ a small tolerance for v , which would yield a similar range of feasible on-times). The further the daily median on-time falls outside this expected range, the more indicative it is of unexpected conditions, either due to a transient event (e.g., a snowstorm) or an improper match between the sensitivity setting and the physical loop's responsiveness. Transient events can be addressed by looking at the results from several days or avoiding results on days with known incidents. If the location is known to have many hours of recurring congestion, the test can be modified to exclude congested traffic (either by time of day, day of week, or via the macroscopic data); though care must be taken to ensure that the late night hours are not over-represented since these periods are often characterized by a higher percentage of trucks in the flow (Coifman, 2001).

Figure A.1 shows daily median on-time at each loop detector in the I-71 corridor on May 1, 2005. The horizontal axis presents the stations in sequential order in the corridor from south to north. The speed limit is 55 mph between stations 102 and 112, then increases to 65 mph for the remaining stations and the range of expected daily median on-time is shown with horizontal dashed lines. Lane 1 is the left-most lane (i.e., median) and the lane numbers increase to the right. Roughly 57% of the loop detectors (61 of 107 northbound and 61 of 108 southbound) show the daily median on-time fell outside of the expected range of on-times. For example, the detectors in all three lanes at station 14 northbound show the daily median on-time is lower than the expected range of daily median on-time. Some stations also show a large difference of on-time across neighboring lanes, e.g., the daily median on-time of lane 2 at station 2 northbound is 5/60 seconds lower than the other lanes. The daily median on-time trends on this particular day are similar the rest of the month (May 2005, not shown), indicating that the sample date did not include a severe transient event. So the sensitivity setting does not appear to be well matched to the responsiveness at the majority of the detectors in this corridor. If one were to choose a higher assumed speed (e.g., assuming most drivers travel 5 mph over the limit) the expected range would move down but discrepancies would remain. Aside from large geometric changes between stations 105 and 1, the corridor is fairly homogeneous, i.e., a given lane should exhibit similar median values across stations 1 through 27 but that clearly does not occur, every lane has median values both above and below our target range. The stations are inconsistently calibrated, which will degrade the aggregate speed and occupancy.

A.2.2 Change of loop detector sensitivity over time

While the daily median on-time is assumed to be nearly constant over extended periods (with occasional transient deviations due to non-recurring events), the daily median on-time trend may abruptly jump to a new value if a technician changes the sensitivity or the responsiveness is impacted by environmental changes, e.g., when the loop begins to fail or lanes are shifted for construction. Figure A.2(a) shows the daily median on-time at station 3 northbound by lane over eight years. The horizontal axis shows the cumulative day since the station became operational and the vertical axis shows the daily median on-time. Vertical delineations on the plot show the start of each month, denoted by the first letter of the month's name. In all four lanes the daily median on-time is stable for long periods, but all four lanes show two abrupt changes (May 23, 2002 and June 9, 2009). After the first five months (January 2002 through May 2002), it stabilizes for approximately seven years. The cause of the first shift was unknown, while the second shift arose due to an engineer increasing the detector sensitivity in response to a request by our team. As noted in Chapter 4, we recently found station 3 exhibited detector dropout errors. To fix this problem, we asked the operating agency (the Ohio Department of Transportation) to increase the detector sensitivity setting of all loop detectors at station 3, as discussed in Section 4.6. The change was made on June 9, 2009 and the engineer reported that the sensitivity levels in all lanes at the station were increased from “Normal” to “High”. In turn, the daily median on-time increased by more than 20% after the change.

Station 23 northbound exhibits a more turbulent trend, abruptly changing several times over eight years, as shown in Figure A.2(b). As with the vast majority of the detector stations in the corridor, even with all of the changes, away from the abrupt jumps all of the detectors exhibit stable trends. After several adjustments, it stabilizes for approximately two years starting in May 2002. The daily median on-time in lane 2 dramatically dropped in July 2004, and the daily median on-time in lane 1 increased after October 2004. These trends continued for almost two years, then both detectors went off line for several months. When they returned, the daily median on-time in each lane took a new value. Closer examination of the station 23 data revealed that lane 2 was set to pulse mode between July 2004 and June 2006. Pulse mode is an option commonly used at intersections to detect the passage of a vehicle for queue measurement. When a loop detector is set to pulse mode it reports a constant on-time for all vehicle passages, independent of their actual on-times. Thus, when a single loop detector is set to be pulse mode, it becomes impossible to estimate speed in that lane. This error in lane 2 persisted for two years before the operating agency corrected it, illustrating how these conceptually simple errors can be very difficult to catch.

A.3 Correction of measurement errors due to incorrect loop detector sensitivity and dual loop spacing

A.3.1 Detector sensitivity at single and dual loop detectors

Conventionally speed is estimated at single loop detectors via Equation 2.3. But some trucks may be four times longer than the mean effective vehicle length, and when present they extend the mean on-time and thus reduce the estimated speed relative to the true speed. To reduce susceptibility to these unusually long vehicles (as well the opposite problem arising from short actuation detector errors such as “flicker”), we calculate a more robust estimate of speed via Equation 2.4. In either case, since the length and speed cannot be measured directly at a single loop detector, effective vehicle length is usually assumed to be some constant value, e.g., $\tilde{L}_{\text{median}} = 20$ ft. As noted earlier, this effective length includes the size of the detection zone, which is a function of the sensitivity and responsiveness. If the detection zone size differs from the expected 6 ft, then $\tilde{L}_{\text{median}}$ should be adjusted accordingly or speed will generally be underestimated or overestimated. Unfortunately, it is difficult to directly measure the size of the detection zone.

Using a 20 ft effective vehicle length, Figure A.3 shows the cumulative distribution function (CDF) of estimated loop speed at each loop detector from Equation 2.4 and the daily median on-time from Figure A.1. The detectors are segregated into two groups by the posted speed limit. For the 55 mph group, 74% (31 of 42) of the detectors yield daily median speeds within 5 mph of the speed limit and 12% (5 of 42) are more than 10 mph above the limit. For the 65 mph group, 32% (55 of 173) of the detectors yield daily median speeds within 5 mph of the speed limit, 30% (52 of 173) are more than 10 mph above or 10 mph below the limit.

To address the discrepancy of speed from a single loop detector, a multiplicative correction factor, ϵ_s , is applied to the initially assumed $\tilde{L}_{\text{median}}$ via Equation A.2.^a Assuming drivers usually keep the posted speed limit in free flow time periods, ϵ_s can be estimated via Equation A.3, where the sample period in Equation A.3 is much longer than the sample periods used in Equation A.2, e.g., all vehicles observed between 10am-3pm or the daily median on-time, and once more, if more information is available a different value of the assumed free flow speed can be used in this equation. The correction factor typically remains stable for a long period (e.g., Figure A.2). Of course the errors that impact the speed estimate also

^a It can be shown that the multiplicative correction factor is functionally equivalent to an additive correction factor.

impact on-time and occupancy. Assuming the speed variance over the sample is negligible, occupancy can be corrected via Equation A.4.

$$\hat{V}'_i = \hat{V}_i \times \varepsilon_s = \frac{\tilde{L}_{\text{median}}}{\text{median}(\text{on-time}_i)} \times \varepsilon_s \quad (\text{A.2})$$

where, $\text{median}(\text{on-time}_i)$ is the median of all on-times observed in sample period i , \hat{V}_i is the uncorrected estimated speed in sample period i , ε_s is a multiplicative correction factor for single loop detectors, and \hat{V}'_i is the new estimated speed corrected by the multiplicative correction factor.

$$\varepsilon_s = \frac{\text{assumed free flow speed}}{\frac{\tilde{L}}{\text{median}(\text{on-time}_j)}} = \frac{\text{speed limit}}{\hat{V}_j} \quad (\text{A.3})$$

$$\text{occ}'_i = \frac{\text{occ}_i}{\varepsilon_s} \quad (\text{A.4})$$

One can further improve the estimate by taking the median from many days. Specifically, we calculated a multiplicative correction factor individually for each loop as follows. First, the daily median on-time is found for all weekdays in a month. Next, the median of these daily median on-times (termed *the monthly median on-time*) is found, thereby reducing the impacts of transient events while still allowing the correction factor to adjust to evolving conditions at the detector station. Then, using Equation A.3 the correction factor is estimated using the monthly median on-time and posted speed limit.

A.3.2 Dual loop detector spacing

Thus far the discussion has centered on correcting the sensitivity at a loop detector, whether it be a single loop or one of the paired loops in a dual loop detector. A very similar problem arises at dual loop detectors with regard to spacing. Ordinarily individual vehicle speed is measured directly from the difference in the vehicle's arrival times at the two loops (or the vehicle's departure times from the two loops), and the known loop spacing via Equation 2.5. But this approach only works when the loop spacing is actually known. While detector designs specify the precise spacing between the pair of loops, as we have found, the crew installing the detectors sometimes does not follow the specifications. Even when the physical spacing between the two loops is known accurately, the effective spacing still depends on the size of the two detection zones. The impacts from a difference in sensitivity between the loop detectors are indistinguishable from the impacts of physical loop spacing on the computed speed, hence in this section, "loop spacing" is used to denote the effective loop spacing after accounting for both the

physical spacing and any modification due to the sensitivity of the two detectors (either with or without the correction in the previous section).

Normally the effective loop spacing (L_D) is assumed to be the physical spacing whether using the arrival or departure times. Clearly, if the two detection zones differ, then L_D should depend on whether Equation 2.5 is using the arrival or departure times since the distance traveled between the leading edges of the detection zones differs from that between the corresponding trailing edges. Again, this discrepancy of arrival and departure spacing can be resolved by first correcting for the differences in the size of the detection zones via Equations A.2-A.4. Without that on-time correction, then the remainder of this section should be applied strictly to the arrival times or strictly to the departure times, the correction for one will not necessarily apply to the other.

In any case the assumed physical spacing between the two loops might not be representative of the effective spacing between the two loops. To calibrate this spacing, we follow a process virtually identical to the one we used above for on-time. Once more a multiplicative correction factor, ε_d , is applied to the initially measured average V_i for sample i via Equation A.5 (thus effectively modifying $1/L_D$ from Equation 2.5). Assuming drivers usually keep the posted speed limit (or a target speed measured by radar, etc.) in free flow time periods ε_d can be estimated from the individual vehicle speed measurements, v , via Equation A.6.

$$V'_i = V_i \times \varepsilon_d \quad (\text{A.5})$$

where V_i is the uncorrected average measured speed in sample period i and V'_i is the corrected average measured speed in sample period i .

As before, to reduce transients, we calculate ε_d over many days

$$\varepsilon_d = \frac{\text{assumed free flow speed}}{V_J} = \frac{\text{speed limit}}{V_J} \quad (\text{A.6})$$

where V_J is either the daily median (v) or monthly median (v).

A.4 Validation of the correction factors

In addition to the loop detector data collection, our group has collected many GPS equipped probe vehicle tours of the I-71 corridor. The tours come primarily from the peak periods and each tour passes almost all of the detector stations used in this work (those shown in Figure A.1). We can extract the time and velocity whenever the probe vehicle passes a detector station. The driver was instructed to

drive in lane 2 (second from left) except when overtaking another vehicle. With 355 probe vehicle passes through the corridor between January 2002 and May 2005, we use these data as an independent measure of speed in lane 2 and then gather the concurrent 5 min loop detector data for the given pass. To verify the correction factors, the corrected single loop detector estimated speeds from Equation A.2 and dual loop detector measured speeds from Equation A.5 are compared against the corresponding GPS velocity measurements from probe vehicle data. Figure A.4(a) shows a typical scatter plot comparing the uncorrected single loop detector estimated speed in lane 2 as the probe vehicle passed versus the corresponding GPS velocity at station 9 northbound. It exhibits a systematic bias, with almost all estimates being too high. After applying the correction factor from Equation A.3, Figure A.4(b) shows that the bias is removed. Without the correction, only 46% of the samples have a loop detector speed within 10 mph of the probe vehicle velocity, but after the correction 98% of the samples do. This detector exhibited a very stable sensitivity level throughout the period with probe vehicle data, so in this case we would get similar results whether using a single month to calibrate via Equation A.3 or the monthly median method described above.

To underscore the importance of using the monthly median method, consider the daily median on-time trend at station 21 northbound, as shown in Figure A.2(c). The daily median on-time at this single loop detector station changes several times over eight years, and in fact the loop detectors did not report any data between October 15, 2003 and November 15, 2004. Figure A.4(c) compares the uncorrected speed estimates against the probe vehicle velocity. The probe vehicle velocity shows that all of the observations at this station come from free flow conditions, yet clearly, no single multiplicative correction factor can bring all of the loop detector data in line with the probe vehicle data. Figure A.4(d) repeats the comparison after using Equations A.2-A.3 and the monthly median method. Without the correction, only 54% of the samples have a loop detector speed within 10 mph of the probe vehicle velocity, but after the correction 97% of the samples do. Figure A.4(e-f) show examples after correction from a single loop detector station and dual loop detector station, respectively, that experienced more congestion. As before, the corrections using the posted speed limit brings most of the loop detector data in line with the probe vehicle data.

To quantify this process, we use the average error (AE), average absolute error (AAE), and average absolute relative error (AARE) between the GPS velocity and the loop detector's speed (estimated speed for single loop detectors and measured speed for dual loop detectors). The statistics are calculated both before and after applying the correction factors, via Equation A.7. A positive AE indicates that on average the loop detector speed is faster than the corresponding GPS velocity. For example, at station 9 northbound (Figure A.4 a-b), the AE before applying the correction factor is 10.8 mph and drops

to 0.4 mph after. But the AE allows positive errors to cancel negative errors since it simply reflects the bias, so we also calculate AAE and AARE. The AAE before and after applying the correction factor at this station is 10.8 mph and 2.2 mph, respectively. The AARE before and after applying correction factor is 17.4% and 3.6%, respectively.

$$AE = \frac{\sum_{n=1}^N v_n^{\text{Loop}} - v_n^{\text{GPS}}}{N}, \quad AAE = \frac{\sum_{n=1}^N |v_n^{\text{Loop}} - v_n^{\text{GPS}}|}{N}, \quad AARE = \frac{\sum_{n=1}^N \left| \frac{v_n^{\text{Loop}} - v_n^{\text{GPS}}}{v_n^{\text{GPS}}} \right|}{N} \quad (\text{A.7})$$

Where, N is the total number of observations with both loop detector and GPS data, v_n^{GPS} is the GPS velocity at n-th probe vehicle passage over the given loop detector, and v_n^{Loop} is the loop speed for 5 min sample corresponding to the n-th probe vehicle passage.

Figure A.5 shows the performance of the single loop detectors before and after applying the correction factor to the estimated speed ("without correction" and "with correction," respectively), thereby rectifying any mismatch between sensitivity and responsiveness. Again, these data come from lane 2, and in the case of dual loop detectors, only the upstream loop is shown. The plots show results for a total of 64 single loop detectors.^b For example, in lane 2 at station 2 northbound, the AE, AAE, and AARE before applying correction factors is 24.6 mph, 24.6 mph, and 47.4%, respectively. After applying correction factors, AE, AAE, and AARE drop to -0.2 mph, 2.4 mph, and 6.7%, respectively.

As designed, the dual loop detectors were supposed to have 20 ft spacing between leading edges of the paired loops, but in some cases the installation contractor was very liberal in their interpretation of the specifications and we call this condition "original fixed". As a result of this problem, the operating agency undertook the task of manually measuring the physical distance between the paired loops and we call this condition "manual calibration". Figure A.6 shows the performance of the dual loop detector measured speed via Equation 2.5 under these two before conditions. The figure also shows performance after applying the correction factor via Equation A.5 to the measured speed (denoted "with correction"), thereby rectifying any remaining error in the paired detector spacing.^c The plots show results for a total of 26 dual loop detectors. For 10 of the 12 detectors with large errors in the *original fixed* data, the *manual*

^b In this case the monthly median is calculated using all of the weekdays in the month in which the observation was made. Obviously this approach could not be implemented in real time. For real time applications, one could instead use the 20 preceding weekdays or the previous calendar month to generate the correction factor. Since the only difference would come near a discrete jump in detector sensitivity, and those are relatively rare (typically less than once per year) the results would be similar no matter how one would define the month of calibration.

^c In this case the correction was applied to the *manual calibration* speeds, but the results would be similar from the *original fixed* speeds since the two differ by a scale factor that is transparent to our method.

calibration made a significant improvement. Though there were a few cases where the manual calibration degraded performance, e.g., station 13 southbound. In almost all cases our correction factor improved performance over both of the before conditions.

Table A.1 summarizes the performance across all detectors, showing the results with and without our monthly median correction factors, sorted by free flow and congested conditions. The GPS velocity is used to differentiate between the two traffic conditions: the given sample is considered free flow if the GPS velocity is higher than 45mph, and congested otherwise. Roughly 10% of observations come from congestion. The right-most columns show the performance across all of the observations, both free flow and congested combined. With the small exception of the congested AE northbound, the AE, AAE, and AARE after applying the correction factors are closer to zero than those before applying the correction factors. Across the different conditions the AARE in free flow are generally smaller than the corresponding AARE in congestion because in congestion the 5 min sample variance is larger and the denominator is smaller. On the other hand, the AAE is roughly consistent between free flow and congestion. In any case, the correction factors improve the loop detector speeds, as measured by the AE, AAE, and AARE.

A.5 Conclusions

This appendix developed a means to quantify detector sensitivity using the daily median and showed how the sensitivity can change over time. It then developed a methodology to correct for unexpected sensitivity errors at a single loop detector by applying a multiplicative correction factor. Key to this work is the fact that for most detector locations, the dominant vehicle will be a free flowing passenger vehicle, and the daily median will usually be representative of such. In other words, the daily median on-time should fall into a small range. The methodology is simple enough that it could be implemented on a model 170 controller. While in an ideal world a technician would be dispatched to the field to correct the sensitivity errors, recognizing that such visits might not always be feasible, we develop a means to generate a correction factor that can be applied to all samples. To reduce sensitivity to transient events, the correction factor is determined by finding the value that brings the monthly median to the target value. This same approach is extended to also correct for errors in the assumed effective spacing at dual loop detectors. Ideally for dual loop detectors one would first individually correct the on-times in both loops via Equations A.2 and A.4, and then correct the spacing via Equations A.5 and A.6, but the methodology would also work without correcting the on-times. Both the single loop and dual loop methods are then validated against concurrent velocity measurements from a GPS equipped probe vehicle.

As demonstrated in Figure A.5-A.6 and Table A.1, the methodology showed good performance compared to the uncorrected data.

Table A.1, Average Error (AE), Average Absolute Error (AAE), and Average Absolute Relative Error (AARE) before and after applying the monthly median correction factors, segregated by free flow and congestion across all observations at all detection stations

Types of loop detectors	Direction	Application of correction factor	Free flow (GPS velocity > 45mph)				Congestion (GPS velocity ≤ 45mph)				Overall (all observations)			
			Number of observations	AE (mph)	AAE (mph)	AARE (%)	Number of observations	AE (mph)	AAE (mph)	AARE (%)	Number of observations	AE (mph)	AAE (mph)	AARE (%)
Single loop detectors	NB	without correction	9,101	-3.3	9.7	15.5	1,096	0.0	5.6	21.7	10,197	-3.0	9.3	16.2
		with correction		0.5	2.6	4.2		-1.0	3.3	14.4		0.3	2.7	5.3
	SB	without correction	8,783	-2.4	10.3	16.3	1,051	-2.1	6.5	26.8	9,834	-2.3	9.9	17.4
		with correction		0.5	2.7	4.3		-0.5	3.7	17.6		0.4	2.8	5.7
Dual loop detectors	NB	original fixed	3,783	8.7	10.4	16.4	453	3.5	6.9	23.1	4,236	8.2	10.0	17.1
		manual calibration		2.9	4.6	7.5		2.2	4.4	15.3		2.8	4.6	8.4
		with correction		0.7	3.1	5.1		-1.8	3.4	13.1		0.5	3.1	5.9
	SB	original fixed	3,544	9.8	10.7	16.7	409	3.1	5.0	19.1	3,953	9.1	10.1	17.0
		manual calibration		6.9	7.7	11.9		1.4	3.8	15.1		6.3	7.3	12.2
		with correction		0.6	2.6	4.2		-1.1	3.1	13.7		0.4	2.7	5.2

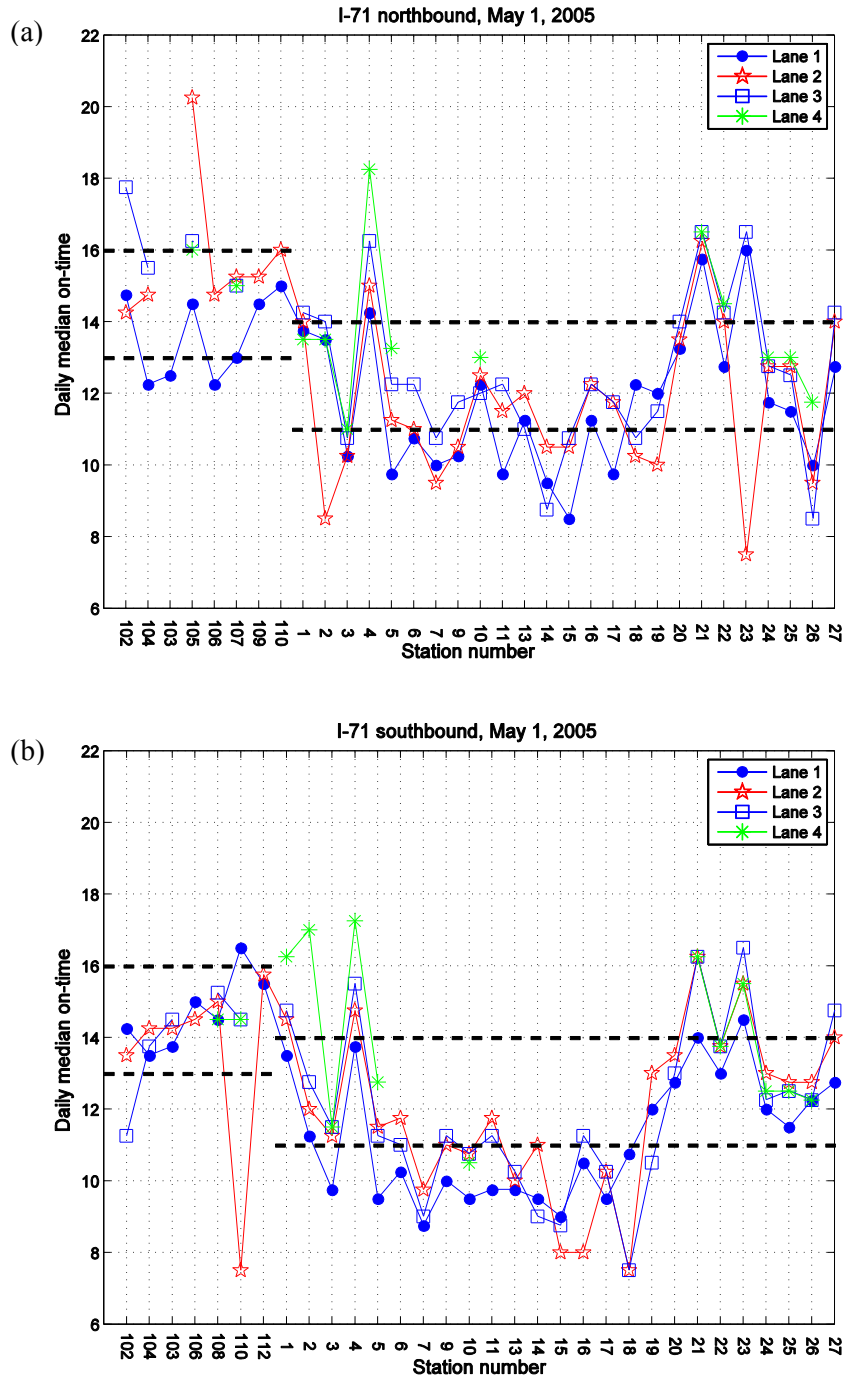


Figure A.1. Daily median on-times at each loop detector in the I-71 corridor on May 1, 2005 (a) 107 loop detectors over 33 stations northbound and (b) 108 loop detectors over 32 stations southbound. The dashed horizontal lines bound the expected range of median on-time given the speed limit at the station. Note that at dual loop detector stations only the upstream detector is shown.

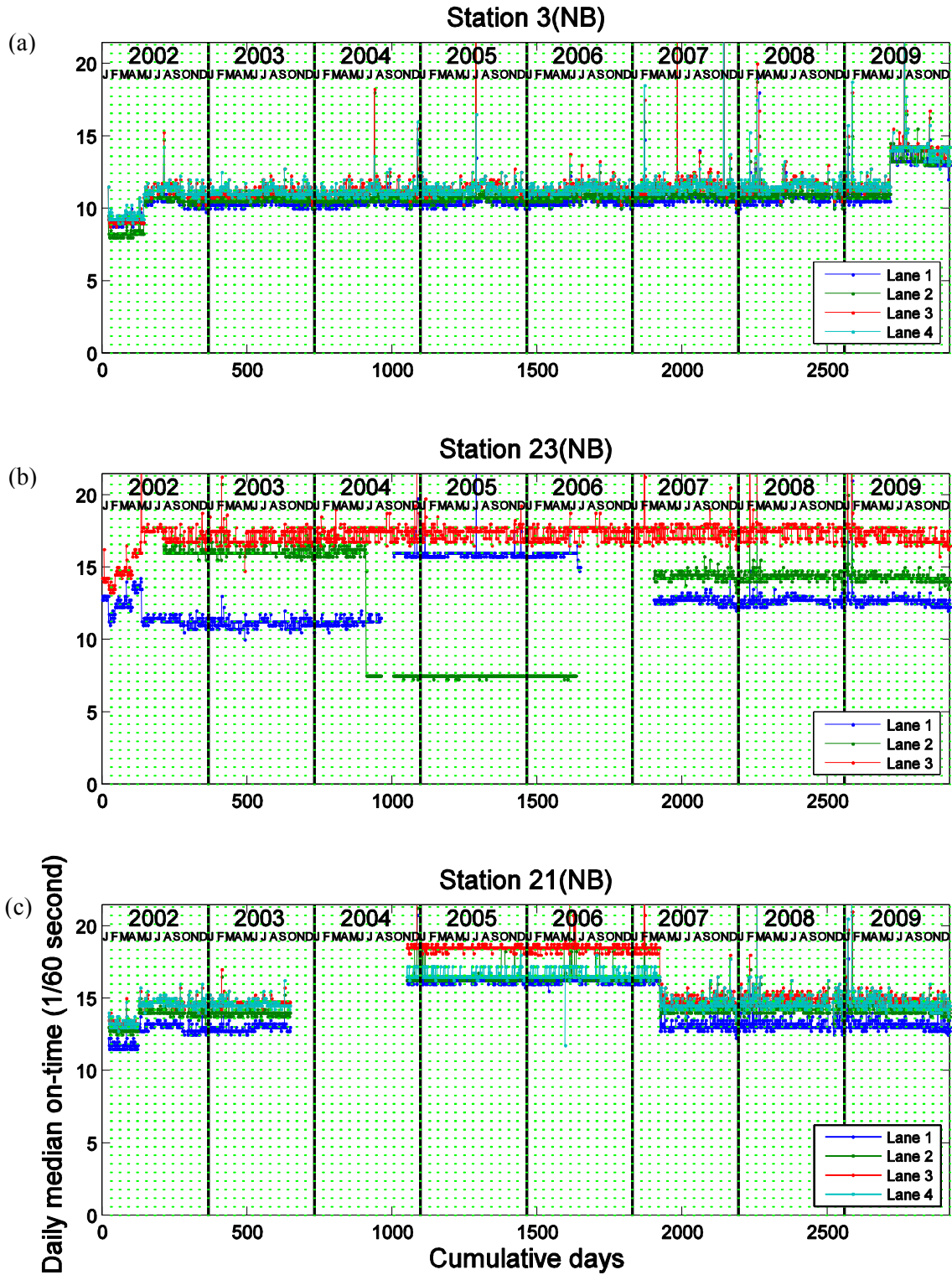


Figure A.2, The trend of daily median on-times by lane over eight years (a) station 3 northbound, (b) station 23 northbound, and (c) station 21 northbound.

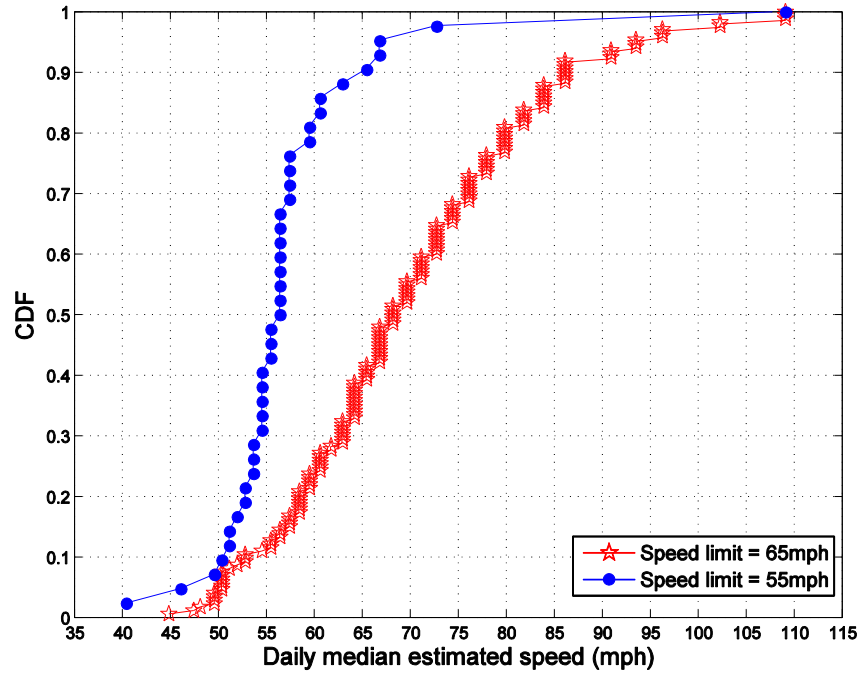


Figure A.3, CDF of daily median estimated speed over 215 loop detections both directions (42 with a 55 mph speed limit and 173 with a 65 mph speed limit). Note that at dual loop detector stations only the upstream detector is shown.

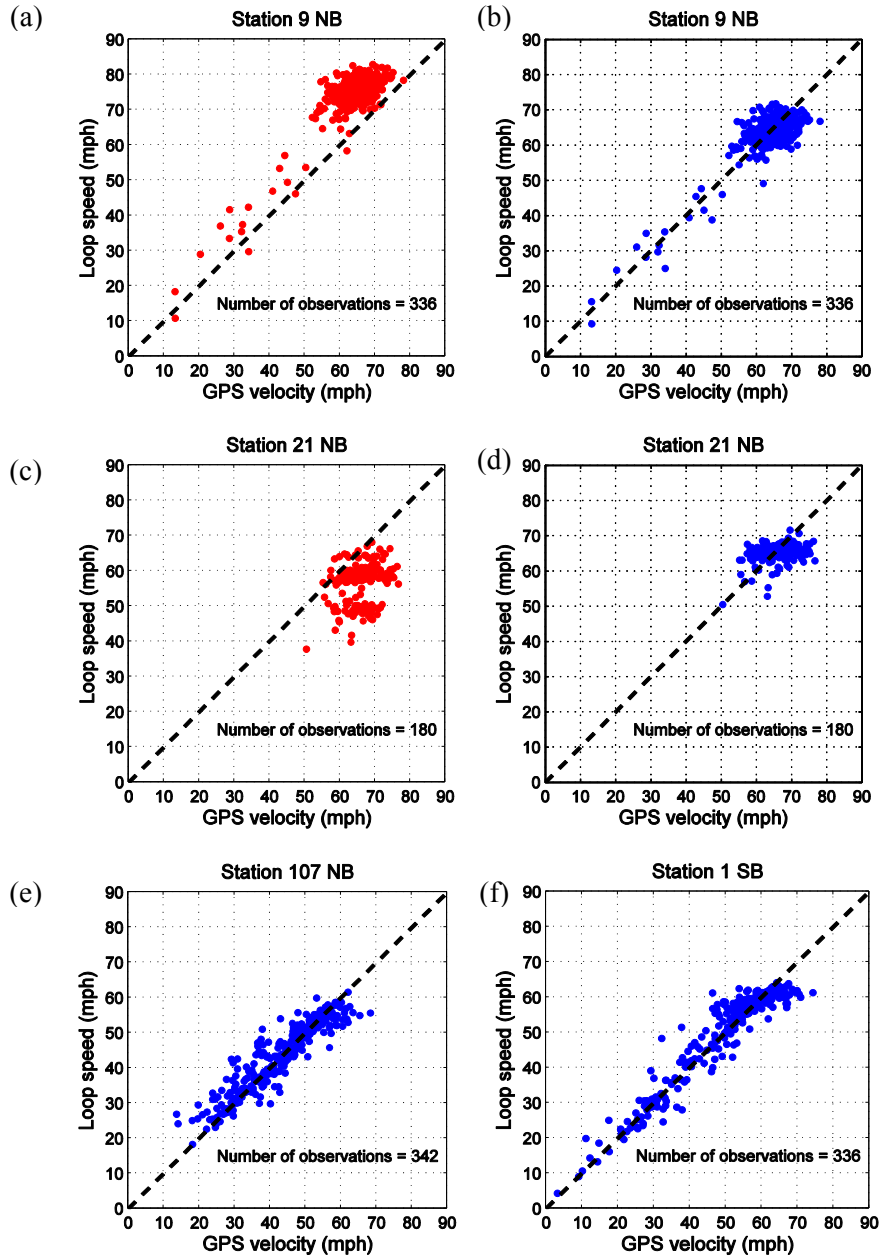


Figure A.4, Comparison of single loop detector estimated speed and GPS velocity (a) from station 9 northbound (lane 2) before applying correction factors. The loop detector speed is systematically higher than the GPS velocity (b) After applying the correction factors at station 9 northbound lane 2 the loop detector speed is unbiased relative to the GPS velocity (c) Repeating the process at station 21 northbound (lane 2), first the raw data show the impact of the changes in the daily median on-time (d) After applying the correction factors from the monthly median method to station 21 northbound the correction factors adjust to the changing detector sensitivity (e) After applying the correction factors to station 107 northbound (f) Comparison of dual loop detector measured speed and GPS velocity from station 1 southbound after applying correction factors.

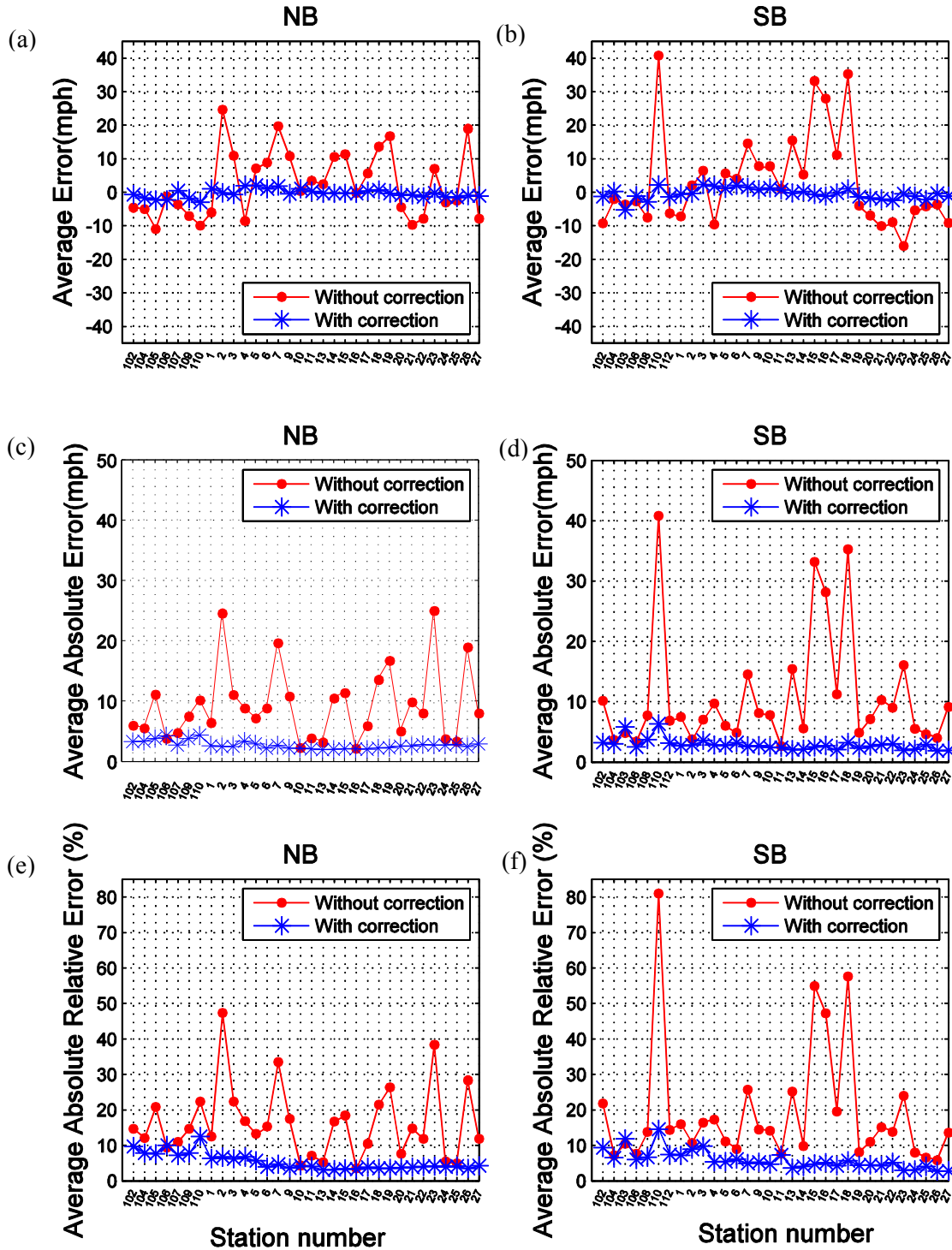


Figure A.5. AE between single loop detector estimated speed and GPS velocity with and without correction factors in lane 2 for (a) northbound and (b) southbound. Next, AAE between single loop detector estimated speed and GPS velocity with and without correction factors for (c) northbound and (d) southbound. Third, AARE between single loop detector estimated speed and GPS velocity with and without correction factors for (e) northbound and (f) southbound.

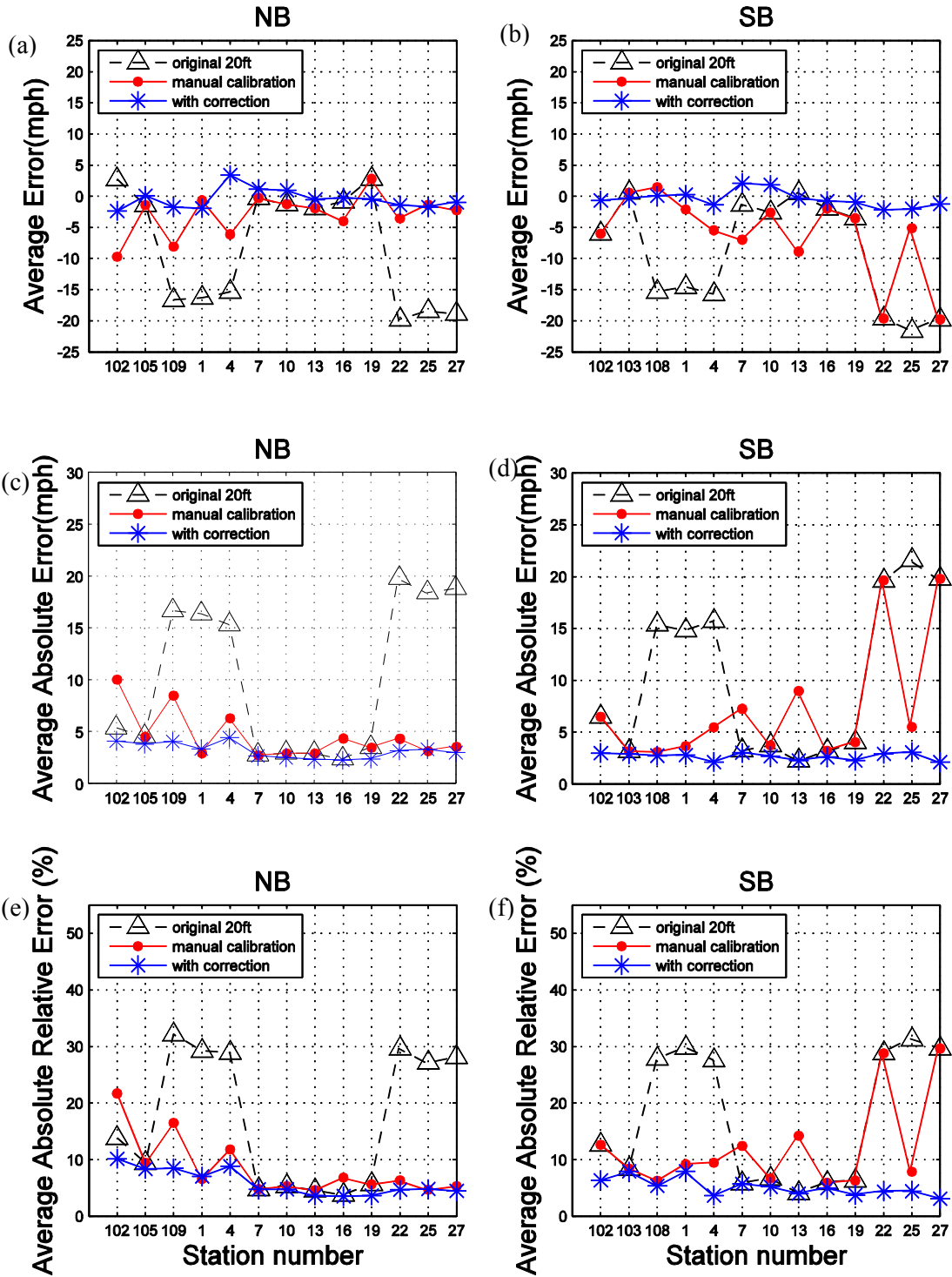


Figure A.6, AE between dual loop detector measured speed and GPS velocity with and without correction factors in lane 2 for (a) northbound and (b) southbound. Next AAE between dual loop detector measured speed and GPS velocity with and without correction factors for (c) northbound and (d) southbound. Third AARE between dual loop detector measured speed and GPS velocity with and without correction factors for (e) northbound and (f) southbound.

APPENDIX B GROUND TRUTHING TOOL

A purpose built software ground truthing tool with a graphical user interface (GUI) was developed in MATLAB to efficiently generate ground truth data. Figure B.1 shows a screen capture of the ground truthing tool while processing the data of lane 2 at station 56 westbound. The GUI window consists of three interfaces: (a) a window for the current video image, (b) a window for a plot of transition pulses from the loop detectors, and (c) a user control panel for entering the ground truth data. Each of these three components is explained in more detail below.

The first step comes before the GUI and it is to synchronize the video and loop detector data. To this end we used the arrival pattern of vehicles across all lanes as follows. First we select roughly 30 seconds from the video and record the time (relative to the start of the short observation period) of all vehicle arrivals at the loop detectors in each lane. Then, we use vehicle reidentification techniques to search the loop detector data to find the same or similar arrival patterns and the fact that we use multiple lanes that are time synchronized leads to much greater accuracy. The offset time between video and loop detector data is then calculated from the difference of times for the first vehicle matched between the video and loop detector data.

After synchronizing the video and detector data we can then use the GUI to step from pulse to pulse at the target detector. Illustrating the general functionality of the GUI, (lane 2, upstream in this case) Figure B.1 part B shows the current pulse denoted with a cyan vertical delineation. So in this case the GUI is at the fifth visible pulse in lane 2 (counted from the left hand side). The GUI shows the concurrent video frame for the same instant in part A and the GUI is ready for the user to assess the pulse using the buttons in part C. In this case the current pulse in lane 2 corresponds to a pick-up truck pulling a trailer, so the user should click the “Medium2” button to classify this pulse as a “vehicle pulling a trailer” and non-detector error.

The user must explicitly classify an event as an error; in the case of non-vehicle detections this classification is straight forward. When a vehicle results in two or more pulses (whether all in one lane, e.g., pulse breakup, or in several lanes, e.g., splashover) the user selects a pulse in the dominant lane of travel and classifies the vehicle as if no error occurred. The remaining pulses are all labeled as errors

without a vehicle class. Finally, when a vehicle triggers a pulse in the correct lane but the pulse is too short, the user would not label that error because this research focuses on detector errors related to non-vehicle detection. The bottom three buttons in the user control panel, part C, allow the user to step the video forward or backwards to get a different view (particularly useful in the presence of occlusions and lane change maneuvers), while the last button allows the user to undo the previous assessment (in which case the GUI jumps back to that pulse). If the user clicks any of the remaining buttons in the user control panel, the input associated with the pulse is logged and the GUI jumps to the next pulse in that lane. The process is repeated for all successive pulses in the given lane.

(A) Current video frame:

The video frames provide information to allow the user to generate the independent ground truth data. After synchronizing the two data sources, the tool automatically presents the concurrent video frame for the given transition pulse. A user then verifies and classifies the source of a pulse from the concurrent video frame. The user is responsible for keeping track of the location of the detectors in the image. Sometimes the location of the detectors are only known approximately, but in most cases knowing the exact location of the detectors is not critical because the small spatial error is canceled by a small temporal offset in the synchronization.

(B) Time series of pulses from the loop detectors:

This plot presents lane number versus time (1/60 seconds) for the loop detector data. Lane numbers increase from top to bottom. In this case the station is equipped with dual loop detectors, so two curves are shown in each lane (upstream in red below, downstream in blue above for a given lane, following the common practice from time-space diagrams where vehicles travel from bottom to top). There are two colors of vertical delineations in this plot, cyan to indicate the current pulse and red to indicate previous pulses in the lane that now have ground truth data.

(C) User control panel:

There are 15 buttons used to assign specific information about a given transition pulse. The user manually records types of vehicles and any detector errors from the direct comparison between concurrent detector and video data.

C1) Start button: click the button to start the ground truthing process. The detector number, detector station source data file path, video data source file path, video time offset, and output file path are

specified at the start of the matlab code for the GUI. The GUI starts at the first pulse from the detector that has a concurrent video image.

C2) Vehicle classification (Refer to Table 2.1 for examples of types of vehicles):

- C2-1) Small: a passenger vehicle,
- C2-2) Medium: a single unit truck or bus,
- C2-3) Medium2: any small or medium vehicle pulling a trailer,
- C2-4) Large: a multiple unit truck

C3) Detector errors:

- C3-1) Exception: A user is not able to see whether a vehicle is present or not for the given pulse because vehicles closer to the camera occlude the lane to the point of precluding differentiation or completely obscure a possible vehicle.
- C3-2) LCM: non-vehicle pulse in a lane changing maneuver,
- C3-3) Semi-S: non vehicle pulse(s) in a splashover error,
- C3-4) Breakup: 1st non-vehicle pulse in a pulse breakup error from a multiple unit truck,
- C3-5) Addi: 2nd (or greater) non-vehicle pulse in a pulse breakup error from a multiple unit truck,
- C3-6) Breakup2: 1st non-vehicle pulse in a pulse breakup error from a vehicle pulling a trailer (i.e., “Medium2”)
- C3-7) Addi2: 2nd (or greater) non-vehicle pulse in a pulse breakup error from a vehicle pulling a trailer

C4) Frame transition:

- C4-1) FWD10: move forward 10 frames of video,
- C4-2) BWD10: move backward 10 frames of video,
- C4-3) UNDO: cancel most recent ground truthed pulse, then automatically move back to that pulse

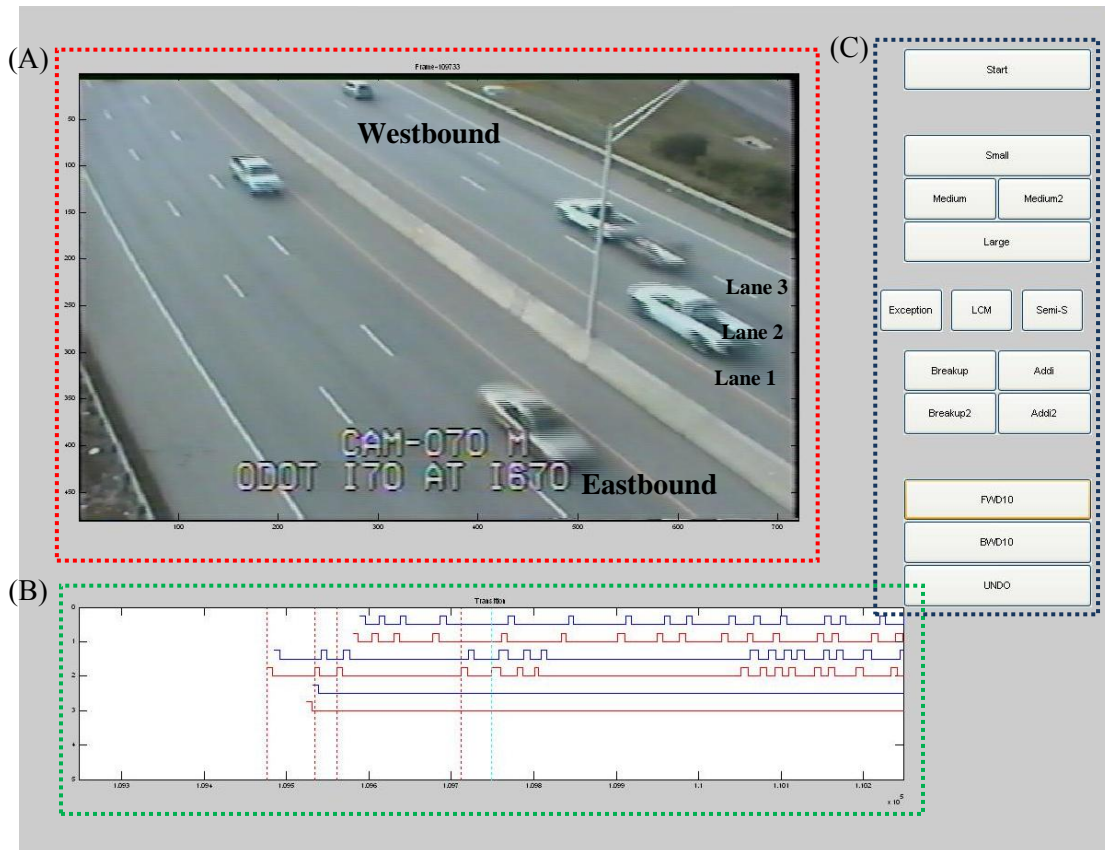


Figure B.1, Screen capture of a ground truthing tool

APPENDIX C SENSITIVITY OF THE SPLASHOVER DETECTION

ALGORITHM WITH RESPECT TO ϵ

Data from station 104 eastbound presented in Table 3.1 are used to evaluate the performance of the splashover detection algorithm with respect to the change of ϵ . When ϵ is set to each integer value from 1 second to 10 seconds, the number of suspected splashover events (nSS) and the expected number of false positives (EnFP) is calculated via Equation 3.2. Figure C.1 shows the difference between nSS and EnFP as being nearly constant for each pair of lanes over the range of ϵ (recall that the splashover detection algorithm arbitrarily sets ϵ to five seconds). For all values of ϵ in this plot the only lane pair that has a positive value is source lane 2-target lane 1 and for all values of ϵ the algorithm correctly identifies the loop detector in lane 2 with splashover.

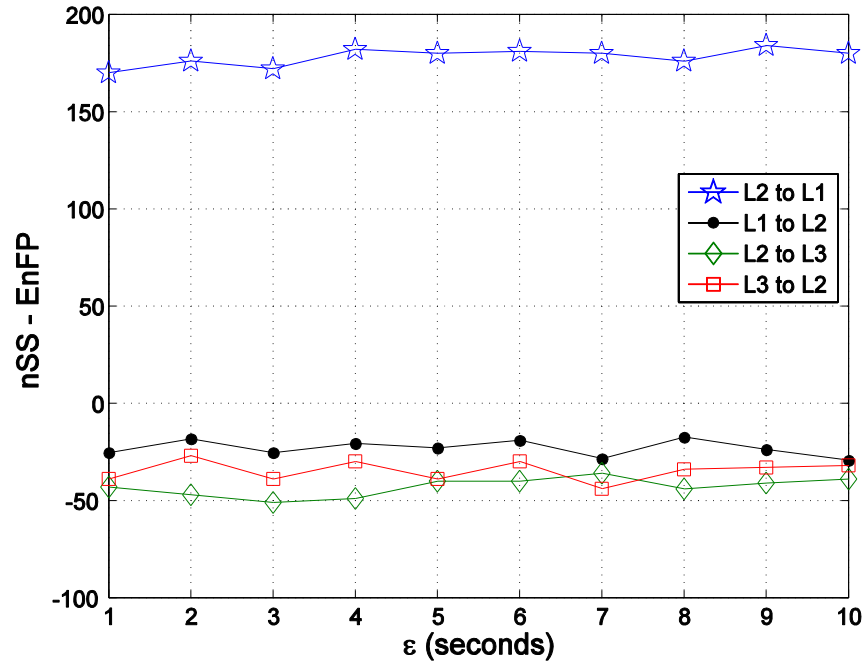


Figure C.1, The number of suspected splashover and expected number of false positives at station 104 eastbound presented in Table 3.1 when ϵ is changed from 1 second to 10 seconds.

**APPENDIX D PERCENTAGE OF ADJUSTED RATE OF SUSPECTED
SPLASHOVER RELATIVE TO SOURCE LANE**

From the Ground Truth Data underlying Table 3.2,

Table D.1, Total number of pulses recorded at each loop detector

Condition	Station number	Direction	Date	Total number of pulses recorded at each loop detector			
				Lane 1	Lane 2	Lane 3	Lane 4
Splashover	38	WB	September 9, 2008	172	242	206	56
	41	EB	September 9, 2008	337	507	-	-
	56	WB	November 21, 2008	345	632	121	-
	104	EB	March 17, 2008	441	349	350	-
Non-splashover	2	NB	March 9, 2009	628	642	526	45
	3	NB	March 17, 2008	310	420	359	168
	3	SB	April 18, 2008	995	1,806	1,537	1,139
	4	SB	March 17, 2008	225	523	533	83
	6	NB	April 18, 2008	2,249	1,962	1,747	-
	9	NB	June 5, 2006	2,386	2,900	2,277	-
	9	SB	June 5, 2006	2,434	2,964	2,288	-
	15	NB	March 10, 2009	1,173	940	899	-
	18	NB	March 9, 2009	197	227	140	-
	19	NB	March 17, 2008	186	297	294	-
	31	NB	November 21, 2008	124	296	220	27
	38	EB	August 29, 2008	355	331	164	-
	43	EB	September 2, 2008	262	419	384	-
	43	WB	September 2, 2008	500	590	444	-
	56	EB	September 3, 2008	596	771	322	-
	102	EB	March 10, 2009	189	320	322	-
104	WB	March 12, 2009	359	415	295	-	

Table D.2, Number of suspected splashover (nSS) of pulse j in the target lane matched to pulse i in the source lane. Shaded cells indicate a loop detector with splashover verified from the ground truth data, while non-shaded cells indicate a loop detector without any observed splashover

Condition	Station number	Direction	Suspected splashover of pulse j in the target lane matched to pulse i in the source lane: P_{ij} in Equation 3.2 [Source lane (S) → Target lane (T)]					
			Lane 1→ Lane 2	Lane 2→ Lane 1	Lane 2→ Lane 3	Lane 3→ Lane 2	Lane 3→ Lane 4	Lane 4→ Lane 3
Splashover	38	WB	4	12	115	2	18	1
	41	EB	18	60	-	-	-	-
	56	WB	8	24	29	6	-	-
	104	EB	32	240	7	35	-	-
Non-splashover	2	NB	30	0	0	24	6	1
	3	NB	0	5	5	5	0	0
	3	SB	2	46	35	28	11	15
	4	SB	1	8	4	6	0	2
	6	NB	15	25	9	37	-	-
	9	NB	18	76	34	36	-	-
	9	SB	9	116	63	50	-	-
	15	NB	1	48	10	8	-	-
	18	NB	7	4	2	2	-	-
	19	NB	2	5	3	5	-	-
	31	NB	3	4	6	12	3	0
	38	EB	4	15	1	3	-	-
	43	EB	1	6	6	13	-	-
	43	WB	6	16	4	12	-	-
	56	EB	5	19	31	19	-	-
102	EB	3	8	7	18	-	-	
104	WB	12	2	7	14	-	-	

Table D.3, Expected number of False Positives (EnFP) of pulse j in the target lane matched to pulse i shifted by the constant delay in the source lane. Shaded cells indicate a loop detector with splashover verified from the ground truth data, while non-shaded cells indicate a loop detector without any observed splashover

Condition	Station number	Direction	Non-splashover of pulse j in the target lane matched to pulse i shifted by the constant delay in the source lane: Q_{ij} in Equation 3.2 [Source lane (S) \rightarrow Target lane (T)]					
			Lane 1 \rightarrow Lane 2	Lane 2 \rightarrow Lane 1	Lane 2 \rightarrow Lane 3	Lane 3 \rightarrow Lane 2	Lane 3 \rightarrow Lane 4	Lane 4 \rightarrow Lane 3
Splashover	38	WB	13	14	15	11	4	3
	41	EB	25	42	-	-	-	-
	56	WB	26	28	15	6	-	-
	104	EB	61	60	47	74	-	-
Non-splashover	2	NB	45	39	30	47	3	3
	3	NB	18	19	28	27	8	8
	3	SB	82	113	183	176	110	78
	4	SB	22	20	51	41	3	2
	6	NB	240	294	219	220	-	-
	9	NB	164	210	194	190	-	-
	9	SB	173	283	273	214	-	-
	15	NB	89	114	103	109	-	-
	18	NB	16	13	10	9	-	-
	19	NB	12	13	13	22	-	-
	31	NB	4	11	11	23	1	0
	38	EB	35	35	10	19	-	-
	43	EB	26	20	26	31	-	-
	43	WB	56	76	43	47	-	-
	56	EB	53	48	36	40	-	-
102	EB	24	31	44	50	-	-	
104	WB	53	38	25	42	-	-	

APPENDIX E MEDIAN ON-TIME OF LOOP DETECTORS WITH GROUND TRUTH DATA

We found the daily median on-times from the source and target lane detectors to ensure that the pair of detectors do not have an extreme difference of loop detector sensitivity. If the absolute difference between the daily median on-times in adjacent lane pairs is greater than $3/60$ seconds, we consider that pair to have an extreme difference of loop detector sensitivity. As a result, the splashover may be in the opposite direction than indicated by Equation 3.2. Table E.1 shows daily median on-time of a loop detector from the corresponding date of the ground truth data underlying Table 3.2 and the difference of daily median on-times at adjacent lane pairs. The absolute difference of daily median on-times is less than $3/60$ seconds for all of the lane pairs in the table, and thus, there does not appear to be an extreme difference of loop detector sensitivity in the lane pairs.

Table E.1, Median on-time of a loop detector used for evaluation of the splashover detection algorithm and the difference of median on-times between two adjacent. Shaded cells indicate loop detectors with splashover verified from the ground truth data, while non-shaded cells indicate loop detectors without any observed splashover

Condition	Station number	Direction	Date	Median on-times [1/60 second]				Difference of median on-times between two adjacent lanes [1/60 second]		
				Lane 1	Lane 2	Lane 3	Lane 4	Lane 1 – Lane 2	Lane 2 – Lane 3	Lane 3 – Lane 4
Splashover	38	WB	September 9, 2008	15.0	15.5	14.5	16.3	-0.5	1.0	-1.8
	41	EB	September 9, 2008	16.5	18.5	-	-	-2.0	-	-
	56	WB	November 21, 2008	14.0	16.5	15.8	-	-2.5	0.8	-
	104	EB	March 17, 2008	15.5	14.3	16.8	-	1.3	-2.5	-
Non-splashover	2	NB	March 9, 2009	13.8	9.0	15.0	14.0	4.8	-6.0	1.0
	3	NB	March 17, 2008	10.5	10.8	11.3	11.5	-0.3	-0.5	-0.3
	3	SB	April 18, 2008	10.0	11.8	12.3	12.5	-1.8	-0.5	-0.3
	4	SB	March 17, 2008	10.8	11.5	12.3	12.0	-0.8	-0.8	0.3
	6	NB	April 18, 2008	10.8	11.3	12.8	-	-0.5	-1.5	-
	9	NB	June 5, 2006	10.5	11.0	12.0	-	-0.5	-1.0	-
	9	SB	June 5, 2006	10.0	11.5	12.3	-	-1.5	-0.8	-
	15	NB	March 10, 2009	8.5	11.0	11.5	-	-2.5	-0.5	-
	18	NB	March 9, 2009	12.5	10.5	11.8	-	2.0	-1.3	-
	19	NB	March 17, 2008	12.0	10.3	12.0	-	1.8	-1.8	-
	31	NB	November 21, 2008	13.0	14.3	14.8	15.3	-1.3	-0.6	-0.4
	38	EB	August 29, 2008	13.3	14.8	16.0	-	-1.5	-1.2	-
	43	EB	September 2, 2008	13.2	14.5	15.5	-	-1.2	-1.0	-
	43	WB	September 2, 2008	14.5	15.5	15.8	-	-1.0	-0.2	-
	56	EB	September 3, 2008	13.8	15.3	16.5	-	-1.5	-1.2	-
	102	EB	March 10, 2009	15.5	15.0	19.3	-	0.5	-4.3	-
104	WB	March 12, 2009	14.0	15.5	14.8	-	-1.5	0.8	-	

**APPENDIX F DETAILED RESULTS FROM THE EARLIER
METHODOLOGIES TO IDENTIFY LOOP DETECTORS WITH
SPLASHOVER**

Table F.1 shows the performance of the three of the earlier error detection methodologies to identify loop detectors with splashover by lane, comparable to Table 3.4 for L&C, and that underlie Figure 3.8 and Table 3.5.

Table F.1, The performance of three of the earlier detection methodologies using the ground truth data. Shaded cells indicate loop detectors with splashover verified from the ground truth data, while non-shaded cells indicate loop detectors without any observed splashover

Condition	Station number	Direction	Chen and May [C&M]				Turochy and Smith [T&S]				Jacobson et al. [JNB]			
			Lane 1	Lane 2	Lane 3	Lane 4	Lane 1	Lane 2	Lane 3	Lane 4	Lane 1	Lane 2	Lane 3	Lane 4
Splashover	38	2	3.5%	0.0%	4.4%	0.0%	0.0%	0.0%	0.0%	0.0%	0.0%	0.0%	11.4%	9.5%
	41	1	4.5%	0.6%	-	-	0.0%	0.0%	-	-	2.2%	1.1%	-	-
	56	2	0.3%	0.6%	2.5%	-	0.0%	0.0%	0.0%	-	0.0%	0.0%	7.9%	-
	104	1	7.7%	0.6%	0.6%	-	4.0%	0.0%	0.0%	-	5.4%	0.0%	0.0%	-
Non-splashover	2	1	1.0%	0.3%	0.4%	0.0%	0.0%	0.0%	0.0%	0.0%	1.2%	55.3%	0.0%	4.9%
	3	1	1.9%	4.8%	2.2%	0.6%	0.0%	0.0%	0.0%	0.0%	18.3%	6.7%	3.3%	3.3%
	3	2	0.5%	0.7%	0.7%	0.5%	0.0%	0.0%	0.0%	0.0%	6.4%	7.0%	1.1%	1.1%
	4	2	0.0%	1.5%	1.7%	0.0%	0.0%	0.0%	0.0%	0.0%	0.0%	4.6%	3.1%	6.4%
	6	1	0.9%	1.5%	0.7%	-	0.0%	0.0%	0.0%	-	1.6%	0.5%	0.0%	-
	9	1	1.1%	5.7%	3.3%	-	0.0%	0.0%	0.0%	-	11.1%	3.3%	0.0%	-
	9	2	1.0%	0.9%	3.6%	-	0.0%	0.0%	0.0%	-	18.0%	3.1%	0.0%	-
	15	1	0.2%	2.6%	0.2%	-	1.6%	0.0%	0.0%	-	87.9%	8.8%	5.5%	-
	18	1	0.5%	4.9%	2.2%	-	0.0%	0.0%	0.0%	-	0.0%	5.9%	5.9%	-
	19	1	1.1%	2.7%	4.1%	-	0.0%	0.0%	0.0%	-	2.2%	6.4%	0.0%	-
	31	1	0.0%	0.3%	0.5%	0.0%	0.0%	0.0%	0.0%	0.0%	2.2%	3.2%	17.2%	8.9%
	38	1	2.3%	0.3%	1.8%	-	0.0%	0.0%	0.0%	-	0.0%	2.2%	8.9%	-
	43	1	2.7%	0.5%	0.5%	-	0.0%	0.0%	0.0%	-	0.0%	0.0%	0.0%	-
	43	2	0.8%	1.0%	0.5%	-	0.0%	0.0%	0.0%	-	1.5%	0.0%	0.0%	-
	56	1	1.7%	0.7%	0.0%	-	0.0%	0.0%	0.0%	-	0.9%	0.0%	2.7%	-
102	1	0.0%	0.3%	1.6%	-	0.0%	0.0%	0.0%	-	0.0%	0.0%	0.0%	-	
104	2	0.6%	0.2%	0.0%	-	0.0%	0.0%	0.0%	-	0.0%	0.0%	0.0%	-	

APPENDIX G SPEED TRENDS OF THE GROUND TRUTH DATA IN CONGESTED CONDITIONS

This appendix presents the speed trends of the ground truth data in congested conditions used to evaluate the pulse breakup detection algorithm.

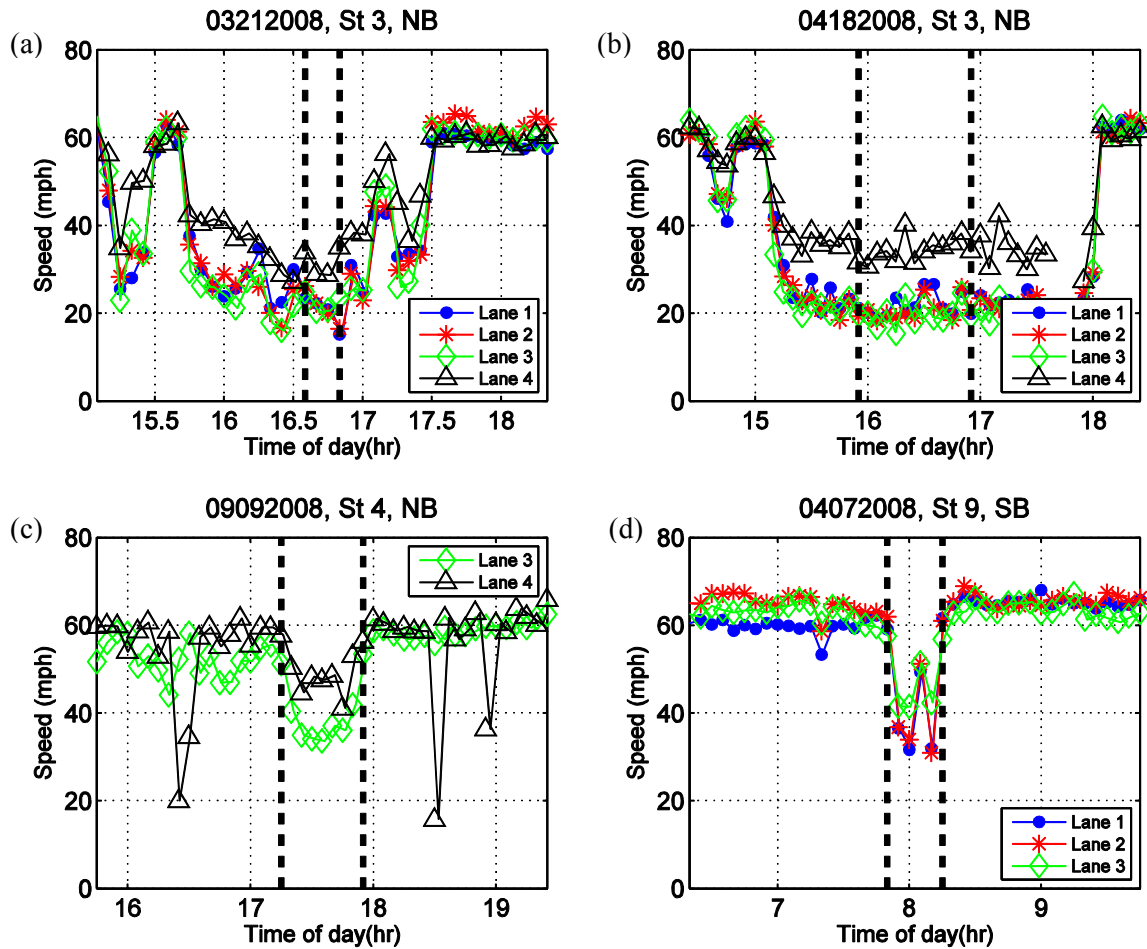


Figure G.1, Speed trends at detector stations in the ground truth data with pulse breakup during congested conditions. The two vertical delineations indicate the time period (start time and end time) when the ground truth data were generated. (a) station 3 northbound on March 21, 2008 (16:35 ~ 16:50), (b) station 3 northbound on April 18, 2008 (15:55 ~ 16:55), (c) station 4 northbound on September 9, 2008 (17:15 ~ 17:55), and (d) station 9 southbound on April 7, 2008 (07:50 ~ 08:10).

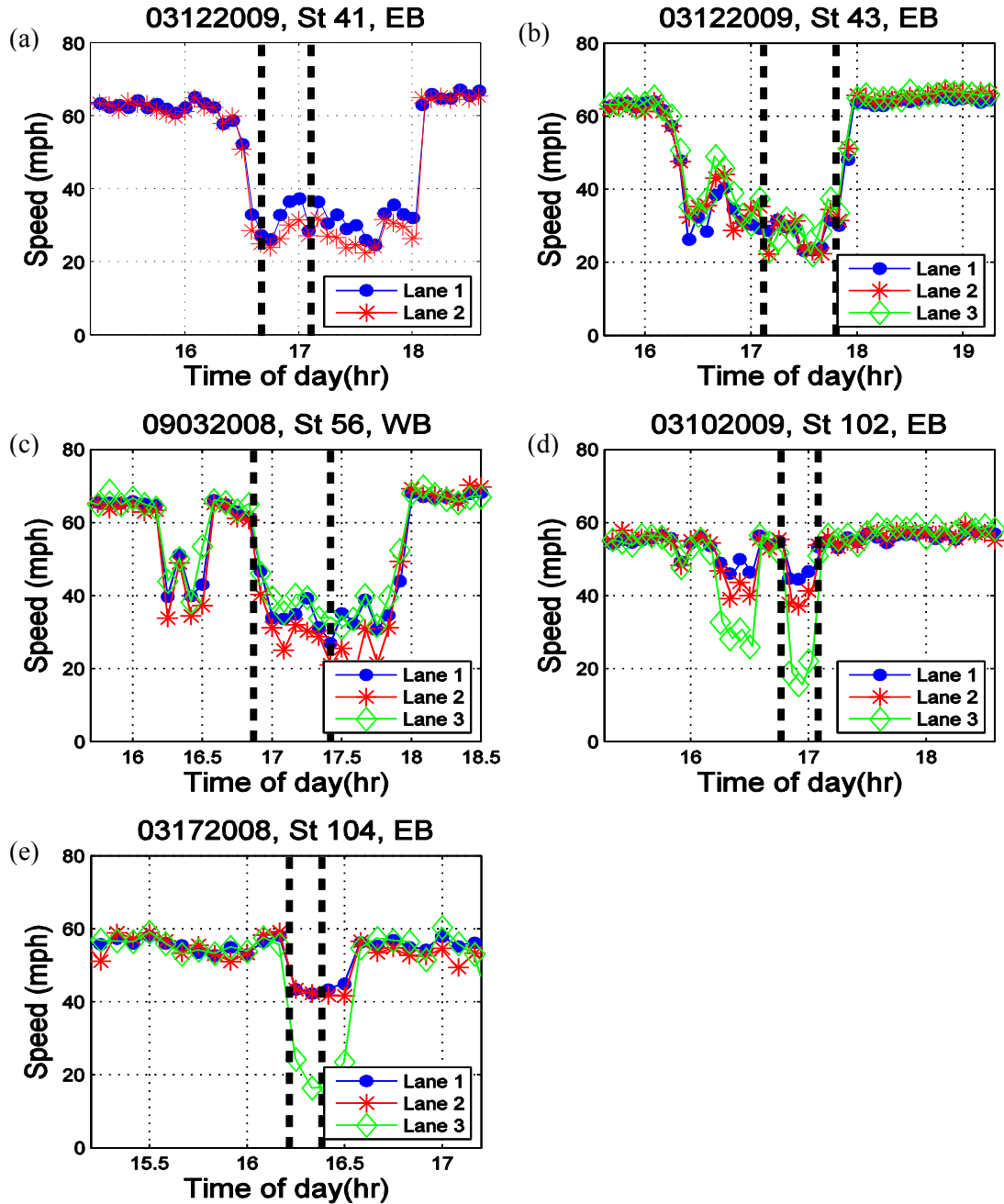


Figure G.2, Speed trends at the detector stations in the ground truth data without observed pulse breakup during congested conditions. The two vertical delineations indicate the time period (start time and end time) when the ground truth data were generated: (a) station 41 eastbound on March 12, 2009 (16:40 ~ 17:06), (b) station 43 eastbound on March 12, 2009 (17:07 ~ 17:48), (c) station 56 westbound on September 3, 2008 (16:40 ~ 17:25), (d) station 102 eastbound on March 10, 2009 (16:46 ~ 17:05), and (e) detector station 104 eastbound on March 17, 2008 (16:10 ~ 16:20).